Thermax 1 2 3 Excel

Research

Design

Fundamentals

2

Thermodynamic Analyses and Optimisation of Energy-Conversion Systems using Excel

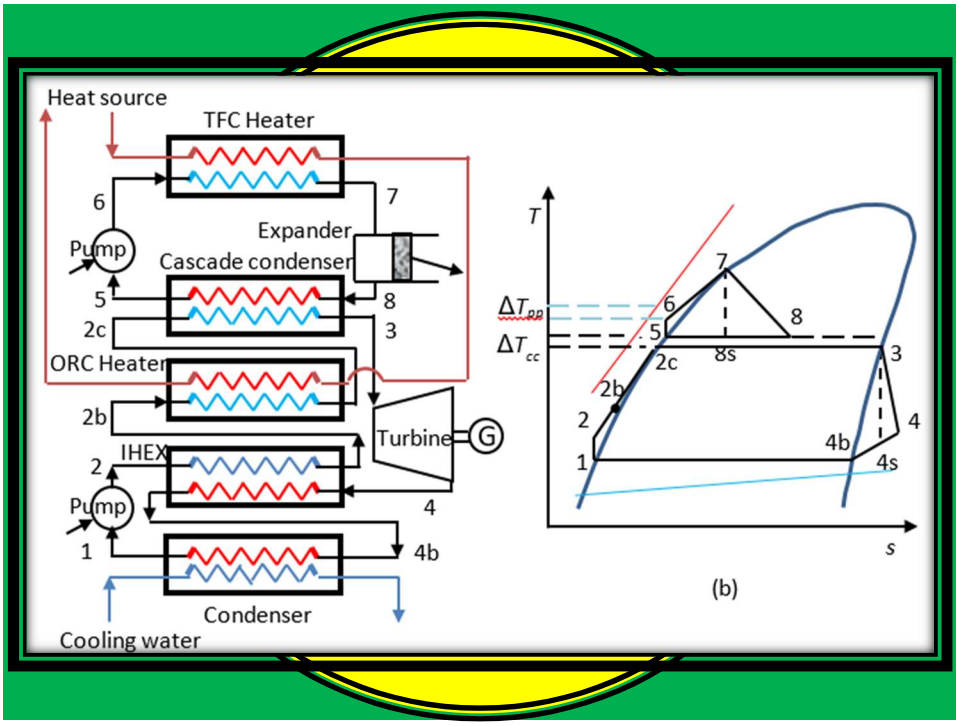

Mohamed M. El-Awad

December, 2025

This book is dedicated to my beloved family; Ghada, Ahmed, and Ula

Thermax (GAS and AIR groups) can be downloaded from:

https://docs.google.com/document/d/15mOzV33K3S8_VJjnVQVN9-ND0mO5VYYqxbV9If3ot8A/edit?usp=drive_link

Preface

The development and application of thermodynamic principles enabled mankind to take the path of civilisation via the invention of the steam engine, the petrol engine, the diesel engine, the steam and gas turbines, the rocket engine, vapour-compression refrigeration systems, vapour-absorption refrigeration systems, water desalination systems and many other man-made systems that enabled the abundant natural energy resources to be utilised for the benefit of the society. The principles and terms of thermodynamics, such the first-law of thermodynamics, the second-law of thermodynamics, entropy, exergy, and thermo-economics have become jargon, not only to scientists and engineers, but to researchers in other areas of knowledge. No doubt, thermodynamics has paved the way, directly or indirectly, to the development of *computers* and *information technology*; the two inventions that have now become vital in our modern daily life and will shape the future of mankind. In return, these two inventions can make the principles of thermodynamic more understandable and properly applicable. Properly understanding and applying these principles by engineering students is more critical than ever before considering the devastating effects of large-scale energy utilisation on the environment and the rapid consumption of conventional energy resources.

Thermodynamics is usually considered a difficult subject by the students. One reason for this is that thermodynamic analyses require the physical properties of the fluids involved to be determined at different phases, temperatures, and pressures by using numerous property tables and charts. Although developing the student's ability to select the relevant table or chart and perform the needed interpolation of data afterwards is an important skill for the future engineers, tables and charts are not suitable for conducting parametric sensitivity analyses that help them to understand the basic principles and concepts of the subject better. Tables and charts are also not suitable for design optimisation analyses that aim to maximise the economic feasibility of energy-conversion systems and minimise their environmental impact. By comparison, computer-aided methods can improve the learning process, firstly, by helping the students to easily conduct such analyses and, secondly, by enabling them to develop more realistic models for their systems than the idealised models that usually adopt many idealisations and simplifying assumptions. Moreover, computer-aided models are interactive and can enhance the learning process by providing immediate answers to "What-if" type of questions without having to repeat the laborious calculations involved. In this respect, the usefulness of computer graphics and animation tools need not be emphasised.

Realising these advantages of computer-aided analyses, most standard textbooks of thermodynamics now include computer-aided exercises by using special software or educational versions of dedicated commercial software. Although this approach can mitigate some of the limitations of the traditional teaching approach, it does not take full advantage of computer-aided methods for equipping the students with the skill of today, which is computer programming, or for enhancing the learning process by gracefully moving from the fundamental exercises to the design and research assignments. This

book presents an approach for teaching engineering thermodynamics by adopting the Learn-By-Examples (LBE) technique and by using a general-purpose software, which is Microsoft Excel, as modelling platform. While LBE has been proven by recent studies as an effective learning technique, Excel enables the students to develop their analytical models without having access to a special software that may not be available to many students particularly in developing countries.

As a modelling platform for engineering analyses, Excel provides a rich library of mathematical functions and powerful graphic tools for data visualisation. Although it does not provide functions for determining fluid properties which are necessary for thermodynamic analyse, such functions can be developed as custom functions with the Visual Basic for Applications (VBA) programming language that comes with Microsoft Applications. This book presents an Excel add-in called Thermax that provides property functions for numerous working fluids that are used in thermodynamic analyses including twenty-nine ideal gases, twenty-eight synthetic and natural refrigerants, two aqua solutions for vapour-absorption refrigeration systems as well as functions for water and superheated steam, humid air for psychrometric analyses, and atmospheric air. While the property functions enable the students to deal with time-consuming parametric studies, the Solver add-in that comes with Excel enables them to perform iterative solutions and optimisation analyses of various energy-conversion systems. As some of the thermodynamic models presented in this book demonstrate, the Excel-based platform enables rather complicated analytical models to be developed with minimum effort.

The first two chapters of the book give a brief review of the basic thermodynamic principles and describe the Thermax add-in in details. The following three chapters shows how Excel and Thermax can be used to deal with thermodynamic analyses of the basic power generation and refrigeration cycles. The two chapters that follow show how they can be used for psychrometric analyses of air-conditioning systems and processes and for combustion analyses. Chapters 8 to 9 deal with thermo-economic optimisation analyses of energy-recovery systems by considering three examples which are the simple gas-turbine cycle with inlet-air cooling, the air-bottoming cycle, and the combined Brayton-Rankine cycle. The last two chapters demonstrate the use of the Excel-based platform for thermodynamic evaluation of two options for utilising low-temperature energy sources which are the vapour-absorption refrigeration cycle and a two-stage power-generation cycle that combines the organic Rankine cycle and the tetrahedral flash cycle. Most of the examples considered in the book have been adopted from popular textbooks and published work so that the students can obtain additional information and verify their results. While relevant exercises are provided at the end of Chapters 2 to 7, more challenging exercises and mini projects are given in the last appendix of the book.

This book is the second volume in a set of books that deal with computer-aided thermofluid analyses by using the Excel-based modelling platform. The books have been written primarily for educational purposes, but it is hoped that they can also be useful for practicing engineers and researchers in the area.

Acknowledgements
The development of Thermax and the writing of this set of books would not have been possible without benefitting from the efforts of many colleagues who have made their publications, data, and software available in the open literature or on their websites. A special gratitude goes to the Mechanical Engineering Department at the University of Alabama (USA) whose initiative "*Excel for Mechanical Engineering*" both inspired and helped me to develop Thermax. I am also indebted to Universiti Putra Malaysia and Universiti Tenaga Nasional (Malaysia), the University of Khartoum (Sudan), and the University of Technology and Applied Sciences (Oman) for their generous support at different periods of my academic career and hope that they find the books a worthy token of appreciation and gratitude. Last, but not least, I am grateful to my beloved family for the unfailing support I needed desperately to complete this work at a a time of conspiracy, betrayal, and war.

CONTENTS

Chapter 1

Introduction

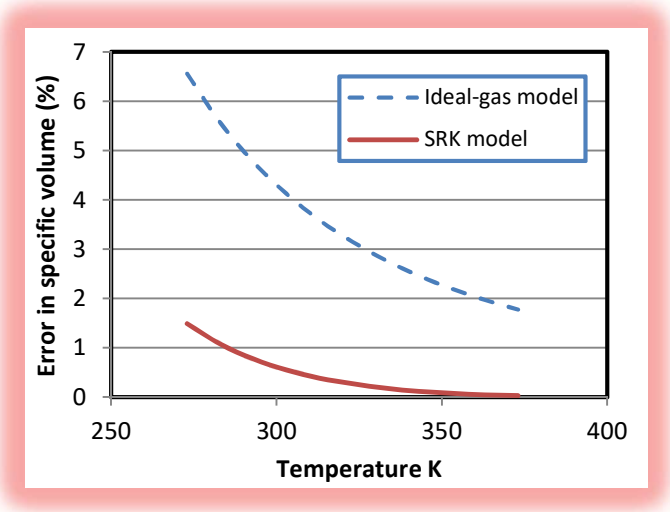

Among the various forms of energy, the two forms that are of primary importance in thermodynamic analyses are thermal energy and work, which is a form of mechanical energy. Depending on their handling of these two forms of energy, energy-conversion systems are divided into two main types; a type that converts thermal energy into work and a type that uses work to produce heating or cooling. In thermodynamics, a system is a specific, definable part of the universe chosen for study, separated from its surroundings (the environment) by a real or imaginary boundary. The system contains matter and/or energy and can exchange these with its surroundings. The type of exchange defines whether the system is an open, closed, or isolated system. Fluids are used in all types of energy-conversion systems because of their ability to change their form so as to facilitate the transfer of thermal energy or work to or from the system. These fluids, called "working fluids", can be gases that change their pressures, temperature, and volume without changing their phase, or liquids and vapours that change their phase as well as their pressures, temperature, and volume. The system's condition is described by thermodynamic properties of the fluid involved. Thermodynamic analyses apply certain physical laws on the processes that take place during the exchange of thermal energy and work between a given system and its surroundings. This chapter briefly reviews the basic principles of thermodynamic analyses of energy-conversion systems and discusses the advantages of computer-aided methods for such analyses. The chapter also highlights the capabilities and limitations of Microsoft Excel as a modelling platform for thermodynamic analyses and optimisation of energy-conversion systems and introduces Thermax, the Excel add-in used to conduct the various analyses presented in this book.

1.1. A brief review of thermodynamics

Engineering thermodynamics determines the amount of energy transfer in the form of work or heat (thermal energy) between any energy-conversion system and its surroundings and the efficiency and effectiveness of the energy transfer process. It has four basic laws the most important of which are the first and the second laws of thermodynamics. While the first law accounts for the *quantity* of energy interaction in a process, the second law accounts for the *quality* of this interaction. To apply these two basic laws, property relationships, tables or charts are used to determine the properties of the particular fluid involved and its phase (a liquid, a liquid-vapour mixture, a gas, or a gaseous mixture). To illustrate the application of thermodynamic laws and relationships in a typical analysis, consider the air-compression system shown in Figure 1.1.a that has two stages of compression separated by an intercooler. Air enters the system at a temperature T_1 and pressure P_1. The first-stage compressor, C_1, compresses the air adiabatically to state 2, after which it enters the intercooler where its temperature is reduced to T_3. The second-stage compressor, C_2, then increases the air pressure to P_4 at which the temperature increases to T_4. Figure 1.1.b shows the compression process on a temperature-entropy diagram. The total compression work is divided between the two compressor stages depending on the intermediate pressure (P_i) and there is a certain value of this pressure that minimises this work. The principles of thermodynamics help us to determine this optimum pressure as shown below.

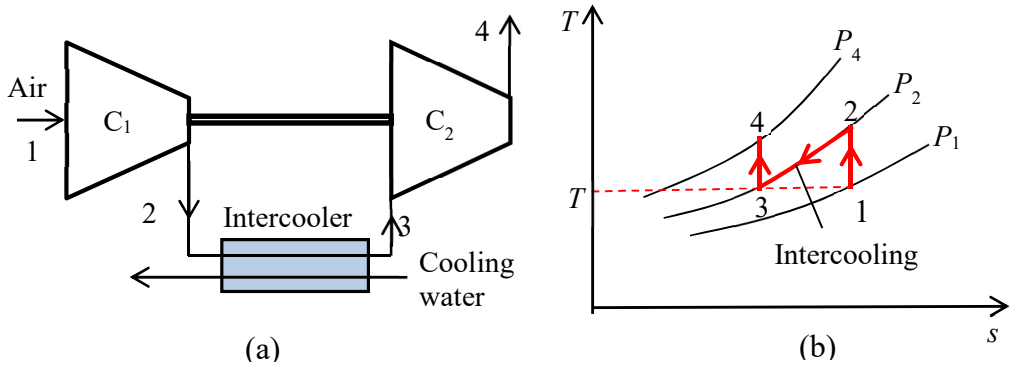

Figure 1.1. Schematic and *T*-*s* diagrams of a two-stage air compressor with intercooling

Treating the two compressor stages as steady-flow processes and neglecting changes in kinetic and potential energy, the first-law of thermodynamics states that [1]:

$$q - w = (h_{out} - h_{in}) \tag{1.1}$$

Where q and w are the amount of heat transfer and work transfer per unit mass flow of air, respectively, and $(h_{out} - h_{in})$ is the resulting enthalpy change over the stage. Equation (1.1) adopts the sign convention that heat into the system is positive, while work into the system is negative. Assuming the compression processes in both stages to be isentropic as shown in Figure 1.1.b could mean that they are adiabatic (q=0) and reversible. Therefore, using an average specific heat for air at constant pressure ($\bar{c}_p$), the compression work per unit mass flow of air in stage 1 (w_1) and in stage 2 (w_2) can be determined from Equation (1.1) as follows:

$$w_1 = -(h_2 - h_1) = -\bar{c}_p (T_2 - T_1) \tag{1.2}$$

$$w_2 = -(h_4 - h_3) = -\bar{c}_p (T_4 - T_3) \tag{1.3}$$

The total compression work (w_{total}) is then given by:

$$w_{total} = w_1 + w_2 = -\bar{c}_p [(T_2 - T_1) + (T_4 - T_3)] \tag{1.4}$$

Assuming perfect intercooling, i.e., $T_3 = T_1$, Equation (1.4) can be rearranged as:

$$w_{total} = \bar{c}_p T_1 \left[\left(1 - \frac{T_2}{T_1} \right) + \left(1 - \frac{T_4}{T_3} \right) \right] = \bar{c}_p T_1 \left[2 - \left(\frac{T_2}{T_1} \right) - \left(\frac{T_4}{T_3} \right) \right] \tag{1.5}$$

Since the two compression processes are assumed to be isentropic and the specific heat for air to be constant, the temperature ratios in Equation (1.5) can be converted into pressure ratios by using the following approximate relationships:

$$\frac{T_2}{T_1} = \left(\frac{P_2}{P_1}\right)^{\frac{k-1}{k}} \tag{1.6}$$

$$\frac{T_4}{T_3} = \left(\frac{P_4}{P_3}\right)^{\frac{k-1}{k}} \tag{1.7}$$

Where k is the ratio of specific heats ($k=c_p/c_v$; c_v is the specific heat for air at constant volume). With another assumption that there is no pressure loss in the intercooler, $P_3 = P_2 = P_i$. Substituting from Equations (1.6) and (1.7), Equation (1.5) becomes:

$$w_{total} = c_p T_1 \left[2 - \left(\frac{P_i}{P_1}\right)^{\frac{k-1}{k}} - \left(\frac{P_4}{p_i}\right)^{\frac{k-1}{k}} \right] \tag{1.8}$$

The variation of the total compression work with the intermediate pressure P_i, can be seen by considering the specific case in which $T_1 = 300$K, $P_1 = 100$ kPa, and $P_4 = 900$ kPa. Using Equation (1.8), the total compression work in the system was calculated for different values of P_i and Figure 1.2 shows the result. The figure shows that the value of P_i at which the total compression work is minimal is around 300 kPa. Increasing or decreasing P_i from this value will increase the compression work.

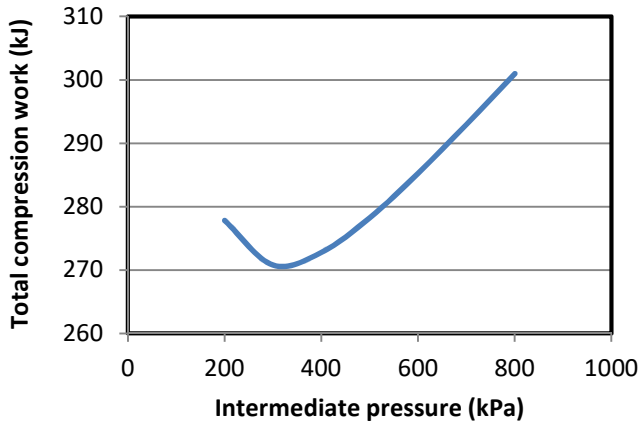

Figure 1.2. Variation of the total compression work with the intermediate pressure

The principles of thermodynamics are also useful for performance evaluation and design optimisation of power-generation and refrigeration systems. For example, consider the

regenerative steam-turbine power plant shown in Figure 1.3. This plant consists of a boiler house for producing superheated steam, a high-pressure steam turbine (HPT), a low-pressure steam turbine (LPT), a condenser, an open feed-water heater (FWH) and two feed-water pumps. A fraction of the steam (y) is extracted after the HPT for preheating the feed-water before going back to the boiler house. Although the extracted steam reduces the work output of the LPT, it reduces the amount of heat added in the boiler and its net effect is to increase the thermal efficiency of the plant. There is also a certain steam-extraction pressure at which the plant's thermal efficiency attains a maximum value. As shown below, the principles of thermodynamics can be used to determine this optimum pressure.

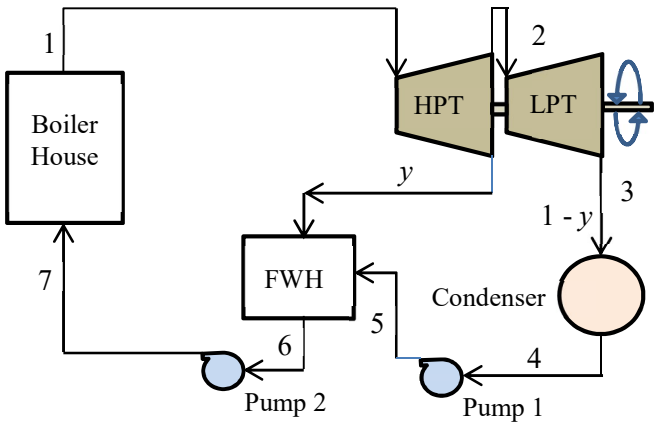

Figure 1.3. Schematic diagram of a regenerative steam-turbine power plant

The total specific work output from the two turbines (w_{out}) and the total specific work input to the two pumps (w_{in}) are given by:

$$w_{out} = w_{HPT} + w_{LPT} \tag{1.9}$$

$$w_{in} = w_{P1} + w_{P2} \tag{1.10}$$

Where w_{HPT} and w_{LPT} are the specific work output from the high-pressure turbine and the low-pressure turbine, respectively, and w_{P1} and w_{P2} are the specific work inputs in pump 1 and pump 2, respectively. Assuming the two turbines and the two pumps to be adiabatic and neglecting the changes in kinetic and potential energies, the work output or input for these devices per each kg of steam generated in the boiler are given by:

$$w_{HPT} = (h_1 - h_2) \tag{1.11}$$

$$w_{LPT} = (1 - y)(h_2 - h_3) \tag{1.12}$$

$$w_{P1} = (1 - y)(h_5 - h_4) \tag{1.13}$$

$$w_{P2} = (h_7 - h_6) \tag{1.14}$$

Mass and energy balance over the feed-water heater gives:

$$yh_2 + (1 - y)h_5 = 1 \times h_6 \tag{1.15}$$

The specific heat input to the boiler (q_{in}) is determined by the relevant enthalpy change as follows:

$$q_{in} = (h_1 - h_7) \tag{1.16}$$

Finally, the net specific work output from the plant (w_{net}) and the thermal efficiency of the plant (η) can be calculated from:

$$w_{net} = w_{out} - w_{in} \tag{1.17}$$

$$\eta = w_{net} / q_{in} \tag{1.18}$$

Both w_{net} and η depend on the fraction of steam extracted for regeneration (y); which in turn depends on the extraction pressure (P_2). Figure 1.4 shows the variation of y and η with P_2 for an ideal cycle in which P_1 = 15 MPa, T_1 = 600°C, and P_4 = 10 kPa. The figure shows that η attains a maximum value of 45.55% when P_2 is in the range of 1000 kPa.

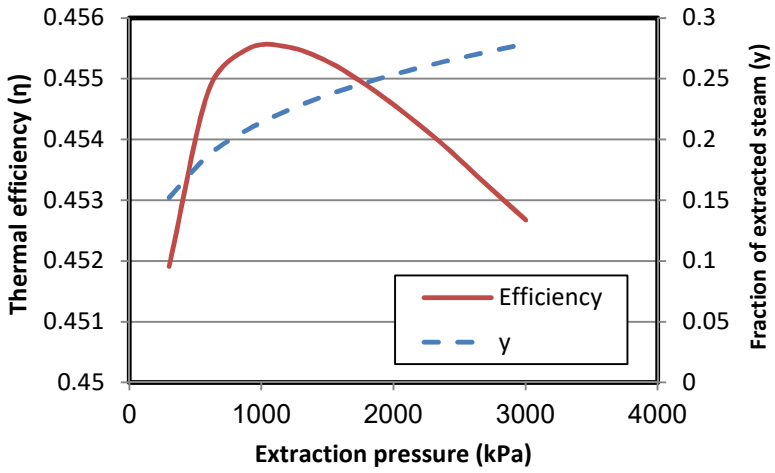

Figure 1.4. The effect of intermediate pressure (P_2) on the fraction of extracted steam (y) and thermal efficiency (η) of an ideal regenerative steam-turbine power plant

It should be mentioned that the working fluid in the above power plant, which is water, changes its phase from liquid to superheated steam in the boiler, to saturated mixture of water and steam in the low-pressure turbine, and returns to liquid water in the condenser. Therefore, appropriate property tables or charts are needed for determining the thermodynamic properties of water at these different states. In general, thermodynamic analyses require many tables and charts for various working fluids. The principles of thermodynamics are also needed for the analyses of air-conditioning systems and processes and for the analyses of the processes that involve combustion and other chemical reactions. For such analyses, thermodynamics provides the basic relationships needed to quantify the effects of fluid mixing and chemical reactions on the properties of the working fluids and to determine the transfer of energy and effluents to or from the system under consideration.

1.2. Advantages of computer-aided thermodynamic analyses

Thermodynamic analyses of energy-conversion cycles that involve phase changes of the working fluid, like the Rankine cycle, require the determination of fluid properties at different phases of the fluid. For these analyses computer-aided methods are more convenient than traditional methods that use property tables and charts. Apart from saving time and eliminating possible human errors, computer-aided analyses offer a number of other advantages over traditional analytical methods. For the cycles that involve gases and do not involve phase changes computer-aided methods allow the application of the variable specific-heat method of analysis instead of the approximate constant specific-heat method which is less accurate. An important advantage of computer-aided methods is their ability to give more realistic results by avoiding unnecessary simplification of the models and by using more accurate formulae for fluid properties. Moreover, they offer reliable techniques for iterative solutions and optimisation analyses. In what follows, these advantages are illustrated by means of relevant examples.

A. Avoiding excessive simplification of the model

In many situations, traditional analytical methods adopt excessive simplifications of the analytical models which makes their results grossly deviate from the behaviour of real systems. A good example of this situation is given by the models of internal-combustion (IC) engines. Traditional air-standard models of IC engines, such as the Otto cycle and the Diesel cycle, neglect heat-transfer and friction losses, treat the combustion process as heat-addition from an external source, and use constant specific heats of the working fluids. These assumptions enable the engine processes to be represented by simple closed-form relations for calculating the amount of heat added to the engine and net work from it [2]. However, air-standard models usually overestimate the engine's output and thermal efficiency. By comparison, computer-aided models of IC engines closely mimic the behaviour of actual IC engines by taking into consideration the geometrical as well as the thermodynamic characteristics of the engines. Therefore, these models can be used to investigate the effect of important design and operation factors such the ignition or

injection timing on the engine performance or the effect of engine' speed on the specific fuel consumption. However, the formulation of these models leads to a set of ordinary differential equations that need to be solved simultaneously by using a numerical method such as the Newton-Raphson method [2].

B. Accurate representation of fluid properties and processes

The ideal-gas law ($Pv=RT$) can be used with reasonable accuracy to determine the specific volume of a superheated vapour. However, when the temperature approaches the saturation line, the value of the specific volume thus determined departs significantly from the actual volume. More accurate estimates can be obtained by using more complex models such as the following Soave-Redlich-Kwong (SRK) equation of state [1]:

$$P = \frac{R_u T}{\tilde{v} - b} - \frac{a\alpha}{\tilde{v}(\tilde{v} + b)} \tag{1.19}$$

Where P is the absolute pressure of the gas, $\tilde{v}$is the molar specific volume, R_u is the universal gas constant, T is the absolute temperature of the gas, and a, b and α are fluid-dependent constants. Figure 1.10 shows the deviations from the tabulated values by those obtained from the ideal-gas law and the SRK equation of state for refrigerant R134a at 0.2 MPa.

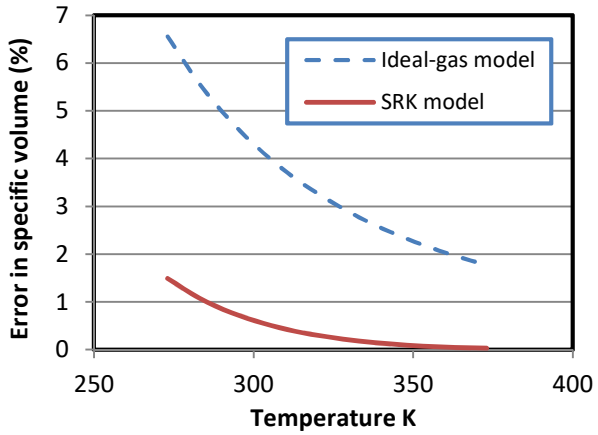

Figure 1.10. Errors in the specific volume of R134a by the ideal-gas law and the SRK equation of state

The figure shows that the error of the ideal-gas law is more that 2% even at high temperatures and increases as the temperature approaches the saturation value, but the accuracy of the SRK equation remained higher than 99% even close to the saturation line. However, the SRK equation is implicit in $\tilde{v}$ and, therefore, it cannot be used directly to determine the specific volume. A number of standard iterative procedures (e.g. Newton-Raphson method) can be used to solve the equation, but they are more suitable for computer-aided analyses than hand calculations. Nonlinear equations like the SRK

equation give advantage to computer-aided thermodynamic analyses by enabling more realistic and accurate estimations.

C. Dealing with iterative solutions and optimisation analyses

Without the simplifying assumptions and approximations, most thermodynamic analyses would require iterative solutions. An example of thermodynamics analyses that require iterative solutions is the determination of the adiabatic flame temperature by first-law analysis of the combustion process. Optimisation analyses are needed for determining the best design for a fluid-thermal system such as the optimum intermediate pressure for the two-stage air-compression system and the optimum steam-extraction pressure for the regenerative Rankine cycle discussed in Section 1.1. While certain simple optimisation analyses that involve a single design parameter can be performed by means of calculus techniques and graphic tools, optimisation analyses that involve multiple design variables and multi-objective optimisation analyses require the use of computer-aided techniques.

1.3. Excel as a modelling platform for thermodynamic analyses

Microsoft Excel provides a rich library of built-in functions and powerful graphical tools. Considering its wide availability, the simplicity of its user-interface, and the flexibility of its graphical tools, it is being increasingly used as a teaching aid in various engineering subjects [3-8]. Although Excel is mostly used for dealing with simple computer-aided operations like matrix inversion and multiplication, it is equipped with other tools that make it a capable modelling platform for more challenging types of "What-if" and optimisation analyses. Two of these tools are the Goal Seek command and the Solver add-in. The Visual Basic for Applications (VBA) programming language that comes with Microsoft Office can be used for developing customised user-defined functions (UDFs) and add-ins for thermodynamic analyses. The Developer ribbon of Excel also allows the use of macros that remove the tedium of parametric studies and repetitive calculations.

The main limitation of Excel as modelling platform for thermodynamic analyses is the lack of built-in functions for fluid properties, but this problem could be solved by developing suitable add-ins. The *Thermotable* add-in developed by the Mechanical Engineering Department at the University of Alabama determines the thermodynamic properties of ideal gases, water and superheated steam, and four refrigerants R134a, R22, R410A, and R407C [9-12]. Goodwin [13] also developed an educational Excel add-in, called *TPX* (Thermodynamic Properties for Excel), that determines the properties of five gases (H_2O, H_2, O_2, N_2, CH_4) and refrigerant R-134a. A number of property add-ins have also been developed for research and industrial applications [14, 15]. The American National Institute of Standards and Technology (NIST) developed *REFPROP* that provides thermophysical properties of various refrigerants and their mixtures [16]. An open-source alternative to *REFPROP*, called *CoolProp*, was developed by Bell [17] at the University of Liege. Optimized Thermal Systems also developed a commercial alternative add-in to *REFPROP* called *XProps* [18].

This book presents an educational add-in, called Thermax, that enables Excel to be used for thermodynamic analyses of various types of energy-conversion systems. Thermax provides property functions for seven groups of working fluids that are used in energy-conversion systems that include:

- Twenty-nine ideal gases,
- Water and superheated steam,
- Twenty-eight refrigerants for vapour-compression refrigeration (VCR) systems,
- Lithium-bromide and ammonia aqua solutions for vapour-absorption refrigeration (VAR) systems,
- Humid air for psychrometric analyses,
- Various types of fuels and chemically-reacting substances,
- Air at standard atmospheric pressure but various temperatures.

In addition to its seven groups of fluid-property functions, Thermax provides a small group of user-defined functions that are useful for general thermofluid analyses. These include two data interpolation functions and a Newton-Raphson solver for non-linear equations such as the SRK equation of state.

1.4. Closure

Chapter 2 describes the fluid property functions provided by Thermax in more details and shows how these functions can be used in Excel's formulae for thermodynamic analyses. The three chapters 3, 4, and 5 illustrate the use of the functions for basic thermodynamic analyses of power generation and refrigeration systems. Chapters 3 and 4 give examples of analysing the Brayton cycle, the Otto cycle, the Rankine cycles with and without regeneration, the combined Brayton-Rankine cycle, and the organic Rankine cycle. Chapter 5 deals with the analyses and optimisation of single-stage, multi-stage compression, and cascade VCR cycles using refrigerant R134a. Chapters 6 and 7 show how the property functions can be used to deal with two types of thermodynamic analyses in which the working fluids are gaseous mixtures. Chapter 6 deals with the analyses of psychrometric processes and illustrates the use of the functions for design analyses of air-conditioning systems, while Chapter 7 focuses on combustion analyses and develops a unified Excel sheet for general steady-flow combustion analyses.

The three chapters 8, 9, and 10 move to design applications of the Excel-based modelling platform by showing how the combination of Excel, Solver, and Thermax can be used in thermo-economic optimisation analyses of three options for utilising the waste energy in the gas turbines' exhaust gas. Chapter 8 deals with utilising the waste energy in a vapour-refrigeration system for cooling the air entering a simple gas-turbine, Chapter 9 deals with utilising the energy in an air-bottoming cycle, and Chapter 10 deals with utilising it in a combined Brayton-Rankine cycle. Beside conducting the thermo-economic analyses for the relevant systems and verifying the results by comparison with published data, Chapters 8 and 9 also highlight the effects of the thermodynamic model and/or solution method on the results, while Chapter 10 shows how the Excel-aided model can be used

to deal with multi-objective optimisation and exrgoeconomic analyses of energy-conversion systems.

Chapter 11 and Chapter 12 venture more into research areas by presenting two options for utilising the energy of low-temperature heat sources. Chapter 11 focusses on thermodynamic analyses of vapour-absorption refrigeration cycles and illustrates the use of Thermax functions for first-law analyses of single-effect and double-effect VAR cycles using ammonia-water and lithium-bromide-water solutions. Chapter 12 present a power-generation cycle that combines the Organic Rankine Cycle (ORC) with the Trilateral Flash Cycle (TFC). The combined cycle enjoys the merits of the two simple cycles by applying the TFC in the high-temperature circuit and the ORC in the low-temperature circuit and connecting the two cycles via a cascade condenser. The chapter evaluates the thermodynamic performance of the combined cycle with five working fluids of low GWP fluids which are R152a, R1234yf, R600, R600a, and R717.

References

[1] Y.A. Cengel, and M.A. Boles, *Thermodynamics an Engineering Approach*, McGraw-Hill, 7th Edition, 2007.

[2] C.R. Ferguson, *Internal Combustion Engines*, John Wiley & Sons, 1986.

[3] M. Niazkar, S.H. Afzali, Application of Excel Spreadsheet in Engineering Education, First International & National Conference on Engineering Education, Shiraz University, 10-12 November 2015

[4] A. Karimi, Using Excel for the thermodynamic analyses of air-standard cycles and combustion processes, ASME 2009 Lake Buena Vista, Florida, USA.

[5] Z. Ahmadi-Brooghani, Using Spreadsheets as a Computational Tool in Teaching Mechanical Engineering, Proceedings of the 10th WSEAS International Conference on computers, Vouliagmeni, Athens, Greece, July 1315, 2006, 305-310

[6] S.A. Oke, Spreadsheet Applications in Engineering Education: A Review, Int. J. Engng Ed. Vol. 20, 2004, No. 6, 893-901

[7] M.M. El-Awad and A. M. Elseory, Excel as a Modelling Platform for Thermodynamic Optimisation Analyses, University of Khartoum Engineering Journal, Vol. 3 Issue 1, pp. 12-18 (February 2013)

[8] M.M. El-Awad and M.S. Al-Saidi, Excel as an Educational Platform for Design Analyses of Fluid-Thermal Systems, World Journal of Engineering and Technology Vol.10 No.2, 2022, 434-443, doi: 10.4236/wjet.2022.102025. Scientific Research Publishing.

[9] The University of Alabama, Mechanical Engineering, Excel for Mechanical Engineering project, Internet: http://www.me.ua.edu/excelinme/index.htm (Last accessed July 11, 2019).

[10] J. Huguet, K. Woodbury, R. Taylor, Development of Excel add-in modules for use in thermodynamics curriculum: steam and ideal gas properties, American Society for Engineering Education, 2008, AC 2008-1751.

[11] K. Mahan, J. Huguet, K. Woodbury, R. Taylor, Excel in ME: Extending and refining ubiquitous software tools, American Society for Engineering Education, 2009, AC 2009-2295.

[12] L. Caretto, D. McDaniel, T. Mincer. Spreadsheet calculations of thermodynamic properties, Proceedings of the 2005 American Society for Engineering Education Annual Conference & Exposition, American Society for Engineering Education, 2005.

[13] D. G. Goodwin, ″TPX: thermodynamic properties for Excel", http://termodinamicaparaiq.blogspot.com/p/tpx_12.html (Last accessed July 11, 2019).

[14] T. K. Jack. Computerised calculations of thermo-physical steam and air properties, *Int. J. Pure Appl. Sci. Technol.*, 9(2) (2012), pp. 84-93 (*Available online at* http://ijopaasat.in/yahoo_site_admin/assets/docs/3_IJPAST-276-V9N2.139104407.pdf (Last accessed July 11, 2019).

[15] C.O.C. Oko and E.O.Diemuodeke. MS Excel spreadsheet add-in for thermodynamic properties and process simulation of R152a, *Energy Science and Technology***,** Vol. 5, No. 2, 2013, pp. 63-69.

[16] E.W. Lemmon, M.L. Huber, M.O. McLinden, *NIST Reference Fluid Thermodynamic and Transport Properties— REFPROP* Version 8.0, User's Guide, National Institute of Standards and Technology, Physical and Chemical Properties Division, Boulder, Colorado 80305, 2007.

[17] I. Bell, CoolProp. Available at https://sourceforge.net/projects/coolprop/files/CoolProp/ (Last accessed July 11, 2019).

[18] Optimized Thermal Systems, XProps, A Quick and easy way to call refrigerant properties, http://optimizedthermalsystems.com/index.php/products/xprops, (Last accessed July 11, 2019).

Chapter 2

Thermax property functions

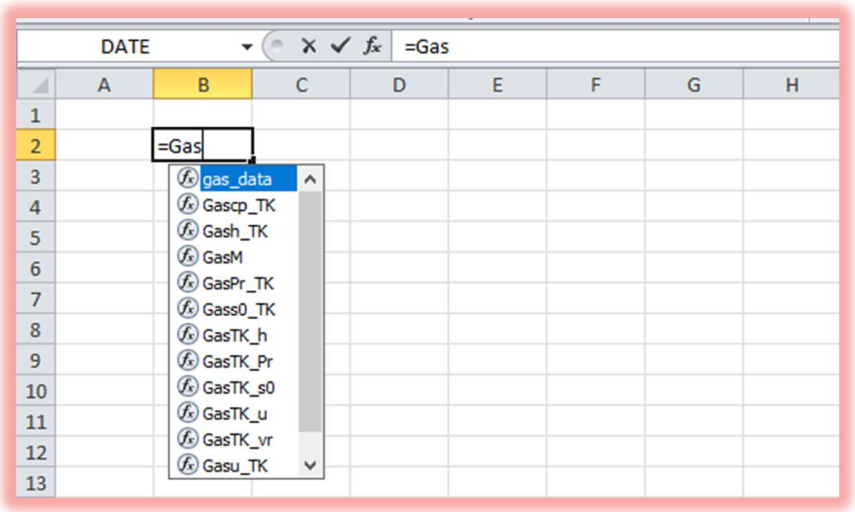

Thermax provides more than a hundred custom functions that determine the key thermo-physical properties for more than eighty working fluids. To help the user select the required property function with ease, Thermax functions are divided into seven groups such that each group deals with similar substances and each group of functions are given a common indicative prefix; e.g. "Gas" for ideal gases and "Ref" for vapour-compression refrigerants. Three groups deal with a single substance which are the "Wat" group for water, the "Psy" group for pyschrometric analyses, and the "Air" group that gives the thermo-physical properties of atmospheric air. The name of each function also indicates its output and input properties. This chapter lists the different Thermax functions for fluid properties and describes the name style adopted for the functions in more details to show how it can be utilised via Excel's function wizard to find the required function without having to memorise the names of all the functions. The chapter also describes the procedure for installing the add-in and using its functions in Excel's formulae for thermodynamic analyses.

2.1. The name style for Thermax property functions

Consider the two Thermax functions shown on Figure 2.1. The function shown on Figure 2.1.a determines the enthalpy of saturated water at a pressure of 500 kPa and quality of 0.8, while that shown on Figure 2.1.b determines the entropy of a superheated refrigerant R134a at a pressure of 200 kPa and temperature of 50°C.

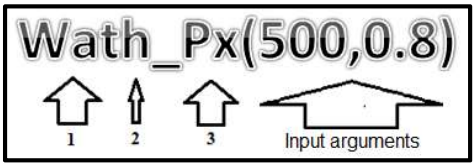

(a)

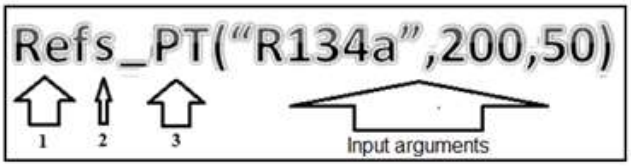

(b)

Figure 2.1. Examples of Thermax functions

Figure 2.1 shows that the name of a function consists of the following three parts:

1. The first three letters (1) refer to the function's group, i.e., "**Wat**" for water/steam and "**Ref**" for vapour-compression refrigerants.
2. The fourth letter (2), which is followed by an underscore, refers to the function's output property, i.e., "**h_**" for enthalpy and "**s_**" for entropy.
3. The letters after the underscore (3) refer to the function's input parameter(s), i.e., "**Px**" for pressure and quality and "**PT**" for pressure and temperature (in °C).

Figure 2.1 also shows the required input parameters for the two functions. While first function (**Wath_Px**) requires two input properties, which are the pressure (500 kPa) and quality (0.8), the second function (**Refs_PT**) requires three input parameters which are the refrigerant name ("R134a"), the pressure (200 kPa), and the temperature (50°C). The other five groups are "**Gas**" for ideal gases, "**Psy**" for psychrometric analyses, "**LiB**" and "**Nh3**" for the two binary solutions used in vapour-absorption refrigeration, "**Chm**" for fuels and chemically reacting substances, and "**Air**" for air at atmospheric pressure. Table 2.1 gives more examples of Thermax functions with their intended usage. As shown in Section 2.3, with this name style the function wizard can be used to find the required function without having to memorise the names of all the functions.

Table 2.1. Examples of Thermax property functions from different groups

#	Thermax function	Property to be determined by the function
1	Gash_TK("Air",350)	The enthalpy (h) for air at 350K
2	GasTK_h("Air",500)	The absolute temperature for air given its enthalpy (h=500 kJ/kg)
3	Wats_Tx(150,0.5)	The entropy (s) of saturated water at a temperature of 150°C and quality of 0.5
4	Wath_PT(90,150)	The enthalpy of superheated steam at 90 kPa and 150°C
5	RefPsat_T("R134a",-5)	The saturation pressure (P_{sat}) for refrigerant R134a at -5°C.
6	PsyRh_PTSh(101,30, 0.001)	The relative humidity (ϕ) of air at 101 kPa, 30°C, and specific humidity (ω) of 0.001 kg/kg
7	Airdv_T(25)	The dynamic viscosity of air at standard atmospheric pressure and 25°C.
8	Chm_f1("C6H6","M")	The molar mass for benzene (C_6H_6)
9	Chm_f3("N2","M")	The molar mass for nitrogen (N_2)
10	LiBh_TX(20,80)	The enthalpy of water-lithium bromide solution at 20°C and 80% concentration.

The following points should be noted regarding the name style of Thermax functions:

1. In the Gas-group, the absolute temperature is represented by "**TK**" while in the other groups the temperature in °C is represented by "**T**".
2. Three groups deal with more than one substance and, therefore, the functions of these groups require the name of the substance as the first input parameter. These groups are the Gas-group, the Ref-group, and the Chm-group.
3. The input and output properties in most of the functions are represented by one or two letters, e.g. **Gash_TK** and **GasTK_h**, but some properties are represented by three letters like the saturation pressure and saturation temperature, which are represented by Psat and Tsat in the Wat and Ref groups. Another example is the density of atmospheric air in the Air-group which is represented by **Airrho**.

2.2. Property functions provided by Thermax

This section lists the functions provided by each group.

2.2.1. Functions for ideal gases (Gas)

This group of functions determine the ideal-gas properties for the 29 gasses listed in Appendix A based on the established ideal-gas relationships [1]. The group provides the 12 functions listed in Table 2.2.

Table 2.2. Functions for thermodynamic properties of ideal gases

#	Function	Input [Unit]	Output [Unit]
1	GasM	Gas name	Molar mass, M [kg/kmol]
2	Gascp_TK	Gas name, T[K]	Specific heat, c_p [kJ/kg.K]
3	Gash_TK	Gas name, T[K]	Specific enthalpy, h [kJ/kg]
4	Gasu_TK	Gas name, T[K]	Specific internal energy, u [kJ/kg]
5	Gass0_TK	Gas name, T[K]	Entropy component, s^0 [kJ/kg.K]
6	GasPr_TK	Gas name, T[K]	Relative pressure, P_r [-]
7	Gasvr_TK	Gas name, T[K]	Relative volume, v_r [K]
8	GasTK_h	Gas name, h[kJ/kg]	Absolute temperature, T [K]
9	GasTK_u	Gas name, u[kJ/kg]	Absolute temperature, T [K]
10	GasTK_s0	Gas name, s^0[kJ/kg.K]	Absolute temperature, T [K]
11	GasTK_Pr	Gas name, P_r [-]	Absolute temperature, T [K]
12	GasTK_vr	Gas name, v_r [-]	Absolute temperature, T [K]

The first five functions in Table 2.2 determine the molar mass (M), specific heat (c_p), enthalpy (h), internal energy (u), and the part of entropy change due to temperature change (s^0), respectively, of the ideal gas from its absolute temperature. The two functions that follow, **GasPr_TK** and **Gasvr_TK**, determine the relative pressure (P_r) and relative specific volume (v_r) of the ideal gas from its absolute temperature, respectively. The last five functions in the table are inversion functions that determine the temperature of the ideal gas from its enthalpy (h), internal energy (u), temperature-dependent entropy change (s^0), relative pressure (P_r) or relative specific volume (v_r).

With the exception of the first function, **GasM**, all the functions in this group involve the gas absolute temperature as an input or output parameter. Note that the temperature in the names of all the functions in this group is represented by "TK". An auxiliary function named "**Gas_data**", not shown in the table, stores the values of the four coefficients a_0, a_1, a_2, and a_3 in Equation (A.1) for the 29 gases [1]. The same function is needed by the function **Chm_f3** in the combustion and chemical reactions group to determine the properties of the gases involved in a combustion or chemical reaction process.

2.2.2. Functions for water and superheated steam (Wat)

This group of functions determine the thermo-physical properties of water and superheated steam. Its functions are divided into two subgroups: (a) the functions for the

properties of saturated water/steam mixture and (b) the functions for the properties of superheated steam. Properties of subcooled liquid water are taken as the corresponding values of saturated liquid water at the given temperature [1].

a) Properties of saturated water/steam mixture

The 20 functions in this subgroup do not use mathematical formulae, but store and interpolate the tabulated data for saturated water provided by ASHRAE [2]. Table 2.3 shows the input and output parameters of the 10 property functions that determine the properties of saturated water/steam mixtures at a given temperature with their relevant units. The corresponding 10 custom functions that provide properties of saturated water-steam mixture at a given pressure are listed in Table 2.4. Properties of water as saturated liquid or saturated vapour can be obtained from the functions number 2 to 9 in the two tables by assigning the value of the quality x as 0 or 1, respectively.

Table 2.3. Property functions for saturated water/steam at a given temperature

#	Function	Input [Unit]	Output [Unit]
1	WatPsat_T	T [°C]	Saturation pressure, p_s [kPa]
2	Watv_Tx	T [°C], x [-]	Specific volume, v [m^3/kg]
3	Watu_Tx	T [°C], x [-]	Specific internal energy u [kJ/kg]
4	Wath_Tx	T [°C], x [-]	Specific enthalpy, h [kJ/kg]
5	Wats_Tx	T [°C], x [-]	Specific entropy, s [kJ/kg.K]
6	Watcp_Tx	T [°C], x [-]	Specific heat c_p , [kJ/(kg·K)]
7	Watk_Tx	T [°C], x [-]	Thermal cond., k [mW/(m·K)]
8	Watdv_Tx	T [°C], x [-]	Viscosity, μ [Pa·s]
9	Watvs_Tx	T [°C], x [-]	Velocity of sound, V_s [m/s]
10	Watst_T	T [°C]	Surface tension, σ [mN/m]

Table 2.4. Property functions for saturated water/steam at a given pressure

#	Function	Input [Unit]	Output [Unit]
1	WatTsat_P	P [kPa]	Saturation temperature, T_s [°C]
2	Watv_Px	P [kPa], x [-]	Specific volume, v [m^3/kg]
3	Watu_Px	P [kPa], x [-]	Specific internal energy u [kJ/kg]
4	Wath_Px	P [kPa], x [-]	Specific enthalpy, h [kJ/kg]
5	Wats_Px	P [kPa], x [-]	Specific entropy, s [kJ/kg.K]
6	Watcp_Px	P [kPa], x [-]	Specific heat c_p , [kJ/(kg·K)]
7	Watk_Px	P [kPa], x [-]	Thermal cond., k [mW/(m·K)]
8	Watdv_Px	P [kPa], x [-]	Viscosity, μ [Pa·s]
9	Watvs_Px	P [kPa], x [-]	Velocity of sound, V_s [m/s]
10	Watst_P	P [kPa]	Surface tension, σ [mN/m]

b) Properties of superheated steam

There are 8 functions in this subgroup that determine the thermodynamic properties of superheated steam as shown in Table 2.5.

Table 2.5. Properties of superheated steam given the pressure and another property

#	Function	Input [Unit]	Output [Unit]
1	Watv_PT	*P*, *T*[°C]	Specific volume, *v* [m^3/kg]
2	Watu_PT	*P*, *T*[°C]	Specific internal energy *u* [kJ/kg]
3	Wath_PT	*P*, *T*[°C]	Specific enthalpy, *h* [kJ/kg]
4	Wats_PT	*P*, *T*[°C]	Specific entropy, *s* [kJ/kg.K]
5	WatT_Ph	*P*, *h*[kJ/kg]	Temperature, *T* [^{0}C]
6	WatT_Ps	*P*, *s*[kJ/kg.K]	Temperature, *T* [^{0}C]
7	Wath_Ps	*P*, *s*[kJ/kg.K]	Specific enthalpy, *h* [kJ/kg]
8	Wats_Ph	*P*, *h*[kJ/kg]	Specific entropy, *s* [kJ/kg.K]

The first four functions determine the specific volume (*v*), internal energy (*u*), enthalpy (*h*), and entropy (*s*) of superheated steam given the pressure and temperature according to the formulae provided by Irvine and Liley [3]. The remaining four functions are inverse functions that use iteration to determine the temperature, enthalpy, or entropy from the pressure and another property.

2.2.3. Functions for vapour-compression refrigerants (Ref)

This group of functions provides the thermo-physical properties for the 28 refrigerants listed in Table A2 of Appendix A. This group can also be divided into two subgroups; (a) for saturated refrigerants and (b) for superheated refrigerants. The two subgroups adopt different methodologies to determine the fluid properties as discussed below.

a) Properties of saturated refrigerants

As for the water group, the functions for saturated refrigerants do not use mathematical formulae, but store and interpolate the tabulated data provided by ASHRAE [2] by using a linear interpolation function. Table 2.6 lists 11 functions in this subgroup that determine the thermo-physical properties of saturated refrigerants at a given pressure while Table 2.7 lists 10 functions that determine the refrigerants properties at a given temperature.

Table 2.6. Properties of saturated refrigerants at a given pressure in kPa and quality

#	Function	Input	Output	Output unit
1	RefTsat_P	*Ref. name, P*, *x*	Saturation temperature, T_{sat}	[^{0}C]
2	Refv_Px	*Ref. name, P*, *x*	Specific volume, *v*	[m^3/kg]
3	Refu_Px	*Ref. name, P*, *x*	Specific internal energy, *u*	[kJ/kg]
4	Refh_Px	*Ref. name, P*, *x*	Specific enthalpy, *h*	[kJ/kg]
5	Refs_Px	*Ref. name, P*, *x*	Specific entropy, *s*	[kJ/kg.K]
6	Refcp_Px	*Ref. name, P*, *x*	Specific heat, c_p	[kJ/kg.K]
7	Refvs_Px	*Ref. name, P*, *x*	Velocity of sound, V_s	[m/s]
8	Refdv_Px	*Ref. name, P*, *x*	Dynamic viscosity, μ	[μPa·s]
9	Refk_Px	*Ref. name, P*, *x*	Thermal conductivity, *k*	[mW/(m·K)]
10	Refst_P	*Ref. name, P*	Surface tension, σ	[mN/m]
11	RefTdew_P	*Ref. name, P*	Dew temperature	[^{0}C]

Table 2.7. Properties of saturated refrigerants at a given temperature in °C and quality

#	Function	Input	Output	Output unit
1	RefPsat_T	*Ref. name, T, x*	*Saturation temperature,* T_{sat}	[^{0}C]
2	Refv_Tx	*Ref. name, T, x*	*Specific volume, v*	[m^3/kg]
3	Refu_Tx	*Ref. name, T, x*	*Specific internal energy, u*	[kJ/kg]
4	Refh_Tx	*Ref. name, T, x*	*Specific enthalpy, h*	[kJ/kg]
5	Refs_Tx	*Ref. name, T, x*	*Specific entropy, s*	[kJ/kg.K]
6	Refcp_Tx	*Ref. name, T, x*	*Specific heat,* c_p	[kJ/kg.K]
7	Refvs_Tx	*Ref. name, T, x*	*Velocity of sound,* V_s	[m/s]
8	Refdv_Tx	*Ref. name, T, x*	*Dynamic viscosity,* μ	[μPa·s]
9	Refk_Tx	*Ref. name, T, x*	*Thermal conductivity, k*	[mW/(m·K)]
10	Refst_T	*Ref. name, T*	*Surface tension,* σ	[mN/m]

Three of the 28 refrigerants are zeotropic blends, which are R404A, R407C, and R410A. For these three refrigerants, the saturation temperature means the bubble temperature, while the dew temperature is given by the last function on Table 2.6, **RefTdew_P**. For the other refrigerants, this function also returns the saturation temperature at the given pressure.

b) Properties of superheated refrigerants

Table 2.9 lists 8 functions that deal with superheated vapours of refrigerants. The first function in Table 2.9 applies the Redlich-Kwong (SRK) equation of state to determine the specific volume of superheated refrigerants. The following five functions apply Equations (C.8) to (C.15) given in Appendix C to determine the relevant property values. The last two function (**Refh_Ps** and **Refs_Ph**) are inversion functions that use an iterative process to determine the fluid's enthalpy or entropy from its pressure and entropy or enthalpy.

Table 2.9. Properties of superheated refrigerants given the pressure in kPa

#	Function	Input [unit]	Output [unit]
1	Refv_PT	*Ref. name, P, T* [°C]	*v* [m^3/kg]
2	Refu_PT	*Ref. name, P, T* [°C]	*u* [kJ/kg]
3	Refh_PT	*Ref. name, P, T* [°C]	*h* [kJ/kg]
4	Refs_PT	*Ref. name, P, T* [°C]	*s* [kJ/kg.K]
5	RefT_Ph	*Ref. name, P, h* [kJ/kg]	*T* [°C]
6	RefT_Ps	*Ref. name, P, s* [kJ/kg.K]	*T* [°C]
7	Refh_Ps	*Ref. name, P, s* [kJ/kg.K]	*h* [kJ/kg]
8	Refs_Ph	*Ref. name, P, h* [kJ/kg]	*s* [kJ/kg.K]

As discussed in Appendix C, the functions in this subgroup determine the properties of superheated refrigerants by extending the compressibility-factor concept to include enthalpy and entropy. Appendix C verifies these functions by comparing their estimations with the data given by ASHRAE [2] for R134a.

2.2.4. Functions for psychrometric analyses (Psy)

The functions of this group provide the thermodynamic properties of atmospheric air, which is a mixture of dry air and water-vapour. Appendix B shows the relations used for the development of these functions which are those commonly used in psychrometric analyses [1]. Table 2.10 lists the 14 functions included in this group together with their input and output arguments. The letters in the function names have the following meanings: h (specific enthalpy), Db (dry bulb), Dp (dew point), P (pressure), Rh (relative humidity), Sh (specific humidity), v (specific volume), Wb (wet bulb). Case 6 in Table 2.1 shows how the function **PsyRh_PTSh** is used to determine the relative humidity for air given its pressure, temperature, and specific humidity.

Table 2.10. Functions for psychrometric analyses

#	Function	Input [unit]	Output [unit]
1	Psyv_PDbRh	P [kPa], T_{db} [°C], ϕ [%]	v [m^3/kg]
2	PsyRh_PDbSh	P [kPa], T_{db} [°C], ω[kg/kg]	ϕ [%]
3	PsyRh_PDbWb	P [kPa], T_{db} [°C], T_{wb} [°C]	ϕ [%]
4	PsySh_PDbRh	P [kPa], T [°C], ϕ [%]	ω [kg/kg]
5	PsySh_PDbWb	P [kPa], T_{db} [°C], T_{wb} [°C]	ω [kg/kg]
6	Psyh_PDbSh	P [kPa], T [°C], ω[kg/kg]	h [kJ/kg]
7	Psyh_PDbRh	P [kPa], T [°C], ϕ [%]	h [kJ/kg]
8	PsyDp_PDbRh	P [kPa], T_{db} [°C], ϕ [%]	T_{dp} [°C]
9	PsyDp_PDbWb	P [kPa], T_{db} [°C], T_{wb} [°C]	T_{dp} [°C]
10	PsyDb_PRhSh	P [kPa], ϕ [%], ω[kg/kg]	T_{db} [°C]
11	PsyDb_PhSh	P [kPa], h [kJ/kg], ω[kg/kg]	T_{db} [°C]
12	PsyWb_PDbRh	P [kPa], T_{db} [°C], ϕ [%]	T_{wb} [°C]
13	PsyWb_PDbSh	P [kPa], T_{db} [°C], ω[kg/kg]	T_{wb} [°C]
14	PsyWb_PRhSh	P [kPa], ϕ [%], ω[kg/kg]	T_{wb} [°C]

2.2.5. Functions for absorption refrigeration solutions (LiB and NH3)

Thermax provides two groups of property functions for the analyses of vapour-absorption refrigeration systems: (a) water-lithium bromide (H_2O-LiBr) solution and (b) ammonia-water (NH_3-H_2O) solution. Each group has 13 property functions to determine properties of the relevant solution, but the two subgroups use different formulae.

A. The H_2O-LiBr solution (LiB)

To determine the enthalpy (h), refrigerant temperature (T_r), and refrigerant concentration (X) of the H_2O-LiBr solution, these functions use the formulae given by ASHRAE [2] and to determine the entropy (s) and specific volume (v) the functions use the formulae given by Kaita [4] and by Patterson and Perez-Blanco [5], respectively. This group needs two functions that determine the saturation pressure and saturation temperature of the refrigerant, which is water in this case. Although the two properties can be obtained by using the relevant functions in the water group, to make this group self-sufficient it has its own functions that determine these properties from the Antoine equations, which are

Equations (B.15) and (B.16) given in Appendix B. Table 2.11 lists the 13 functions in the Lib-group.

Table 2.11. Functions for water-lithium bromide solution

#	Function	Input [unit]	Output [unit]
1	LiBh_TX	*T* [°C], *X* [%]	*h* [kJ/kg]
2	LiBv_TX	*T* [°C], *X* [%]	*v* [m^3/kg]
3	LiBs_TX	*T* [°C], *X* [%]	*s* [kJ/kg.K]
4	LiBT_trX	*Tr* [°C], *X* [%]	*T* [°C]
5	LiBT_prX	*Pr* [kPa], *X* [%]	*T* [°C]
6	LiBT_hX	*h* [kJ/kg], *X* [%]	*T* [°C]
7	LiBTr_TX	*T* [°C], *X* [%]	*Tr* [°C]
8	LiBPr_TX	*T* [°C], *X* [%]	*Pr* [kPa]
9	LiBX_Ttr	*T* [°C], *Tr* [°C]	*X* [%]
10	LiBX_Tpr	*T* [°C], Pr [kPa]	*X* [%]
11	LiBT_sX	*s* [kJ/kg.K], *X* [%]	*T* [°C]
12	LiBpr_tr	*T* [°C]	P_{sat} [kPa]
13	LiBtr_tr	*P* [kPa]	T_{sat} [°C]

B. The ammonia-water solution (NH3)

To determine the enthalpy of the ammonia-water solution, this group applies the formulae given by Patek and Klomfar [6] and to determine the specific volume it applies that given by Sun [7]. The entropy of NH_3-H_2O solution in the liquid state (s_l) and the vapour state (s_v) are obtained by using the formulae given by El-Shaarawi et al [8]. The relations between refrigerant pressure and temperature of the solution with concentration are taken from Bourseau and Bugarel [9]. Table 2.12 lists the 13 functions in the NH3-group.

Table 2.12. Functions for ammonia-water solution

#	Function	Input [unit]	Output [unit]
1	NH3h_TX	*T* [°C], *X* [%]	*h* [kJ/kg]
2	NH3v_TX	*T* [°C], *X* [%]	*v* [m^3/kg]
3	NH3sl_prX	*Pr* [kPa], *X* [%]	s_l [kJ/kg.K]
4	NH3sv_prX	*Pr* [kPa], *X* [%]	S_v [kJ/kg.K]
5	NH3T_trX	*Tr* [°C], *X* [%]	*T* [°C]
6	NH3T_prX	*Tr* [°C], *X* [%]	*T* [°C]
7	NH3T_hX	*h* [kJ/kg], *X* [%]	*T* [°C]
8	NH3tr_TX	*T* [°C], *X* [%]	*Tr* [°C]
9	NH3pr_TX	*T* [°C], *X* [%]	*Pr* [kPa]
10	NH3X_Ttr	*T* [°C], *Tr* [°C]	*X* [%]
11	NH3X_Tpr	*T* [°C], Pr [kPa]	*X* [%]
12	NH3pr_tr	*T* [°C]	P_{sat} [kPa]
13	NH3tr_pr	*P* [kPa]	T_{sat} [°C]

The NH3-group also needs two functions that determine the saturation pressure and saturation temperature of the refrigerant, which is ammonia. In order to make the group self-sufficient, the group has its own functions that determine these properties instead of using the functions provided by the refrigerants group. Accordingly, the saturation pressure (P_{sat}) of ammonia is obtained from the following equation [7]:

$$P_{sat} = 10^3 \sum_{i=0}^{6} a_i T^i \tag{2.1}$$

Where, T is in ºC, P in kPa and values of the six coefficients a_1 to a_6 can be found in Sun [7]. The saturation temperature (T_{sat}) is obtained from Equation (2.1) by iteration.

2.2.6. Functions for combustion and chemical reactions (Chm)

The analyses of combustion and other chemical reactions involve mass and energy balances of the substances involved as reactants or products that can be solids, liquids, or gases. The gases involved are treated as ideal and, therefore, the group of functions for ideal gases "Gas" can be used here. However, combustion analyses require additional data like the heating value, enthalpy of formation, and Gibbs function of formation. The group provided by Thermax for the analyses of combustion processes and chemical reactions consists of the three general functions shown in Table 2.13.

Table 2.13. Functions for thermodynamic properties of reacting systems

#	Function	Input argument	Output property
1	Chm_f1	Substance; property	M, $\bar{h}_f^0$, $\bar{g}_f^0$, $\bar{s}^0$
2	Chm_f2	Substance; property	M, Q_H, Q_L, AF, Hv, α, β, γ, δ
3	Chm_f3	Substance; property, temperature	$\bar{c}_p$, $\bar{h}$, $\bar{u}$, $\bar{s}^0$

All three functions require as input arguments the substance name and the name of the required property. In addition to those, the third function requires the temperature of the substance involved to be provided. The first function, **Chm_f1**, provides the molar mass (M), molar enthalpy of formation ($\bar{h}_f^0$), molar Gibbs function of formation ($\bar{g}_f^0$), and molar absolute entropy ($\bar{s}^0$) for the 29 reacting substances and reaction products that are listed in Table A.3 of Appendix A. Case 8 in Table 2.1 illustrates the use of this function. The second function, **Chm_f2**, provides additional data needed for combustion analyses involving the 20 fuels and reacting substances listed in Table A.5. These include values of the molar mass (M), gravimetric higher and lower heating values (Q_H and Q_L), stoichiometric air-fuel ratio (AFR_s) and heat of vaporisation (H_v). This function also provides the carbon, hydrogen, oxygen, and nitrogen contents of the substance (α, β, γ, δ) based on the general chemical representation $C_\alpha H_\beta O_\gamma N_\delta$. The third function, **Chm_f3**, determines four properties of ideal gases needed for combustion analyses on a unit-mole basis. Case 9 in Table 2.1 shows the required input and the output of this function.

2.2.7. Functions for air at standard atmospheric pressure (Air)

Fluid-dynamics and heat-transfer analyses require the thermo-physical properties of air at standard atmospheric pressure. This group provides these properties based on the tabulated data given by Cengel and Ghajar [10]. The functions use a linear interpolation function to determine the air density (ρ), specific heat (c_p), thermal conductivity (k), thermal diffusivity (α), dynamic viscosity (μ), kinematic viscosity (ν) and Prandtl number (Pr) at temperatures in the range -150°C to 2000°C. Table 2.14 shows the names of the seven functions in this group with their corresponding output properties. Note that this group also provides a function for determining the specific-heat for air at constant pressure (c_p) which can be used instead of the function provided by the ideal-gas group.

Table 2.14. Properties of air at 1 atm pressure given the temperature in °C

#	Function	Output	Output unit
1	Airrho_T	Density (ρ)	kg/m^3
2	Aircp_T	Specific heat (c_p)	J/Kg.°C
3	Airk_T	Thermal conductivity (k)	W/m.°C
4	Airdf_T	Thermal diffusivity (α)	m^2/s
5	Airdv_T	Dynamic viscosity (μ)	kg/m·s
6	Airkv_T	Kinematic viscosity (ν)	m^2/s
7	AirPr_T	Prandtl number (Pr)	-

2.3. Using Thermax property functions in Excel formulae

Before Thermax functions can be used in Excel's formulae, it has to saved it in the computer as an add-in. To do that, open the **Thermax** file and then save it in your computer as an "**Excel Add-in**". Excel comes with a number of add-ins that extend the application's functionality such as the Solver add-in. All add-ins are saved in one folder and active add-ins are automatically loaded when Excel starts up. In order to activate Thermax after saving it, open a new Excel sheet and then do the following:

1. Go to **File**, click **Options** and then select **Add-Ins**.
2. From the **Manage** ribbon at the bottom of the menu select **Excel Add-ins** and then press **Go**. The pull-down menu shown on Figure 2.2 will appear to you.
3. To add **Thermax** to the add-ins menu, tick (√) the corresponding box. If for any reason the add-in does not appear in the list, then click on **Browse** and search for it in the destination folder and select it.

The add-in functions can now be used in Excel's formulae just like its built-in functions. The following sections illustrate two methods for using these functions in Excel.

2.3.1. Accessing Thermax functions via the Function Wizard

This method suits the first-time users. To illustrate the method, let us start a formula by entering the equal sign (=) in any cell (say, cell B2). If you now press the *fx* button in the formula ribbon, the **Function Wizard** shown on Figure 2.3 will come up. The Function

Wizard firstly lists the various categories of built-in functions provided by Excel, e.g., financial, mathematical, statistical, etc. Scroll down the list of function categories and select the **User-defined** functions. Then, all the functions provided by Thermax will be listed alphabetically as shown on Figure 2.4.

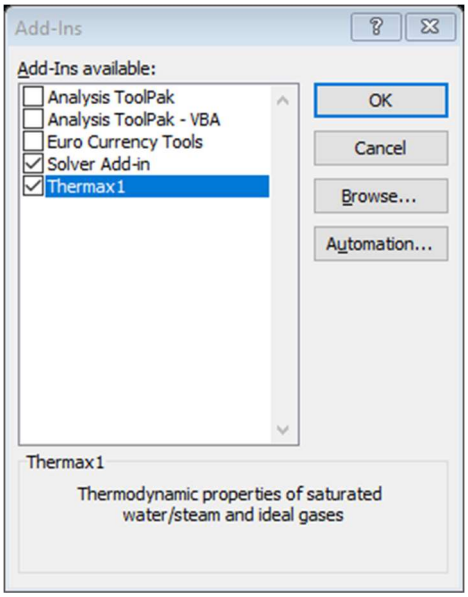

Figure 2.2. Adding Thermax to the menu of Excel add-ins

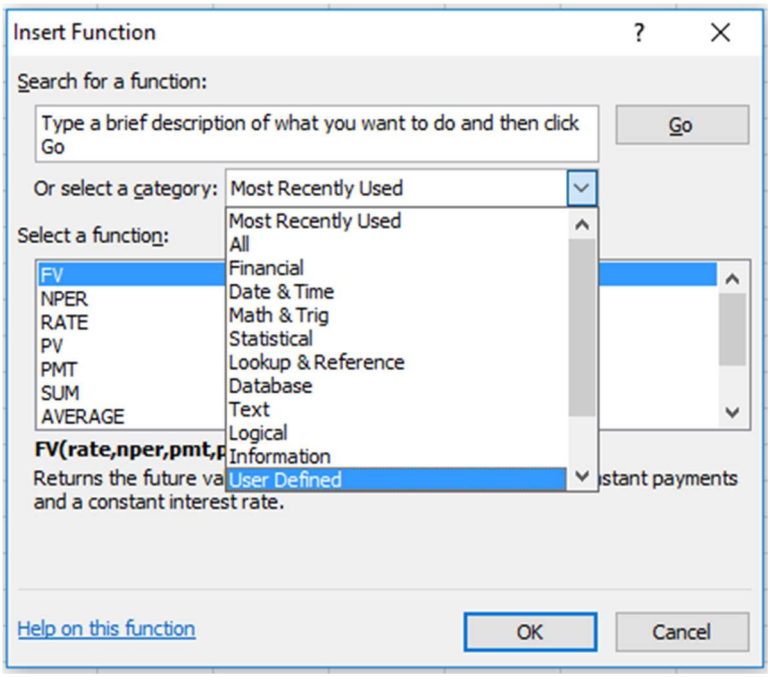

Figure 2.3. Finding the add-in user-defined functions in the Function Wizard

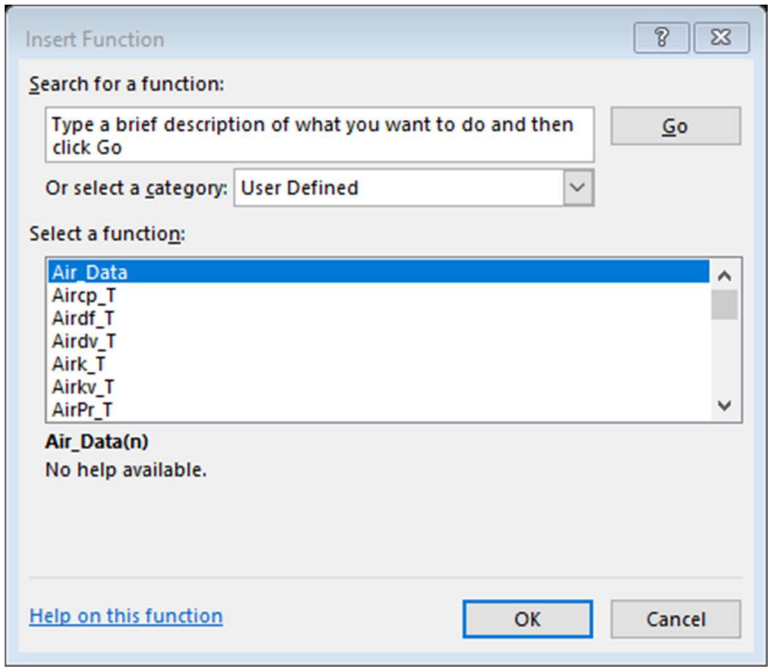

Figure 2.4. Thermax functions listed alphabetically in the User Defined category

The first function in the list of Figure 2.4, **Air_Data**, is an auxiliary function that stores the data for the seven thermophysical properties of air at standard atmospheric pressure. This function is called by other functions in the Air-group in order to determine the values of their respective properties at the required temperature. To start using the add-in functions, let us use it to determine the thermal conductivity (k) of air at 25°C. To do that, go down the list and select the function named **Airk_T**. Upon pressing the OK button, the **Function Arguments** box shown on Figure 2.5 will appear to you.

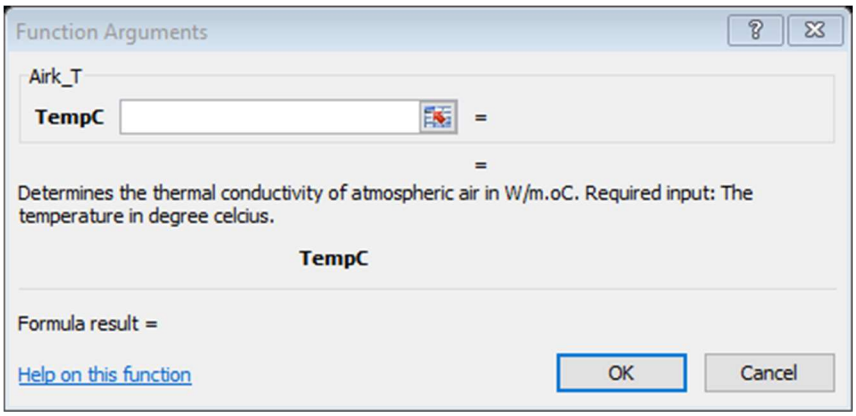

Figure 2.5. The Function Arguments box for the "Airk_T" function

Figure 2.5 shows that this function has one input parameter, which is the temperature in °C "TempC", and gives a brief description of its intended use. Fill the form by entering

the given value of the temperature, 25, as shown on Figure 2.6. Note that the formula ribbon now shows the formula in cell B2, which is "=Airk_T(25)", and the Function Arguments form shows the calculated value of k, which is 0.02551 W/m.^{o}C. When you press the "**OK**" button, this value will appear in the cell B2. Compare this value with the tabulated data for atmospheric air.

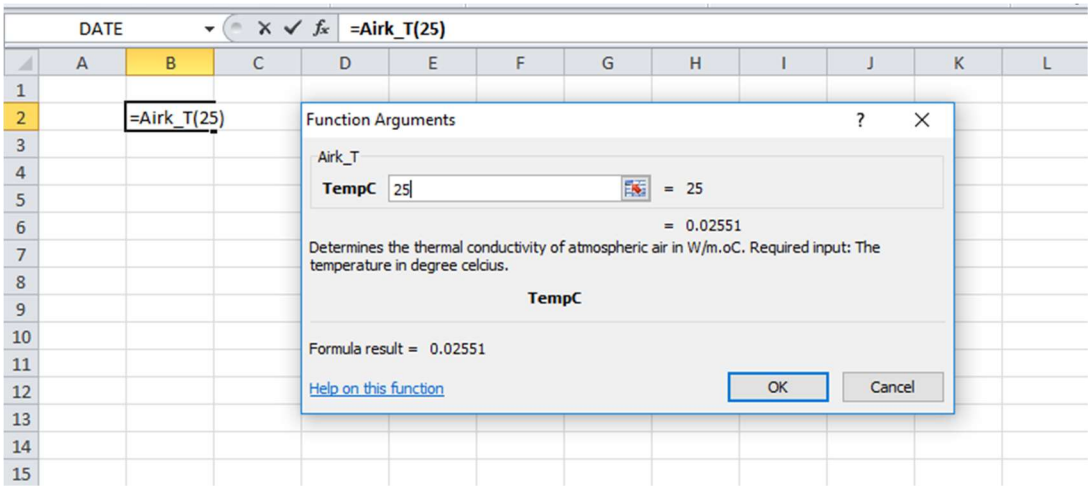

Figure 2.6. Using the function "Airk_T" to determine the thermal conductivity of atmospheric air at 25^{o}C

2.3.2. Direct use of Thermax functions in Excel formulae

After some practice with the procedure described above it becomes unnecessary to follow that lengthy procedure. Instead, one can simply type in the formula that contains the property function in the required Excel cell by first identifying the group, e.g., Gas, Wat, etc., and then the functions letter(s), e.g., h for enthalpy, s for entropy, etc. The required function and the its input parameters can then be determined easily with the help of Excel's user-interface. For illustration, suppose that we want to determine the temperature of carbon-dioxide (CO_2) at which the value of its enthalpy (h) equals 750 kJ/kg. In this case, we need to use the function in the "**Gas**" group that determines the temperature for a given enthalpy value of the gas. Therefore, we start an Excel formula by typing the equal sign "=" in any cell and then type the prefix "Gas". As shown on Figure 2.7, as soon as we type the prefix "Gas" after the equal sign, the user-interface will display all Thermax functions in the ideal-gases group for us to select from. Since the property we want to find is the temperature, which the Gas-group functions require in absolute degree, we continue the name of the function by adding the letters "TK" immediately after the three-letter prefix "Gas" followed by an underscore. As shown on Figure 2.8, the user-interface will then list only the five functions in Table 2.2 that determine the gas temperature given h, P_r, s^0, u, or v_r. To find the temperature from a known value of enthalpy, we have to select the "**GasTK_h**" function as shown on Figure 2.9. Excel will then ask you to enter the required input parameters. This function requires the name of the gas, which is "CO2", and the value of enthalpy, which is 750 kJ/kg, as

shown on Figure 2.10. Press the "**Enter**" key, and the answer shown on Figure 2.11, which is 817.5544K, will be displayed.

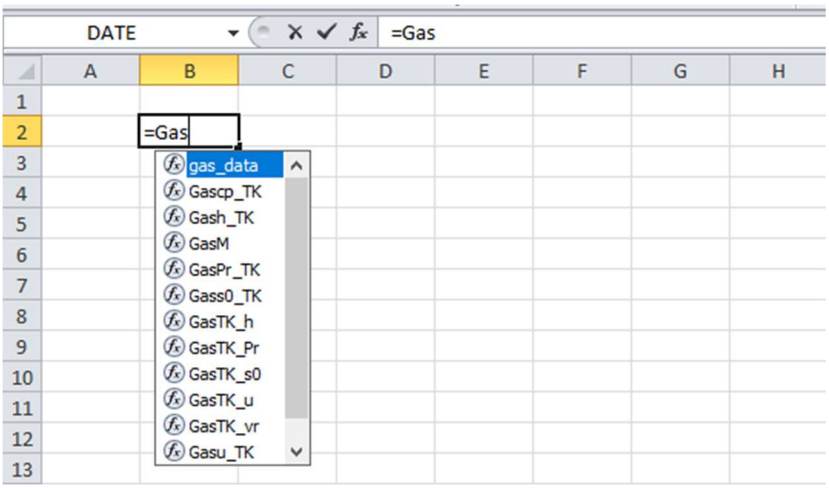

Figure 2.7. Excel UI showing all the functions in the Gas-group

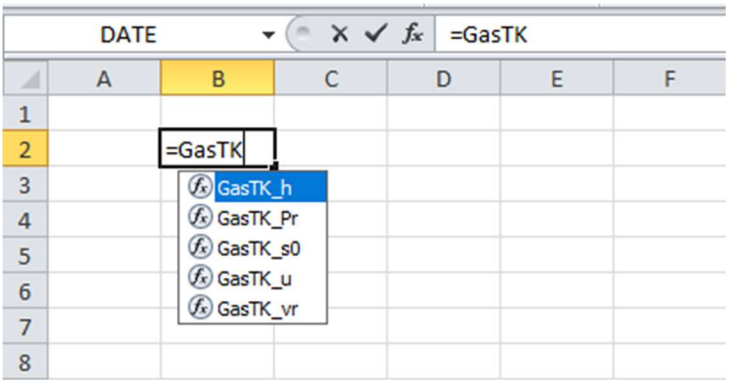

Figure 2.8. The UI showing only the five functions that determine the temperature of an ideal gas from known values of h, p_r, s^0, u, or v_r

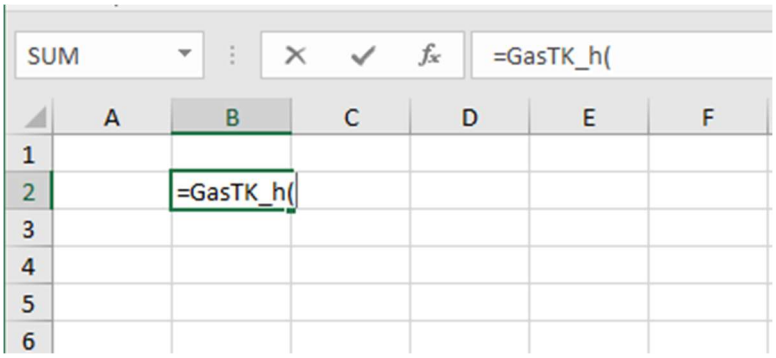

Figure 2.9. Selecting the required function from the five functions that determine the gas temperature

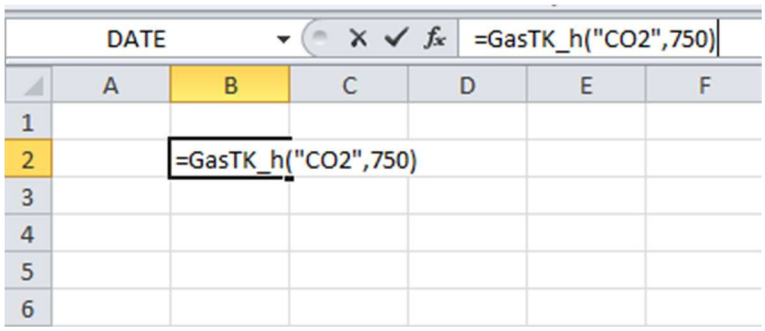

Figure 2.10. Entering the required input for the GasTK_h function

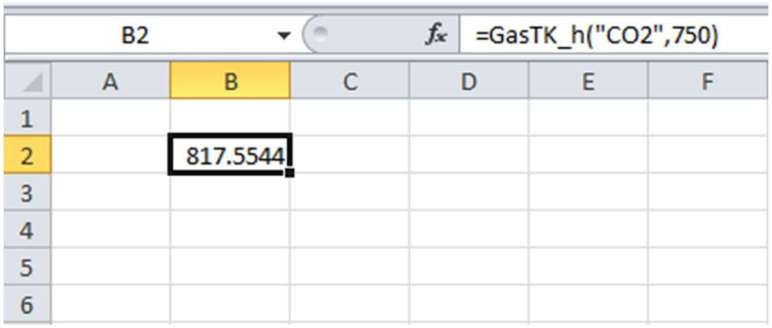

Figure 2.11. The gas temperature as determined by the GasTK_h function

You can always call the **Function Wizard** if you are not certain about the required input parameters by pressing the *fx* button in the formula ribbon and the form shown on Figure 2.12 will appear to you. The form shows the two required input parameters for you to provide. Pressing the "Enter" key or the "OK" button after entering the required data, the function will calculate the corresponding temperature which is 817.5544K as shown on Figure 2.11. This value can be checked by comparison with the tabulated data.

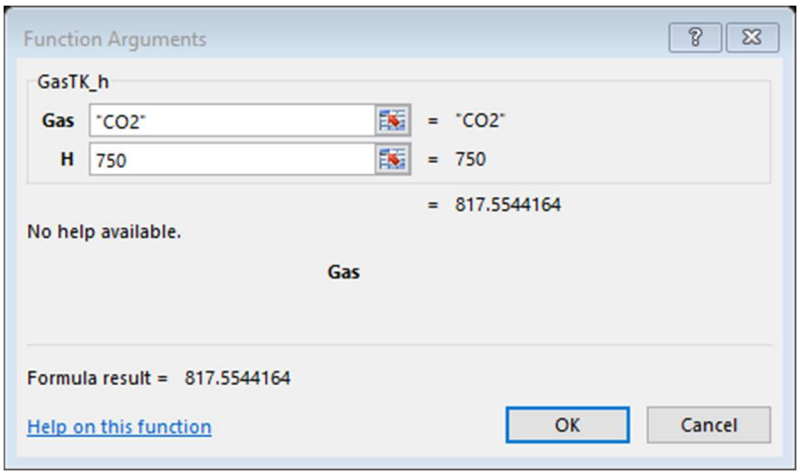

Figure 2.12. The Function Wizard showing the required input for the GasTK_h function

2.4. Closure

This chapter introduces the Thermax add-in and its seven groups of property functions that determine the thermo-physical properties of various types of working fluids and shows how the functions can be used in Excel formulae. Thermax property functions are named in a way that helps the user to find the appropriate function via Excel's user-interface and function wizard. The functions for ideal-gases, superheated steam, atmospheric humidified air, the two vapour-absorption fluids, and combustion gases use verified formulae for these substances [1,3-9]. The functions for saturated water and saturated refrigerants determine the properties by interpolation of the verified data provided by ASHRAE [2]. The functions for atmospheric air at standard pressure also use interpolation of published data [10]. The group of functions developed for superheated refrigerants use an extended compressibility-factor concept. The verification of these functions is discussed in Appendix C and in [11].

References

[1] Y. A. Cengel and M. A. Boles. *Thermodynamics an Engineering Approach*, McGraw-Hill, 7th Edition, 2007.

[2] American Society of Heating, Refrigeration and Air-Conditioning Engineers, (ASHRAE), Handbook of fundamentals, Atlanta, 2017.

[3] T.F. Irvine Jr. and P.E. Liley. Steam and gas tables with computer equations. Orlando, (FL): Academic Press, 1984.

[4] Y. Kaita, Thermodynamic properties of lithium bromide-water solutions at high temperatures, Int. J. Refrig., vol. 24, no. 5, pp. 374–390, 2001, doi: 10.1016/S0140-7007(00)00039-6.

[5] M.R. Patterson and H. Perez-Blanco, Numerical fits of the properties of lithium-bromide water solutions, *ASHRAE Trans*. Volume 94, Issue 2, pp. 2059-2077, 1988.

[6] J. Patek and J. Klomfar, Simple functions for fast calculations of selected thermodynamic properties of the ammonia-water system. *International Journal of Refrigeration,* Vol. 18, No. 4, 1995, pp. 228 -234.

[7] D-W Sun. Comparison of the performances of NH_3-H_2O, NH_3-$LiNO_3$ and NH_3-NaSCN absorption refrigeration systems. *Energy Convers. Mgmt*, Vol. 39, No. 5/6, 1998, pp. 357-368.

[8] M.A.I. El-Shaarawi, S.A.M. Said, M.U. Siddiqui, New correlation equations for ammonia-water vapor liquid equilibrium (VLE) thermodynamic properties, *ASHRAE Transactions*, 2013, pp. 293-298.

[9] P. Bourseau and R. Bugarel, Absorption-diffusion machines: comparison of the performances of NH_3-H_2O and NH_3-NaSCN. *International Journal of Refrigeration*, Vol. 9, Issue 4, pp. 206-214.

[10] Y. A. Cengel and A. J. Ghajar. *Heat and Mass Transfer: Fundamentals and Applications*. McGraw Hill, 2011.

[11] M.M. El-Awad, M.S. Al Nabhani, K.S. Al Hinai, A. Younis, Development and Validation of an Excel Add-In for determining the Properties of Various Refrigerants, Proceedings of the 1st National Conference on Applied Science, Engineering & Technology 2019, CASET – 2K19, 11th June 2019, Ibri, Oman

Exercises

1. Complete the following table by specifying the usage of the given Thermax function according to its name:

#	Function	Output property	Input /properties
1	Gascp_TK("CO2",300)		
2	WatTsat_P(200)		
3	WatT_Ph(200, 3487.7)		
4	RefPsat_T("R134a",0.0)		
5	PsyTs_P(100)		
6	Nh3Pr_TX(200,80)		
7	Airdv_T(500)		
8	Chm_f2("HDL","QL")		

2. Name the appropriate Thermax functions that determine the following properties:

#	Task	Thermax function
1	The enthalpy of saturated liquid water at 25°C	
2	The internal energy of oxygen at 300K	
3	The entropy of superheated steam at 10 kPa, 200°C	
4	The absolute temperature at which the relative pressure of air is equal to 15	
5	The saturation pressure for R-134a at -15°C	
6	The dry-bulb temperature of humid air at P = 101 kPa, ϕ = 50%, ω = 0.01	
7	The enthalpy of ammonia-water solution at 30°C, X= 50%	
8	The higher heating value for gasoline	

3. Using Thermax functions, determine the values of the following fluid properties:

#	Fluid	Given properties	Required property	Value
1	Saturated water	100 kPa, x = 0.5	Enthalpy (h)	
2	Steam	100°C, x = 1.0	Entropy (s)	
3	Air	700K	Relative volume (v_r)	
4	CO_2	450K	Specific heat (c_p)	
5	Hydrogen	h = 2000 *kJ/kg*	Temperature (T)	
6	R134a	1000 kPa, 50°C	Enthalpy (h)	
7	R134a	50°C, x = 0.5	Entropy (s)	

Chapter 3

Analyses of gas power cycles

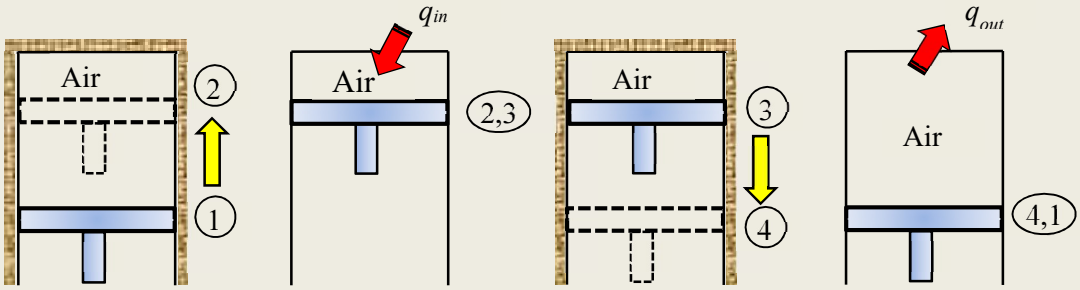

1-2: Isentropic compression

2-3: Heat addition at constant *v*

3-4: Isentropic expansion

4-1: Heat rejection at constant *v*

This chapter illustrates the use of Thermax functions for analysing two basic gas power cycles, which are the Brayton cycle for gas turbine and the Otto cycle for spark-ignition internal-combustion engines. For the Brayton cycle both the simple and the regenerative cycles are analysed and for the Otto cycle both energy and exergy analyses are presented. Values of the key parameters of the cycles determined by using Thermax functions are verified against the relevant values given in standard thermodynamics textbooks. The results obtained for the simple Brayton cycle and the Otto cycle are also compared with those obtained by using another property add-in which is the "Ideal-Gas" add-in [1].

3.1. The ideal Brayton cycle

The Brayton cycle is the ideal cycle for gas-turbines. Unlike the real gas-turbine cycle, it is a closed cycle with a constant mass of the working fluid going through the system's components as shown on Figure 3.1. The cycle consists of four processes; compression in an ideal gas compressor, heat-addition from a high-temperature source, expansion in an ideal gas turbine, and heat-rejection to a low-temperature sink. Figure 3.2 shows the Brayton cycle on a *T-s* diagram.

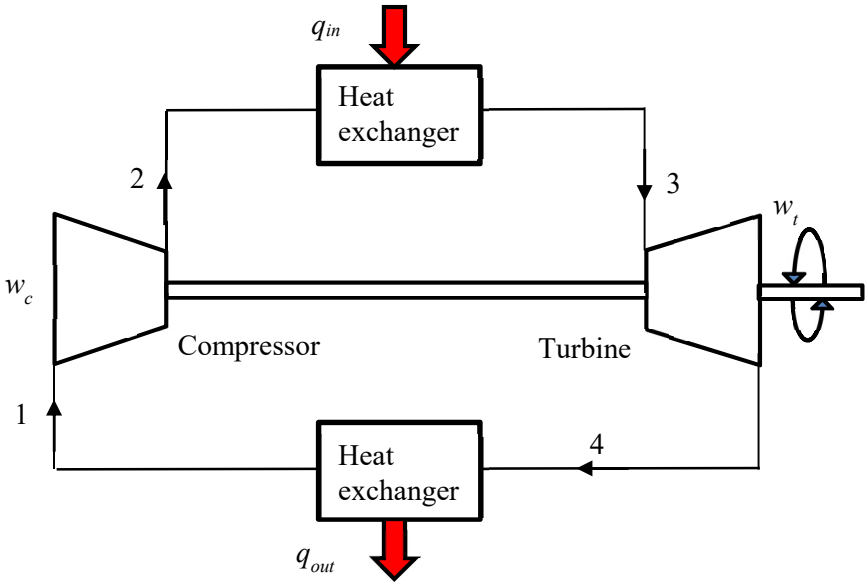

Figure 3.1. Schematic diagram of the closed-cycle gas-turbine

In the following analysis, the working fluid in the closed cycle is assumed to be air, but it can be any other suitable gas. Given the compressor's inlet temperature, T_1, and the turbine's inlet temperature, T_3, the discharge temperature from the compressor (T_2) and that from the turbine (T_4) are determined by using the variable specific-heat method of analysis from the corresponding relative pressures P_{r2} and P_{r4} given by:

$$P_{r2} = P_{r1} \times \left(P_2 / P_1\right) \tag{3.1}$$

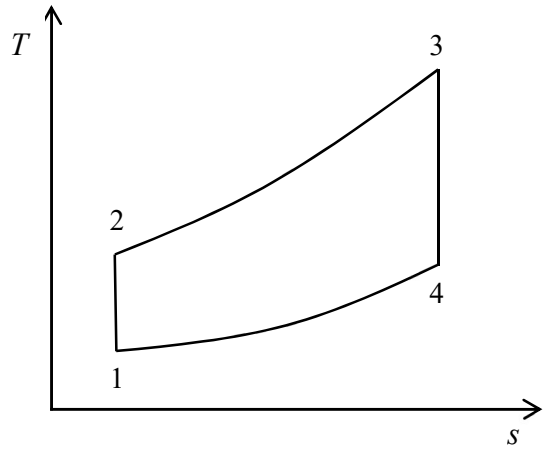

Figure 3.2. *T-s* diagram for the ideal Brayton cycle

$$P_{r4} = P_{r3} \times \frac{P_4}{P_3} \tag{3.2}$$

Where P_{r1} and P_{r2} are the relative pressures at states 1 and 2, respectively. For the ideal cycle without pressure losses, $P_3 = P_2$ and $P_4 = P_1$.

The compressor work (w_c) and turbine work (w_t), per unit mass flow rate of the air, are determined from:

$$w_c = (h_2 - h_1) \tag{3.3}$$

$$w_t = (h_3 - h_4) \tag{3.4}$$

Where h_1, h_2, h_3, and h_4 are values of the enthalpy at states, 1, 2, 3, and 4, respectively. The amount of heat addition (q_{in}) per unit mass flow of the air is given by:

$$q_{in} = (h_3 - h_2) \tag{3.5}$$

Therefore, the net work (w_{net}), back-work ratio (BWR), and thermal efficiency (η) of the cycle are determined from:

$$w_{net} = w_t - w_c \tag{3.6}$$

$$BWR = w_c / w_t \tag{3.7}$$

$$\eta = w_{net} / q_{in} \tag{3.8}$$

The following example illustrates the procedure for using Thermax property functions for analysing the cycle . The example is based on Example 9.5 in Cengel and Boles [2].

Example 3.1. Analysis of the simple ideal Brayton cycle
A gas-turbine power plant that operates on an ideal Brayton cycle with air as the working fluid has a pressure ratio of 8. The gas temperature at the compressor inlet is 300 K and at the turbine inlet is 1300 K. Determine (a) the net work per unit mass flow rate of the working fluid, (b) the back work ratio, and (c) the thermal efficiency.

Solution
Figure 3.3 shows the Excel sheet developed for this example using Thermax functions. The figure shows the general layout adopted in this book for developing the Excel sheets according to which the sheet is divided from left to right into three main parts: (i) Input data, (ii) Intermediate calculations, and (iii) Final results. In the present case, the input data include the two values of the temperature at states 1 and 3 (T_1 and T_3) and the pressure ratio (rp). The middle part of the sheet, which is reserved for the calculation of intermediate results, shows the calculated values of the two unknown temperatures T_2 and T_4 and the enthalpy values at the four states in the cycle. The final results are the compressor work (w_c), the turbine work (w_t), the heat input (Q_in), the back work ratio (BWR), and thermal efficiency (η) as shown on the right side of the sheet.

η | fx | =(w_t-w_c)/q_in

	A	B	C	D	E	F	G	H	I	J	K	L
1	*Input Data*				*Intermediate calculations*					*Final results*		
2	T_1	300	K	Pr_2	11.06829198		h_1	299.8455		w_c	243.6869	
3												
4	rp	8		T_2	538.1465495		h_2	543.5324		w_t	606.014	
5												
6	T_3	1300	K	Pr_4	41.69167583		h_3	1396.057		q_in	852.5248	
7												
8				T_4	769.2393498		h_4	790.0433		BWR	0.402114	
9												
10										η	0.425005	
11												

Figure 3.3. The Excel sheet developed for Example 3.1 using Thermax functions

Figure 3.4 shows the formula entered in each cell of the calculations part using Thermax functions. Note that "cell-labelling" has been used in the formulae. Only three Thermax functions from the Gas-group have been used in the Excel model with air as the gas which are: **GasPr_TK**, **GasTK_Pr**, and **Gash_TK**. For the purpose of comparison, a similar Excel sheet was developed by using the IdealGas add-in developed at the University of Alabama [1]. Figure 3.5 shows this Excel sheet and Figure 3.6 reveals the function used in it. Note that the IdealGas functions have the advantage of allowing two systems of

units to be used, but they can only be used for air. By comparison, Thermax functions only use the "SI" system, but they can be used for different gases.

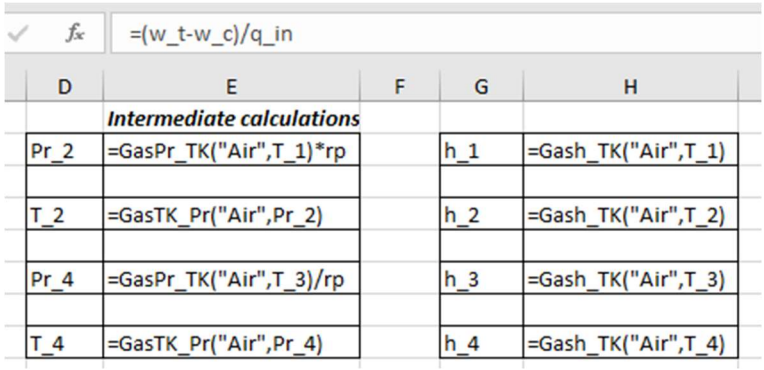

	D	E	F	G	H
		Intermediate calculations			
	Pr_2	=GasPr_TK("Air",T_1)*rp		h_1	=Gash_TK("Air",T_1)
	T_2	=GasTK_Pr("Air",Pr_2)		h_2	=Gash_TK("Air",T_2)
	Pr_4	=GasPr_TK("Air",T_3)/rp		h_3	=Gash_TK("Air",T_3)
	T_4	=GasTK_Pr("Air",Pr_4)		h_4	=Gash_TK("Air",T_4)

Figure 3.4. Thermax functions used in the Excel sheet of Example 3.1

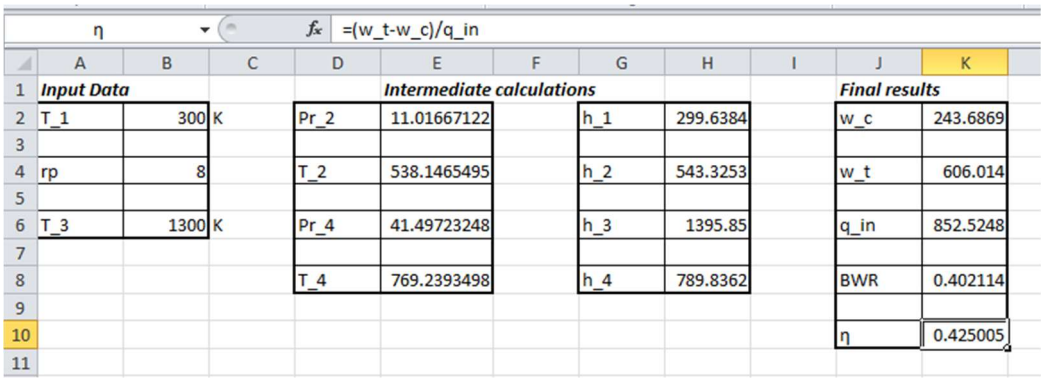

	A	B	C	D	E	F	G	H	I	J	K
1	*Input Data*				*Intermediate calculations*					*Final results*	
2	T_1	300	K	Pr_2	11.01667122		h_1	299.6384		w_c	243.6869
3											
4	rp	8		T_2	538.1465495		h_2	543.3253		w_t	606.014
5											
6	T_3	1300	K	Pr_4	41.49723248		h_3	1395.85		q_in	852.5248
7											
8				T_4	769.2393498		h_4	789.8362		BWR	0.402114
9											
10										η	0.425005
11											

Figure 3.5. Excel sheet for Example 3.1 using the IdealGas add-in

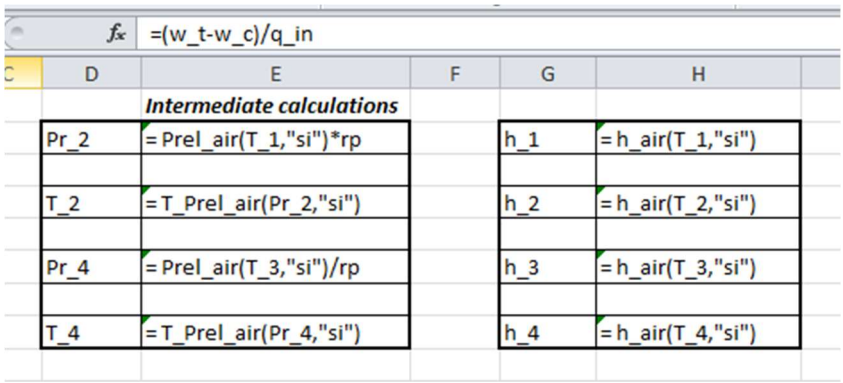

	D	E	F	G	H
		Intermediate calculations			
	Pr_2	= Prel_air(T_1,"si")*rp		h_1	= h_air(T_1,"si")
	T_2	= T_Prel_air(Pr_2,"si")		h_2	= h_air(T_2,"si")
	Pr_4	= Prel_air(T_3,"si")/rp		h_3	= h_air(T_3,"si")
	T_4	= T_Prel_air(Pr_4,"si")		h_4	= h_air(T_4,"si")

Figure 3.6. IdealGas functions used in the Excel sheet of Example 3.1

Table 3.1 shows the values determined by the two property add-ins for the key cycle parameters and their corresponding values given by Cengel and Boles [2]. The figures of

the table show only minor differences between the values obtained by the two property add-ins and those given by Cengel and Boles [2].

Table 3.1. Verification of the two add-ins' results with those of Cengel and Boles [2]

Parameter	Cengel and Boles [2]	Thermax	IdealGas
w_c	244.16	243.69	243.69
w_t	606.60	606.01	606.01
q_{in}	851.62	852.52	852.52
BWR	0.403	0.402	0.402
η	0.426	0.425	0.425

3.2. The regenerative Brayton Cycle

Gas turbines can sustain higher combustion temperatures than those typically met in internal-combustion engines, but the higher combustion temperatures lead to higher exhaust temperatures that can reach more than 500°C. By adding a regenerator to the simple gas-turbine system, as shown on Figure 3.7, the energy in the hot exhaust gases is utilised to preheat the compressed air before it goes to the combustion chamber. This arrangement, called *regeneration*, reduces the fuel combustion and improves the plant's thermal efficiency, but requires the addition of a heat-exchanger plant increases the cost of the plant. The economic benefit due to regeneration depends not only on the cost of the heat-exchanger, but also on the system's pressure ratio. While the cost of the heat-exchanger depends on its size and effectiveness, there is a certain value for the pressure ratio that maximises the system's thermal efficiency and minimises the fuel cost.

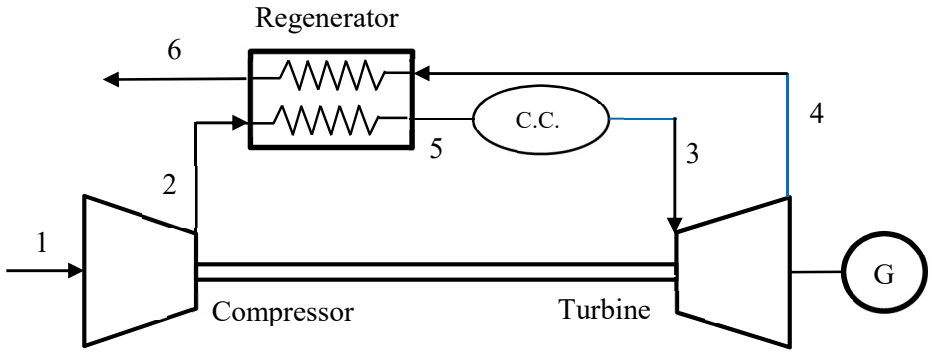

Figure 3.7. Schematic diagram of the regenerative gas-turbine

Figure 3.8 shows the *T-s* diagram for the regenerative Brayton cycle assuming zero pressure losses in the combustion chamber and heat-exchanger. Due to friction losses in both compressor and turbine, the actual exit temperatures from these devices (i.e., T_2 and T_4) are different from the ideal values obtainable by the isentropic compression and expansion processes (T_{2s} and T_{4s}).

Chapter 4

Analyses of vapour and combined power cycles

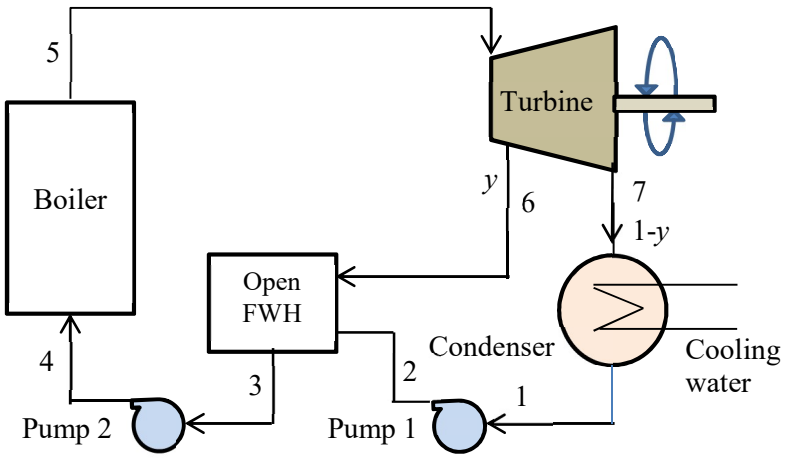

This chapter illustrates the use Excel with Thermax property functions for analysing various vapour power cycles including the simple Rankine cycle, Rankine cycle with superheat and reheat, and the regenerative Rankine cycle with one and two feed-water heaters. The results obtained for the key parameters of these cycles are verified against the relevant values given by standard textbooks [1,2]. The chapter also illustrates the use of the functions for analysing the combined Brayton-Rankine cycle and the simple organic Rankine cycle using three different working fluids.

4.1. The ideal simple Rankine cycle

The Rankine cycle is the ideal cycle for steam-turbine power plants. The basic plant shown on Figure 4.1 consists of four components: a boiler, a turbine, a condenser, and a pump. The working fluid, which is water, is pumped at a low temperature to the boiler where it is heated to become saturated steam. The high-pressure steam is then taken to the turbine where it expands to produce work. The steam is completely condensed in the condenser before being pumped back to the boiler. Cooling water removes the heat rejected in the condenser. Figure 4.2 shows the *T-s* diagram for the ideal cycle.

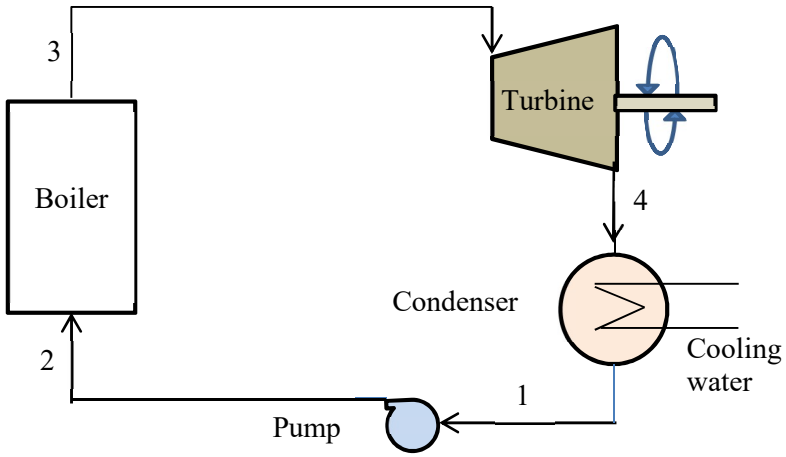

Figure 4.1. Schematic diagram of a simple steam-turbine power plant

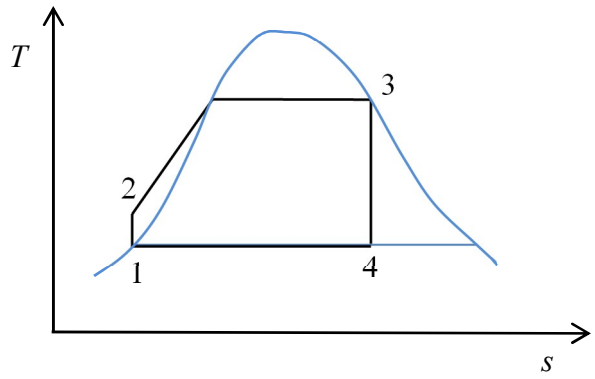

Figure 4.2. *T-s* diagram for the ideal simple Rankine cycle

The pump-work (w_p), turbine-work (w_t), rate of heat addition in the boiler (q_{in}), and rate of heat rejection in the condenser (q_{out}) per unit mass flow of the working fluid are given by:

$$w_p = (h_2 - h_1) \tag{4.1}$$

$$w_t = (h_3 - h_4) \tag{4.2}$$

$$q_{in} = (h_3 - h_2) \tag{4.3}$$

$$q_{out} = (h_4 - h_1) \tag{4.4}$$

Where h_1, h_2, h_3, and h_4 are enthalpy values of the working fluid at the four states indicated on Figures 4.1 and 4.2. The two enthalpy values h_1 and h_3 can be obtained directly from the given pressures by using the relevant Thermax functions, but h_2 and h_4 have to be calculated from:

$$h_2 = h_1 + v_1(P_2 - P_1) \tag{4.5}$$

$$h_4 = h_1 + x_4 h_{fg,P1} \tag{4.6}$$

Where v_1 is the specific volume of saturated liquid water at the condenser pressure, x_4 is the quality at point 4, and $h_{fg,P1}$ is the enthalpy of vaporisation (the difference between the specific enthalpy of saturated steam and saturated liquid water) at the condenser pressure P_1. The quality x_4 is determined from the following equation:

$$x_4 = \frac{s_4 - s_1}{s_{fg,P1}} \tag{4.7}$$

Where s_1 and s_4 are the specific entropy values at points 1 and 4, respectively, and $s_{fg,P1}$ is the difference between the specific entropy of saturated steam and saturated liquid water at the condenser pressure P_1. For the ideal isentropic process, $s_4 = s_3 = s_{g,P2}$.

Once enthalpy values at the states 1 to 4 are determined, and the values of w_p, w_t, q_{in}, and q_{out} are calculated, the different cycle parameters can be calculated as follows:

(a) The thermal efficiency (η):

$$\eta = (w_t - w_p) / q_{in} \tag{4.8}$$

(b) The back work ratio (BWR):

$$BWR = w_p / w_t \tag{4.9}$$

(c) The mass flow rate of the steam (kg/h):

$$\dot{m} = \frac{\dot{W} \times 1000 \times 3600}{\left(w_t - w_p\right)} \tag{4.10}$$

Where $\dot{W}$ is the net power of the plant in MW.

(d) The rate of heat transfer in the boiler, ($\dot{Q}_{boiler}$), into the working, in MW:

$$\dot{Q}_{boiler} = \dot{m} q_{in} / 3600 \tag{4.11}$$

(e) The rate of heat transfer from the condenser ($\dot{Q}_{condenser}$), in MW:

$$\dot{Q}_{condenser} = \dot{m} q_{out} / 3600 \tag{4.12}$$

(f) The mass flow rate of the cooling water in kg/h:

$$\dot{m}_{cw} = \frac{\dot{Q}_{out} \times 1000 \times 3600}{\left(h_{cw,o} - h_{cw,i}\right)} \tag{4.13}$$

Where $h_{cw,i}$ and $h_{cw,o}$ are the enthalpy values of the cooling water entering and exiting the condenser, which are approximated with those of saturated water at the relevant temperatures. The following example, which is based on Example 8.1 in Moran and Shapiro [1], shows how the cycle can be analysed with Thermax property functions.

Example 4.1. Analysis of the simple and ideal Rankine cycle

A steam-turbine power plant that operates on the ideal Rankine cycle has a net power output of 100 MW. Saturated steam enters the turbine at 8.0 MPa and saturated water exits the condenser at 8 kPa. Determine (a) the thermal efficiency of the cycle, (b) the back work ratio, (c) the mass flow rate of the steam, in kg/h, (d) the rate of heat transfer, Q_{in}, into the working fluid as it passes through the boiler, in MW, (e) the rate of heat transfer, Q_{out}, from the condensing steam as it passes through the condenser, in MW, (f) the mass flow rate of the condenser cooling water, in kg/h, if cooling water enters the condenser at 15ºC and exits at 35ºC. Also, study the effect of increasing the condenser pressure from 8 to 20 kPa on the thermal efficiency, mass-flow rate of the steam, and mass-flow rate of the cooling water.

Solution

The Excel sheet developed for this example is shown on Figure 4.3. The left side of the sheet stores the given data which include the condenser pressure (P_1), the boiler pressure (P_2), the power of the cycle (Power), the temperature of the cooling water entering the condenser (T_cwi), and the temperature of the cooling water leaving the condenser (T_cwo). The central part of the sheet performs the intermediate calculations that determine the values of enthalpy at the four states in the cycle. Table 4.1 shows the formulae used in these calculations with the various property functions provided by Thermax. For example, the enthalpy at point 1 (h_1), which equals the enthalpy of saturated liquid water at the condenser pressure, is obtained by using the function **Wath_Px** with the two input parameters being the condenser pressure and the quality x =0.

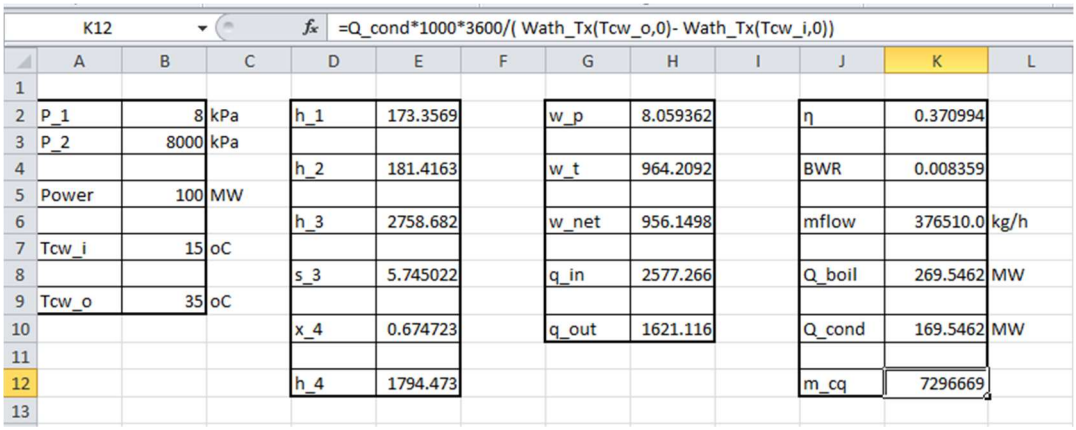

Figure 4.3. The Excel sheet developed for Example 4.1

Table 4.1. Excel formulae with Thermax functions in the sheet of Example 4.1

Cell	Parameter	Excel formula
E2	h_1	=Wath_Px(P_1,0.0)
E4	h_2	=h_1+Watv_Px(P_1,0.0)*(P_2-P_1)
E6	h_3	=Wath_Px(P_2,1.0)
E8	s_3	=Wats_Px(P_2,1.0)
E10	x_4	=(s_3-Wats_Px(P_1,0.0))/(Wats_Px(P_1,1.0) - Wats_Px(P_1,0.0))
E12	h_4	=h_1+x_4*(Wath_Px(P_1,1.0) - Wath_Px(P_1,0.0))

The cells H2 to H10 calculate the values of the pump-work (w_p), the turbine-work (w_t), the net work (w_net = w_t – w_p), the rate of heat addition in the boiler (q_in), and rate of heat rejection in the condenser (q_out). The final results given in the right-side of the sheet include the thermal efficiency (η), the back-work ratio (BWR), the rate of heat addition in the boiler (Q_boil), the rate of heat rejection in the condenser (Q_cond), and the mass flow rate of the cooling water (m_cw). The formula bar in Figure 4.3 reveals the formula in the cell K12 that calculates the mass flow rate of the cooling water using Equation (4.13). As the figure shows, the thermal efficiency is 37.1% and x_4 is 0.675.

Table 4.2 compares the values obtained by Thermax functions and those given by Moran and Shapiro [1] for the cycle parameters in the question. The figures show close agreements between the two results.

Table 4.2. Verification of Thermax results for Example 4.1

	Parameter	Moran and Shapiro [1]	Thermax	Deviation (%)
(a)	η	0.371	0.3709	-0.189
(b)	BWR	0.0084	0.0084	0
(c)	$\dot{m}$ (kg/h)	3.77×10^5	3.77×10^5	0.265
(d)	Q_{boiler} (MW)	269.77	269.546	-0.083
(e)	$Q_{condenser}$ (MW)	169.75	169.546	-0.120
(f)	$\dot{m}_{cw}$ (kg/h)	7.3×10^6	7.3×10^6	0

The Excel sheet was used to analyse the effect of increasing condenser pressure on the cycle's efficiency, mass flow rate of the steam and mass flow rate of the cooling water. The resulting percentage changes of the three parameters are shown on Figure 4.4. The figure shows that the thermal efficiency decreases by nearly 6%, while the mass flow rates of both the steam and the cooling water increase by more than 10%.

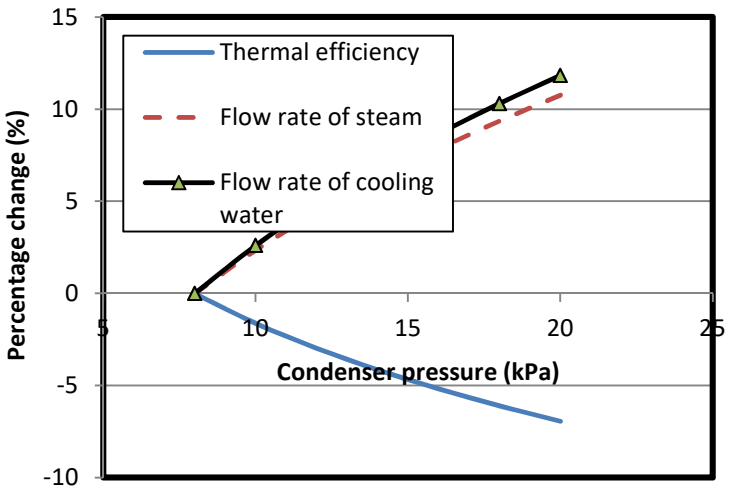

Figure 4.4. Effect of increasing the condenser pressure on the cycle's efficiency, mass flow rate of the steam, and mass flow rate of the cooling water

4.2. The Rankine cycle with superheat and reheat

The thermal efficiency of the simple Rankine cycle can be improved by increasing the boiler pressure and/or reducing the condenser pressure. However, both of these changes increase the wetness fraction of the steam in the last stages of the turbine and may cause erosion of the turbine blades in these stages. This problem can be solved by superheating

Chapter 5

Analyses of simple, multi-stage compression, and cascade VCR cycles

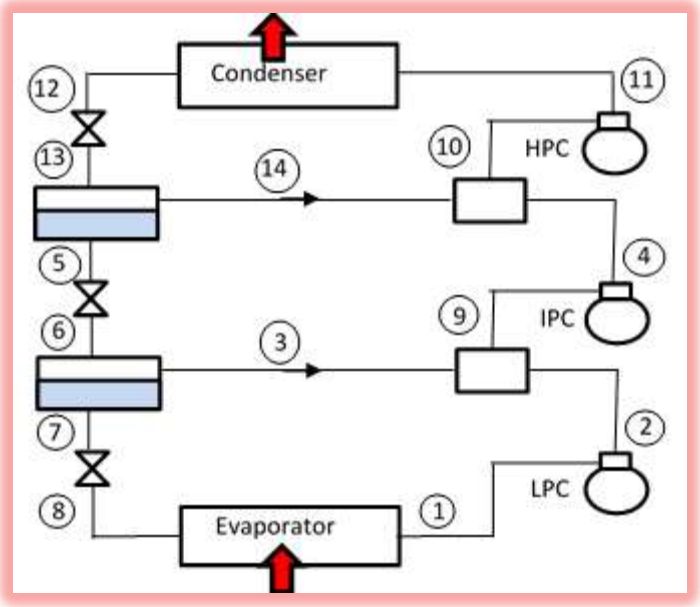

The vapour-compression refrigeration (VCR) systems used in various residential, commercial, and industrial applications are the main contributor to the ozone-layer depletion problem and a major contributor to the global-warming problem. Improving the performance of these systems will help us to curb the adverse effects of these two problems. One approach to improve the performance of the simple single-stage VCR system, which deteriorates when there is a large difference between the evaporator and condenser temperatures, is to use multi-stage compression VCR systems that split the compression process into two or more stages. Another approach is to use cascade systems that split the VCR cycle into two or more cycles usually using different refrigerants with heat-exchangers between them. This chapter illustrates the use of Thermax property functions for the analyses of simple, two-stage and three-stage compression, and cascade VCR cycles. The results obtained by using the property functions for refrigerant R134a are verified against those given by Moran and Shapiro [1] and Cengel and Boles [2] and compared to those obtained by using the add-in developed for R134a at the University of Alabama [3].

5.1. Analysis of the ideal vapour-compression refrigeration cycle

Figure 5.1 shows a schematic diagram of the basic VCR system and Figure 5.2 shows the *T-s* diagram for the ideal VCR cycle that consists of the following four processes:

1. Process 1-2: reversible adiabatic compression process
2. Process 2-3: constant-pressure heat-rejection process in the condenser
3. Process 3-4: expansion process in an expansion value or a capillary tube
4. Process 4-1: constant-pressure heat-addition process in the evaporator

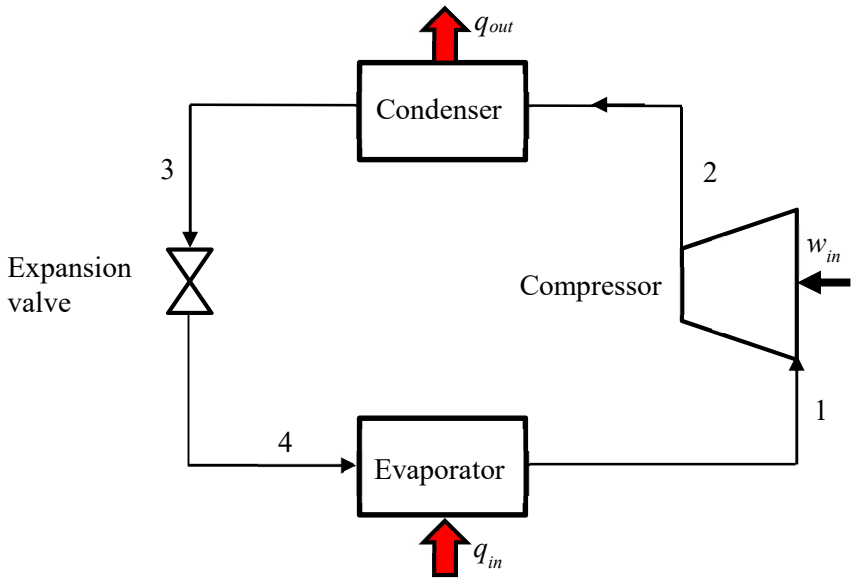

Figure 5.1. Schematic diagram of the single-stage vapour-compression refrigeration system

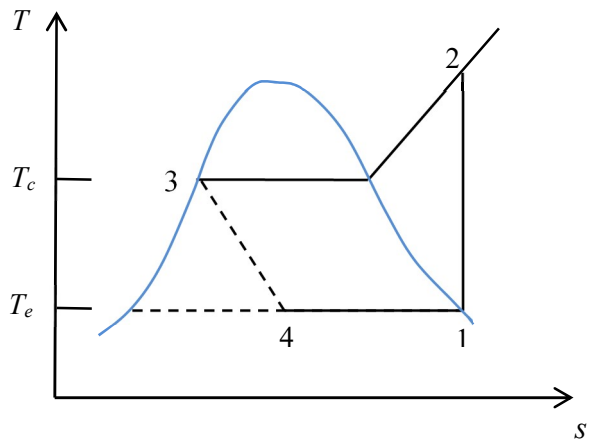

Figure 5.2. *T-s* diagram for the ideal vapour-compression refrigeration cycle

Assuming steady operation of all the system components and neglecting the changes in kinetic and potential energy across each component, the energy interactions with the surroundings in the different components per unit mass flow rate of the refrigerant in the system are described by the following relationships.

Compressor input work:

$$w_c = (h_2 - h_1) \tag{5.1}$$

Heat rejection in the condenser:

$$q_{out} = (h_2 - h_3) \tag{5.2}$$

Heat input in the evaporator:

$$q_{in} = (h_1 - h_4) \tag{5.3}$$

Adiabatic expansion process in the expansion valve or capillary tube:

$$h_4 = h_3 \tag{5.4}$$

Three parameters measure the performance of the VCR system; which are its coefficient of performance (*COP*), cooling capacity (*CC*) in ton of refrigeration, and the compressor power ($\dot{W}_c$), which are defined as follows:

$$COP = \frac{q_{in}}{w_c} \tag{5.5}$$

$$CC = \frac{60\dot{m}q_{in}}{211} \tag{5.6}$$

$$\dot{W}_c = \dot{m}(h_2 - h_1) \tag{5.7}$$

Where $\dot{m}$ is the mass flow rate of the refrigerant in the system in kg/s. The following example, which is based on Example 10-1 in Moran and Shapiro [1], illustrates the use of Thermax and the UA add-in "R134a" for analysing the cycle.

Example 5.1. Analysis of the ideal vapour-compression refrigeration cycle
An ideal VCR cycle thermally connected to a cold region at 0°C and a warm region at 26°C uses refrigerant R134a as the working fluid. The refrigerant enters the compressor as saturated vapour at 0°C and leaves the condenser as saturated liquid at 26°C. The mass flow rate of the refrigerant is 0.08 kg/s. Determine (a) the compressor power, in kW, (b) the refrigeration capacity, in tons, and (c) the coefficient of performance.

Solution
Figure 5.3 shows the Excel sheet developed for this example by using the functions provided by the refrigerants group (Ref) of Thermax. The given data for the evaporator and condenser temperatures and refrigerant mass flow rate are shown on the left side of the sheet as T_e, T_c, and m_ref, respectively. The middle part of the sheet shows the formulae used for determining the different enthalpy values using the relevant functions. For example, the enthalpy at state 1, h_1, is determined by using the function **Refh_Tx** that returns the enthalpy of saturated vapour (h_v) at a given temperature. The entropy at this point (s_1) is found by using another function, **Rehs_Tx**, that determines the entropy of saturated vapour at a given temperature (T) and quality (x).

COP =q_in/w_c

	A	B	C	D	E	F	G	H	I
1									
2	T_e	0	oc	h_1	398.600	=Refh_Tx("R134a",T_e,1)	w_c	1.409	kW
3				s_1	1.727	=Refs_Tx("R134a",T_e,1)			
4	T_c	26	oc				q_in	13.010	kW
5				P_c	685.430	=RefPsat_T("R134a",T_c)			
6	m_ref	0.08	kg/s				CC	3.700	Ton
7				h_2	416.207	=Refh_Ps("R134a",P_c,s_1)			
8							COP	9.237	
9				h_3	235.970	=Refh_Tx("R134a",T_c,0)			
10									
11				h_4	235.970	=h_3			
12									

Figure 5.3. Excel sheet developed for Example 5.1 using Thermax

The right-hand side of the sheet calculates the compressor power, w_c, according to Equation (5.7), the cooling capacity, CC, according to Equation (5.6), and the coefficient of performance (COP) according to Equation (5.5). Figure 5.4 shows a similar sheet that was developed by using property functions from the R134a add-in provided by the University of Alabama [3]. Note that this add-in supports two systems of units, but its functions can only be used for refrigerant R-134a. Table 5.1 that compares the calculated values for the key cycle parameters by the two add-ins shows a good agreement between the add-in results with their corresponding values given by Moran and Shapiro [1].

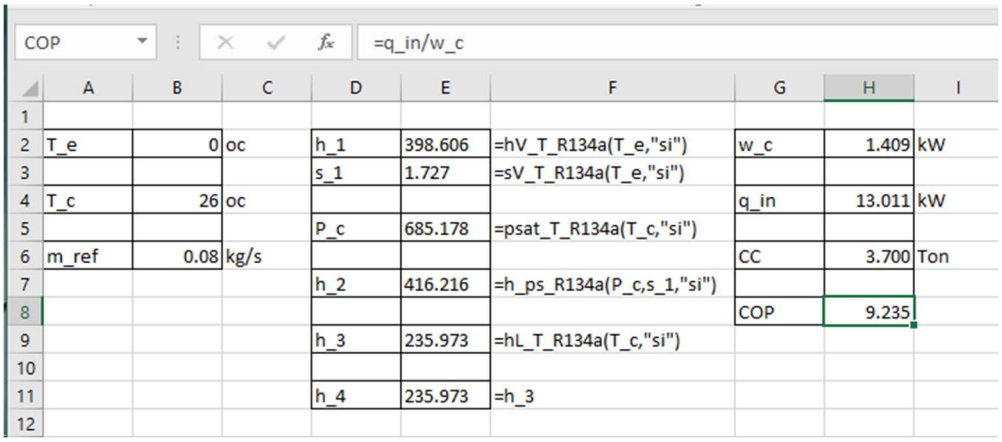

Figure 5.4. Excel sheet developed for Example 5.1 using the UA add-in for R134a

Table 5.1. Comparison of the ideal VCR cycle key parameters given by the two add-ins with their values given by Moran and Shapiro [1]

Parameter	Moran & Shapiro [1]	Thermax	UA Add-in R134a
Compressor work [kW]	1.40	1.409	1.409
Refrigeration capacity (ton)	3.67	3.700	3.700
COP	9.24	9.237	9.235

5.2. Analysis of the actual vapour-compression refrigeration cycle

The ideal cycle shown on Figure 5.2 does not account for the irreversibility and pressure losses in the system components. Moreover, the compression process is assumed to be adiabatic and reversible which means that it is isentropic. The COP of actual CVR systems is much lower than the figures shown in Table 5.1 because of pressure and heat-transfer losses and irreversibilties. In actual VCR cycles, all four processes are irreversible because of friction losses in the compressor and heat-transfer with finite temperature differences in the evaporator and condenser. Some degree of subcooling also occurs in actual cycles at the condenser discharge. These deviations from the ideal cycle affect both the cooling capacity and COP of the VCR system. Figure 5.5 shows the *T*-*s* diagram for the actual VCR cycle.

Chapter 6

Analyses of air-conditioning processes and systems

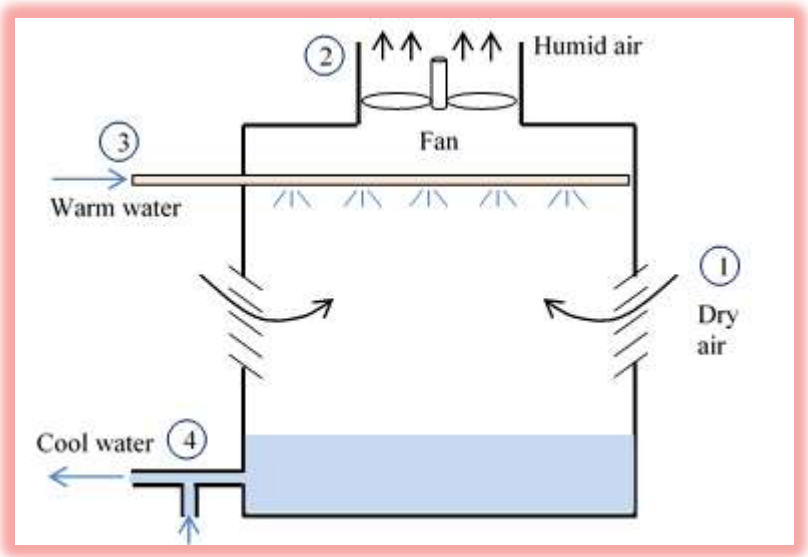

Psychrometric analyses of air-conditioning processes and systems, which treat air as a mixture of two gases, dry air and water vapour, require the properties of the mixture to be evaluated. The traditional method of determining the properties of humid air by visual interpolation of psychrometric charts is not suitable for design optimisation analyses and can be inaccurate. A suitable alternative is provided by Excel with Thermax functions from the "Psy" group or the "Thermotables" add-in developed at the University of Alabama [1]. This chapter shows how the functions can be used for such analyses. The chapter initially describes the basic functions of the psychrometric chart before using Thermax functions for analysing two basic air-conditioning processes; which are the cooling-with-dehumidification process and the process of adiabatic mixing of two moist-air streams. Thermax functions are then used to analyse two relevant systems, which are the evaporative cooler and the wet cooling tower. Finally, the chapter shows how the property functions can be used for solving a design optimisation problem that minimises the energy consumption of an air-conditioning system by air re-circulation.

6.1. The psychrometric chart and the basic air-conditioning processes

The psychrometric chart is used in the analyses of air-conditioning systems and processes to determine the state of humid air at a given pressure in terms of its properties at various temperatures and humidity levels. The pressure is usually the standard atmospheric pressure of 1 atm (equivalent to 101.325 kPa). Figure 6.1 shows a typical layout of the psychrometric chart.

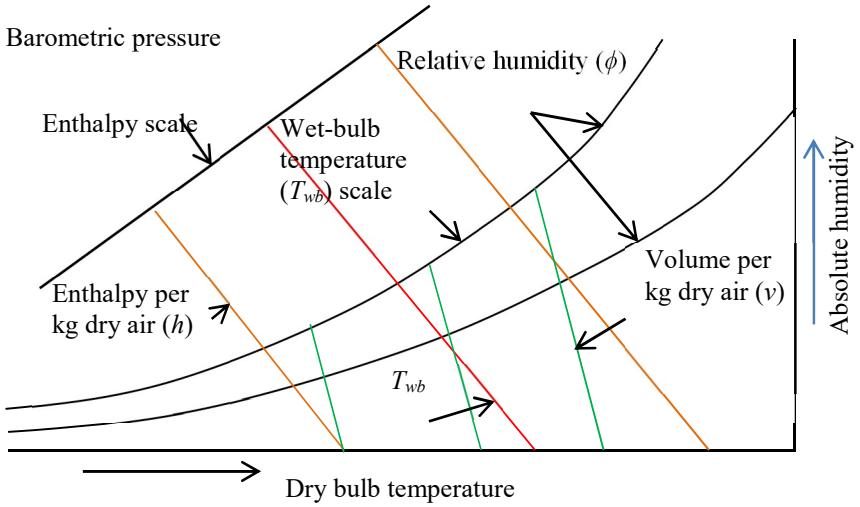

Figure 6.1. The psychrometric chart

On the horizontal axis, the chart shows the dry-bulb temperature, which is the normal temperature as measured by a mercury thermometer. The vertical axis on the right-side of the chart shows the absolute humidity of air (ω), also called the specific humidity,

6.6. Design analysis of an air-conditioning system

The previous sections utilised the property functions for the analyses of basic psychrometric processes and systems that did not involve repetitive calculations. However, property functions are more advantageous over psychrometric charts when dealing with repetitive parametric or optimisation analyses of air-conditioning systems. This is demonstrated by the following design case which is based on a design problem given by Moran and Shaprio [3].

The design case

The energy requirements of large air-conditioning systems can be reduced by re-circulating part of the discharged conditioned air and mixing it with the fresh unconditioned air. Figure 6.14 shows a system for supplying a space with 2100 m^3/min of conditioned air at a dry-bulb temperature of 22°C and a relative humidity of 60% when the outside air is at a dry-bulb temperature of 35°C and a relative humidity of 55%.

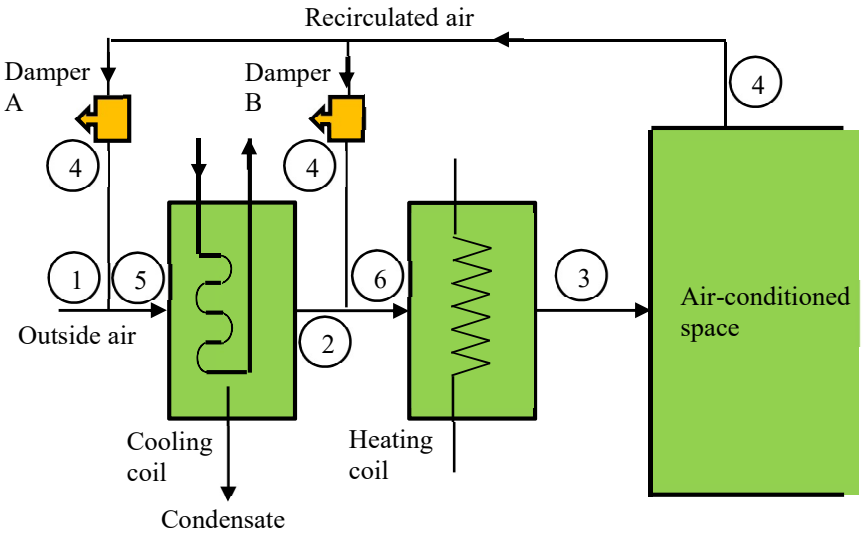

Figure 6.14. Schematic diagram of the air-conditioning system (adapted from Moran and Shapiro [3])

Dampers A and B can be set to give three alternative operating modes:

(a) Both dampers closed (zero recirculated air).
(b) Damper A open and damper B closed. One-third of the conditioned air comes from outside air.
(c) Both dampers open. One-third of the conditioned air comes from outside air. One-third of the recirculated air bypasses the dehumidifier via open damper B, and the rest flows through the damper A.

It is required to determine which of the three operating modes gives the minimum cooling and heating loads?

Option (a)

Since there is no air re-circulation in this mode, both the cooling and heating loads will be at their maximum values. Therefore, this option will be the reference against which the savings of the other two modes are evaluated and compared. The air-conditioning process in this mode consists of only two operations; a cooling and dehumidification process followed by a simple heating process. Referring to Figure 6.14, the cooling load (Q_c) and heating load (Q_h) can be calculated from:

$$\dot{Q}_c = \dot{m}_{a1}(h_1 - h_2) - \dot{m}_w h_{fg} \tag{6.25}$$

$$\dot{Q}_h = \dot{m}_{a1}(h_3 - h_2) \tag{6.26}$$

Where $\dot{m}_{a1}$ and h_1 are the mass-flow rate of dry air and enthalpy of humid air at state 1, h_2 and h_3 are the enthalpy of humid air at states 2 and 3, respectively, and $\dot{m}_w$ is the rate of water removal by condensation at state 2. The values of $\dot{m}_{a1}$ and $\dot{m}_w$ are calculated from:

$$\dot{m}_{a1} = \frac{\dot{V}_1}{v_{a1}} = \frac{2100}{v_{a1}} \tag{6.27}$$

$$\dot{m}_w = \dot{m}_{a1}(\omega_1 - \omega_2) \tag{6.28}$$

The condition of air at states 1 and 3 are known and its condition at state 2 is specified by the fact that ϕ_2 = 100% and ω_2=ω_3. Figure 6.15 shows the Excel sheet prepared for this mode of operation.

Qin23_ | =mflow_a1*(h3_-h2_)

	A	B	C	D	E	F	G	H	I	J
1										
2		CASE A								
3		T1_	35	oC	ω1	0.019796	=PsySh_PDbRh(P1_,T1_,ϕ1)	mflow_a1	2441.159	=mflowa_3
4		ϕ1	55	%				mflow_w	23.93922	=mflow_a1*(ω1-ω2)
5					ω3	0.009989	=PsySh_PDbRh(P1_,T3_,ϕ3)			
6		ϕ2	100	%				h1_	85.94336	=Psyh_PDbSh(P1_,T1_,ω1)
7					ω2	0.009989	=ω3	h2_	39.20629	=Psyh_PDbSh(P1_,T2_,ω2)
8		T3_	22	oC	T2_	13.90176	=PsyDb_PRhSh(P1_,ϕ2,ω2)	h3_	47.49226	=Psyh_PDbSh(P1_,T3_,ω3)
9		ϕ3	60	%						
10		Flow3	2100	m3/min	Pv3_	1.580615	=ϕ3/100*PsyPsat_T(T3_)	Qout12	112696.7	=mflow_a1*(h1_-h2_)-mflow_w*PsyhL_T(T2_)
11					Pa3_	98.41939	=P1_-Pv3_	Qin23	20227.35	=mflow_a1*(h3_-h2_)
12		P1_	100	kPa	va3_	0.860247	=0.287*(T3_+273)/Pa3_			
13					mflowa_3	2441.159	=Flow3/va3_			
14										

Figure 6.15. Excel sheet for option (a)

The given data for T_1, P_1, ϕ_1, ϕ_2, T_3, ϕ_3, and $\dot{V}_{a3}$ is shown on the left side of the worksheet. The specific humidities ω_1 and ω_3 are calculated by calling the add-in function **PsySh_PDbRh** with relevant values of P, T and ϕ at the two points. At point 2, $\omega_2 = \omega_3$, ϕ_2=100% and P_1=100 kPa. The temperature T_2 is then determined by using the function **PsyDb_PRhSh**. Values of the enthalpy h_1, h_2, and h_3 are calculated by calling the function **Psyh_DbSh**. The auxiliary function **PsyhL_T** is also used here (cell I10) to determine the temperature of saturated liquid water at T_2. Substituting in Equations (6.25) and (6.26), the values obtained for the cooling and heating loads (Q_c =Qout12 and Q_h = Qin23) for this option are 112,696.7 kJ/min and 20,227.4 kJ/min, respectively.

Option (b)

In this case, two-thirds of the discharged air is recirculated through damper A and only one-third of the conditioned air comes from outside air. As shown later, this mode reduces the cooling load, but keeps the heating load unchanged. Referring to Figure 6.14, the mass flow rate of dry air at state 3 is given by:

$$\dot{m}_{a3} = \frac{\dot{V}_3}{v_{a3}} = \frac{2100}{v_{a3}} \tag{6.29}$$

The mass flow rates of dry air at states A, 1, 2, and 5 are given by:

$$\dot{m}_{aA} = \dot{m}_{a3}/3 \tag{6.30}$$

$$\dot{m}_{a1} = \dot{m}_{a3}/3 \tag{6.31}$$

$$\dot{m}_{a2} = \dot{m}_{a3} \tag{6.32}$$

$$\dot{m}_{a5} = \dot{m}_{a3} \tag{6.33}$$

The condition of air at the states 1, 2, and 3 are the same as in case (a). The condition at state 4 is specified by the given values of T = 27°C and ϕ=49%. Assuming adiabatic mixing, the condition of the air after the mixing process at state 5 is determined as follows:

$$h_5 = \left(\dot{m}_1 h_1 + \dot{m}_A h_4\right)/\dot{m}_5 \tag{6.34}$$

$$\omega_5 = \left(\dot{m}_1 \omega_1 + \dot{m}_A \omega_4\right)/\dot{m}_5 \tag{6.35}$$

The rate of water removal in the dehumidifier is calculated from:

$$\dot{m}_w = \dot{m}_{a3}\left(\omega_5 - \omega_2\right) \tag{6.36}$$

The cooling load and heating loads for this case are calculated from:

$$\dot{Q}_c = \dot{m}_{a3}(h_1 - h_2) - \dot{m}_w h_{fg} \tag{6.37}$$

$$\dot{Q}_h = \dot{m}_{a3}(h_3 - h_2) \tag{6.38}$$

Figure 6.16 shows the Excel sheet prepared for this operation mode. In addition to the input-data of the sheet shown in Figure 6.15, the input-data part of this sheet provides the condition at point 4. The mass flow rate of outside air (mflowa_1) is reduced to one third of the total flow rate and two-thirds of the total the mass flow rate passes through damper A (mflowa_A). The calculation part is also expanded to include the calculations of humidity and enthalpy of the air mixture at point 5. The cooling and heating loads are now determined according to Equations (6.37) and (6.38). As Figure 6.16 shows, the cooling and heating capacities for this option are 63,575.9 kJ/min and 20,227.4 kJ/min, respectively. Compared to option (a), this mode reduced the cooling capacity but the heating capacity remained unchanged.

Qin23_ =mflowa_3*(h3_-h2_)

	A	B	C	D	E	F	G	H	I	J
1										
2		CASE B								
3		T1_	35	oC	ω1	0.019796	=PsySh_PDbRh(P1_,T1_,ϕ1)	ω4	0.011025	=PsySh_PDbRh(P1_,T4_,ϕ4)
4		ϕ1	55	%				h4_	55.24902	=Psyh_PDbSh(P1_,T4_,ω4)
5					ω3	0.009989	=PsySh_PDbRh(P1_,T3_,ϕ3)	h5_	65.48047	=(mflowa_1*h1_+mflowa_A*h4_)/mflowa_3
6		ϕ2	100	%				ω5	0.013949	=(mflowa_1*ω1+mflowa_A*ω4)/mflowa_3
7					ω2	0.009989	=ω3	T5_	29.69421	=PsyDb_PhSh(P1_,h5_,ω5)
8		T3_	22	oC	T2_	13.90176	=PsyDb_PRhSh(P1_,ϕ2,ω2)	mflow_w	9.665144	=mflowa_3*(ω5-ω2)
9		ϕ3	60	%						
10		Flow3	2100	m3/min	Pv3_	1.580615	=ϕ3/100*PsyPsat_T(T3_)	h1_	85.94336	=Psyh_PDbSh(P1_,T1_,ω1)
11					Pa3_	98.41939	=P1_-Pv3_	h2_	39.20629	=Psyh_PDbSh(P1_,T2_,ω2)
12		P1_	100	kPa	va3_	0.860247	=0.287*(T3_+273)/Pa3_	h3_	47.49226	=Psyh_PDbSh(P1_,T3_,ω3)
13										
14		T4_	27	oC	mflowa_3	2441.159	=Flow3/va3_	Qout52	63575.85	=mflowa_3*(h5_-h2_)-mflow_w*PsyhL_T(T2_)
15		ϕ4	49	%	mflowa_1	813.7196	=mflowa_3/3	Qin23	20227.35	=mflowa_3*(h3_-h2_)
16					mflowa_A	1627.439	=mflowa_3*2/3			
17										

Figure 6.16. Excel sheet for option (b)

Option (c)

In this option, one-third of the conditioned air bypasses the dehumidifier via the open damper B. Another one-third of the air-flow is recirculated via damper A, while the remaining air comes from the outside. As shown below, this mode reduces the cooling as well as the heating capacities of the system. Referring to Figure 6.14, the mass flow rate of dry air at state 3 is:

$$\dot{m}_{a3} = \frac{\dot{V}_3}{v_{a3}} = \frac{2100}{v_{a3}} \tag{6.39}$$

The mass flow rates of dry air at states A, B, and 1, which are equal are, given by:

$$\dot{m}_{aA} = \dot{m}_{aB} = \dot{m}_{a1} = \dot{m}_{a3} / 3 \tag{6.40}$$

Conservation of mass applied over the mixing processes after damper A and damper B gives:

$$\dot{m}_{a5} = 2\dot{m}_{a3} / 3 \tag{6.41}$$

$$\dot{m}_{a2} = \dot{m}_{a5} \tag{6.42}$$

$$\dot{m}_{a6} = \dot{m}_{a3} \tag{6.43}$$

The air conditions at the states 1, 3 and 4 are the same as in case (a) and case (b). The condition at state 2 is also specified by the fact that ϕ_2 = 100% and ω_2=ω_3. Assuming adiabatic mixing, the condition after the mixing process at state 5 is determined by:

$$h_5 = \left(\dot{m}_1 h_1 + \dot{m}_A h_4\right) / \dot{m}_5 \tag{6.44}$$

$$\omega_5 = \left(\dot{m}_1 \omega_1 + \dot{m}_A \omega_4\right) / \dot{m}_5 \tag{6.45}$$

Similarly, the condition at state 6 is determined as follows:

$$h_6 = \left(\dot{m}_2 h_2 + \dot{m}_B h_4\right) / \dot{m}_{a6} \tag{6.46}$$

$$\omega_6 = \left(\dot{m}_2 \omega_2 + \dot{m}_B \omega_4\right) / \dot{m}_6 \tag{6.47}$$

The rate of water removal in the dehumidifier is calculated from:

$$\dot{m}_w = \dot{m}_{a5}\left(\omega_5 - \omega_2\right) \tag{6.48}$$

Finally, the cooling and heating loads for this case are calculated from:

$$\dot{Q}_c = \dot{m}_{a5}\left(h_1 - h_2\right) - \dot{m}_w h_{fg} \tag{6.49}$$

$$\dot{Q}_h = \dot{m}_{a3}\left(h_3 - h_6\right) \tag{6.50}$$

Figure 6.17 shows the Excel sheet prepared for this option. Compared to the sheet shown on Figure 6.16, the calculation part is expanded to calculate the mass flow rates after damper B and at states 5 and 2. The additional calculations also include enthalpy and humidity values and the temperature at state 6. The rates of cooling and heating capacities calculated for this option are 50,570.1 kJ/min and 7,173.1 kJ/min, respectively. These figures indicate that both the cooling and heating capacities of this option are significantly

less than those of options (a) and (b). Table 6.5 summarises the results of the cooling and heating capacities for the three options. Compared to option (a), options (b) and (c) save about 37% and 57% of the total load, respectively. Therefore, option (c) is the preferred mode of operation.

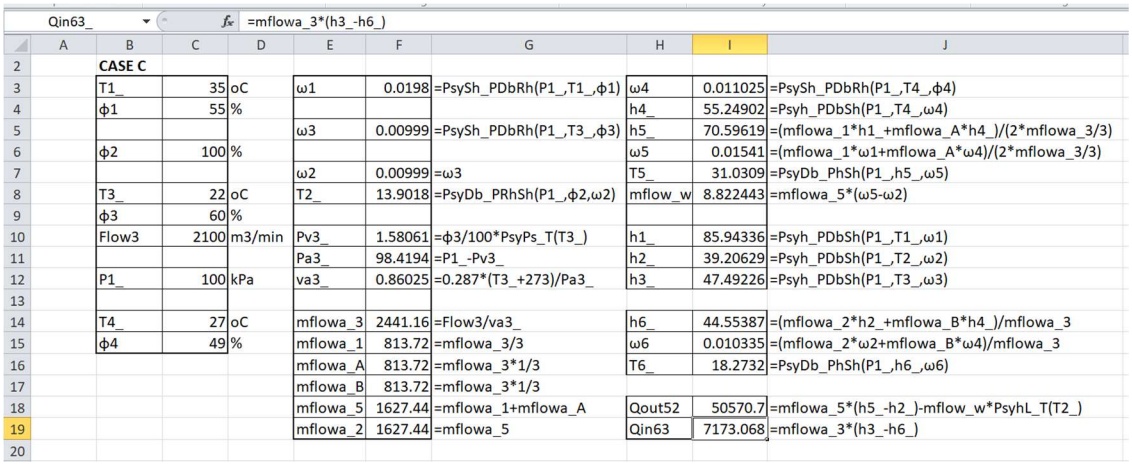

Qin63_ =mflowa_3*(h3_-h6_)

	A	B	C	D	E	F	G	H	I	J
2		CASE C								
3		T1_	35	oC	ω1	0.0198	=PsySh_PDbRh(P1_,T1_,ϕ1)	ω4	0.011025	=PsySh_PDbRh(P1_,T4_,ϕ4)
4		ϕ1	55	%				h4_	55.24902	=Psyh_PDbSh(P1_,T4_,ω4)
5					ω3	0.00999	=PsySh_PDbRh(P1_,T3_,ϕ3)	h5_	70.59619	=(mflowa_1*h1_+mflowa_A*h4_)/(2*mflowa_3/3)
6		ϕ2	100	%				ω5	0.01541	=(mflowa_1*ω1+mflowa_A*ω4)/(2*mflowa_3/3)
7					ω2	0.00999	=ω3	T5_	31.0309	=PsyDb_PhSh(P1_,h5_,ω5)
8		T3_	22	oC	T2_	13.9018	=PsyDb_PRhSh(P1_,ϕ2,ω2)	mflow_w	8.822443	=mflowa_5*(ω5-ω2)
9		ϕ3	60	%						
10		Flow3	2100	m3/min	Pv3_	1.58061	=ϕ3/100*PsyPs_T(T3_)	h1_	85.94336	=Psyh_PDbSh(P1_,T1_,ω1)
11					Pa3_	98.4194	=P1_-Pv3_	h2_	39.20629	=Psyh_PDbSh(P1_,T2_,ω2)
12		P1_	100	kPa	va3_	0.86025	=0.287*(T3_+273)/Pa3_	h3_	47.49226	=Psyh_PDbSh(P1_,T3_,ω3)
13										
14		T4_	27	oC	mflowa_3	2441.16	=Flow3/va3_	h6_	44.55387	=(mflowa_2*h2_+mflowa_B*h4_)/mflowa_3
15		ϕ4	49	%	mflowa_1	813.72	=mflowa_3/3	ω6	0.010335	=(mflowa_2*ω2+mflowa_B*ω4)/mflowa_3
16					mflowa_A	813.72	=mflowa_3*1/3	T6_	18.2732	=PsyDb_PhSh(P1_,h6_,ω6)
17					mflowa_B	813.72	=mflowa_3*1/3			
18					mflowa_5	1627.44	=mflowa_1+mflowa_A	Qout52	50570.7	=mflowa_5*(h5_-h2_)-mflow_w*PsyhL_T(T2_)
19					mflowa_2	1627.44	=mflowa_5	Qin63	7173.068	=mflowa_3*(h3_-h6_)
20										

Figure 6.17. Excel worksheet for option (c)

Table 6.5. Cooling and heating capacities for the three options

Option	Cooling capacity [kJ/min]	Heating capacity [kJ/min]	Total load [kJ/min]	Saving [%]
(a)	112,696.7	20,227.4	132,924.10	-
(b)	63,575.2	20,227.4	83,802.60	36.95
(c)	50,570.1	7,7173.1	57,743.20	56.56

Table 6.6 lists Thermax function used in the analysis of option (c) of the design case; which involves more state points than the other two options. As the table shows, from the total of 18 functions provided by the "Psy" group of Thermax, only six functions have been used in this design analysis. This indicates the adequacy of the add-in functions in this group for a wide range of air-conditioning and psychrometric analyses.

Table 6.6. Thermax function used in the analysis of option (c) of the design case

Function	Usage
PsySh_PDbRh	ω_1, ω_3, ω_4
PsyDb_PRhSh	T_2
Psyh_PDbSh	h_1, h_2, h_3, h_4
PsyDb_PhSh	T_5, T_6
PsyPsat_T	P_{v3}
PsyhL_T	$\dot{Q}_c$

Chapter 7

Combustion analyses

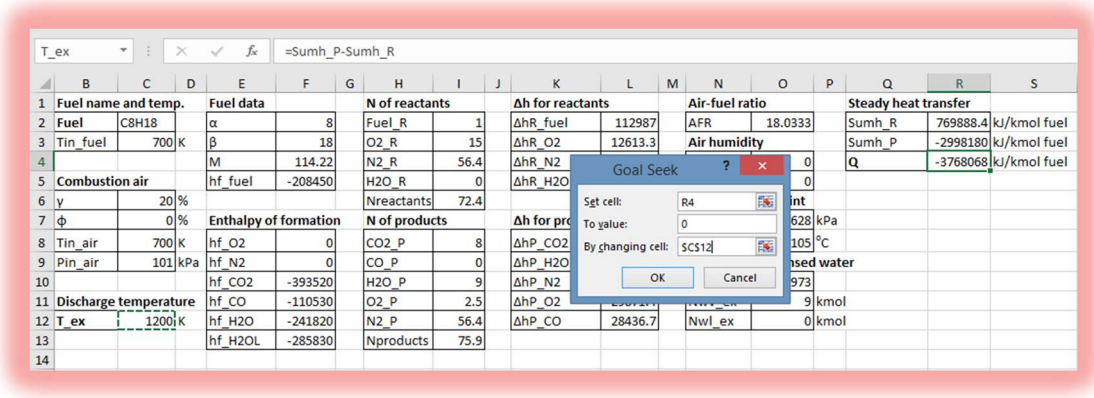

Combustion analyses involve multiple reactants (fuel, air, and water-vapour) and multiple combustion products (CO_2, CO, H_2O, O_2, and N_2) and determining the thermodynamic properties of the numerous reactants and products at different temperatures makes combustion analyses tedious for hand calculations using property tables and charts. This chapter shows how the analyses can be automated by using the property functions provided by Thermax to develop an Excel sheet for first-law combustion analyses of various fuels. The required input includes the fuel itself, the amount of excess air, the inlet temperatures and pressures of the fuel and the air, the moisture content of the air, and the discharge temperature of the combustion products. With this information, the sheet determines the air-fuel ratio, the dew-point temperature of the combustion products, and the amount of heat released from combustion. Excel's Goal Seek command is used for determining the fuel's adiabatic flame temperature (T_{af}) for steady-flow combustion that requires an iterative solution. Finally, the chapter shows how the Developer tools and the Data Validation tools of Excel can be used to develop macros and drop-down lists that eliminate the tedium of repetitive parametric analyses and make the sheet more user-friendly.

7.1. The basic equations for combustion analyses

Combustion analysis of a hydrocarbon fuel in air determines: (i) the amount of air needed for the combustion process (or the air-fuel ratio), (ii) the temperature at which water vapour condensation in the combustion products occurs (the dew-point temperature of combustion products), (iii) the fraction of condensed water-vapour at temperatures lower than the dew-point temperature, and (iv) the amount of heat released by the combustion process. The following subsections describe the basic equations involved.

7.1.1. The combustion equation for a hydrocarbon fuel in excess air

Ideal combustion of a hydrocarbon fuel $C_\alpha H_\beta$ in pure oxygen is expressed by:

$$C_\alpha H_\beta + aO_2 \rightarrow bCO_2 + cH_2O \tag{7.1}$$

Balances of the number of C moles, O_2 moles, and H_2 moles on both sides of Equation (7.1) lead to:

$$b = \alpha \tag{7.2}$$

$$c = \beta / 2 \tag{7.3}$$

$$a = b + c/2 \tag{7.4}$$

Substituting from Equations (7.2) and (7.3) in Equation (7.4) gives:

$$a = \alpha + \beta / 4 \tag{7.5}$$

8

Thermo-economic optimisation of the gas-turbine cycle with inlet-air cooling

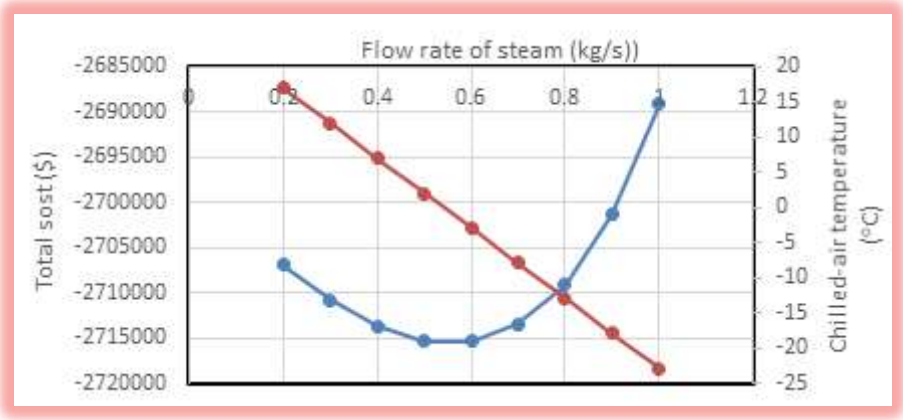

Thermo-economic optimisation analyses of energy-conversion systems seek to find a trade-off between the two conflicting objectives of maximising the thermodynamic efficiency of the plant (i.e. thermal or exergetic efficiency or coefficient of performance) and minimising the costs of its equipment by minimising the *total* cost of the system. Having formulated the objective function for optimisation that relates the total cost of the system to its initial and running costs, the optimisation procedure then requires: (i) the development a thermodynamic model, (ii) development of an economic model, and (iii) selection of an optimisation method. Usually a ready-made solver is used for step (iii) such as Excel's Solver. For the traditional thermo-economic analyses (i.e. excluding exergoeconomic analyses [1,2]) a generalised economic model is also available for step (ii) [3,4]. However, the thermodynamic model is system-specific and, depending on the underlying assumptions used, different models can be formulated that yield different answers for the same objective function and the same optimisation method used.

This chapter highlights the roles of the thermodynamic model and the optimisation method in thermo-economic optimisation analyses of energy-conversion systems by considering the gas-turbine with inlet air-cooling described by Burmeister [5]. The system uses vapour-absorption refrigeration (VAR) for cooling the inlet-air, a heat-recovery steam generator (HRSG) for producing the steam needed by the VAR system, and an air-preheater for heating the compressed air before going to the combustion chamber. The total cost of the system includes that of the air preheater, the HRSG, the VAR system, the combustion chamber, and the sales of produced electricity. The chapter initially describes the analytical model developed by Burmeister [5] to optimise the ideal cycle by using the approximate method. Two Excel-aided models for the system are then described that apply the exact variable specific-heat method for the ideal cycle and the actual cycle by using Thermax property functions. For these two models, optimised solutions are obtained with the two methods offered by Solver, viz., the GRG Nonlinear method and the Evolutionary method. The results obtained by the two thermodynamic models with the two solution methods provided by Solver are compared.

8.1. Analytical optimisation of the ideal cycle with the approximate method

Due to the reduction in air density, both the output power and thermal efficiency of the simple-cycle gas turbines deteriorate during summer time particularly in hot climates. Therefore, cooling the air before the compressor can be cost-effective. The gas-turbine power generation plant shown on Figure 8.1 is equipped with a VAR system for cooling the inlet air that extracts part of the waste energy in the exhaust gas to produce steam which is used to supply the heat needed for operating the VAR system. The system also utilises part of the exhaust-gas energy to raise the temperature of the compressed air before going to the combustion chamber so as to minimise the fuel consumption of the plant. The total cost (C_T) of the system is given by [5]:

C_T = fuel cost + air-cooler cost + boiler cost + air-preheater cost - sale of power

9

Thermo-economic optimisation of the air-bottoming cycle

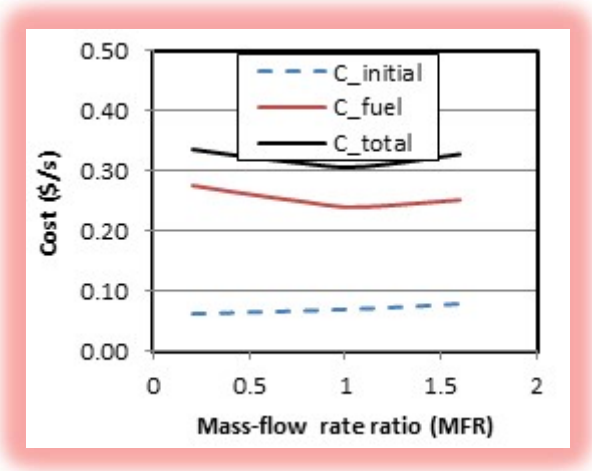

The exhaust gases of gas-turbines' carry away with them significant portions of the fuels' energy that can be recovered and used for improving the turbines' thermal efficiency in a number of ways. One of the attractive options in this regard is the air-bottoming cycle (ABC) in which the exhaust-gas energy is used as the high-temperature source for a low-pressure gas turbine. The ABC produces more work output than the basic system without additional energy input, but it costs more because of the additional equipment. Therefore, the economic feasibility of the ABC requires a compromise to be made between the thermodynamic improvement of the system and the additional cost of equipment. This chapter presents optimisation analyses of the ABC with three objectives; thermodynamic, economic, and thermo-economic. While the thermodynamic optimisation aims to maximise the system's thermal efficiency and the economic optimisation aims to minimise its initial cost, the thermo-economic optimisation aims to minimise its total annualised cost for the same generation capacity. The chapter also illustrates the advantage of the Evolutionary method of Solver over the GRG Nonlinear method for the thermo-economic analysis that involves nine design variables by proving its ability to find an optimised system with a lower total cost as well as a higher thermal efficiency.

9.1. Description of the air-bottoming gas-turbine system

Figure 9.1 shows a schematic diagram of a power generation plant that works on the ABC in which the two gas turbines work in parallel. According to Korobitsyn [1], the bottom cycle adds 20–30% to the power output of the plant and boosts the plant's efficiency by up to 45%. Compared to the more conventional combined Brayton-Rankine cycle, the main advantage of the ABC is that it doesn't require abundant supply of cooling water or expensive water treatment facilities. Considering its low initial cost, short installation period, and its ability to run unmanned, the ABC has become an attractive option for small power plants of up to 50 MWe [2].

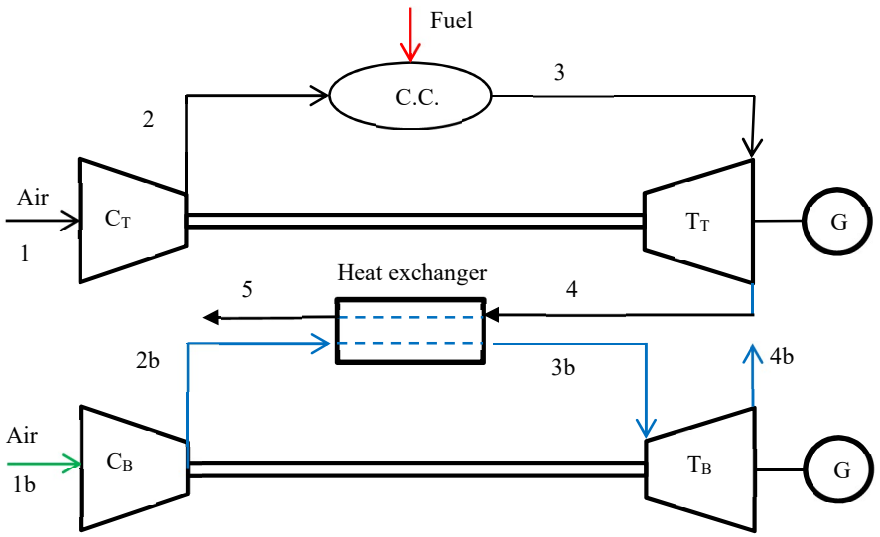

Figure 9.1. Schematic diagram of the air-bottoming gas-turbine plant

10

Thermo-economic optimisation of the combined cycle power plant

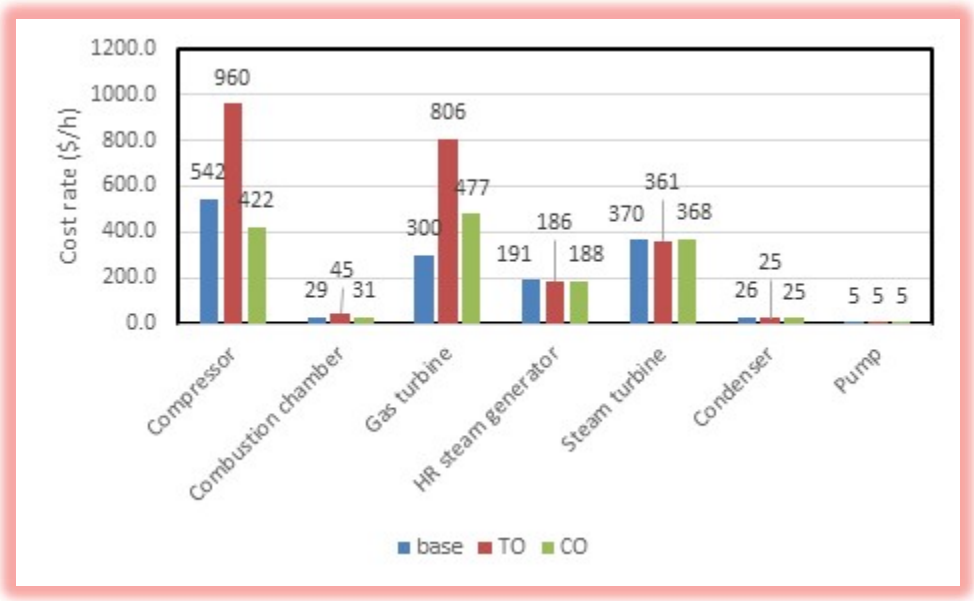

The combined-cycle uses the exhaust heat from the gas turbine to produce steam in a heat recovery steam generator (HRSG) which is then expanded in a steam turbine to increase the generation of electricity of the plant by up to 50% without additional fuel [1]. The resulting increase in the thermal efficiency can exceed 64% [2]; which reduces the emission levels of the combined-cycle power plant (CCPP) and improves its reliability. These merits make the CCPP a favoured option for power providers. Although the growing share of renewables in the energy mix poses a big challenge to conventional thermally driven power plants, with respect to CCPPs the market is projected to grow at a compound annual growth rate (CAGR) of 5.4% during 2024–2029 [3,4]. This chapter presents an Excel-aided model for thermodynamic and thermo-economic analyses and optimisation of the basic CCPP cycle. The model is first validated with the data provided by Baghernejad and Anvari-Moghaddam [5], who compared three configurations of the CCPP from energy, exergy, exergoeconomic and environmental perspectives. The model is then used to conduct a parametric analysis and conventional single-objective thermodynamic and thermo-economic optimisation of the CCPP by using Excel's Solver. Finally, the chapter explains how the model can also be used to conduct multi-objective optimisation and exergoeconomic analyses for the CCPP.

10.1. System description and input data

Figure 10.1 shows a schematic diagram of the basic CCPP that adds a simple Rankine cycle to the simple Brayton cycle. Various modifications to the two cycles that constitute the combined cycle can be adopted to improve the performance of the plant. Ref. [5] used the input data shown in Table 10.1 for analysing the basic configuration shown on Figure 10.1 which they referred to as Configuration 1.

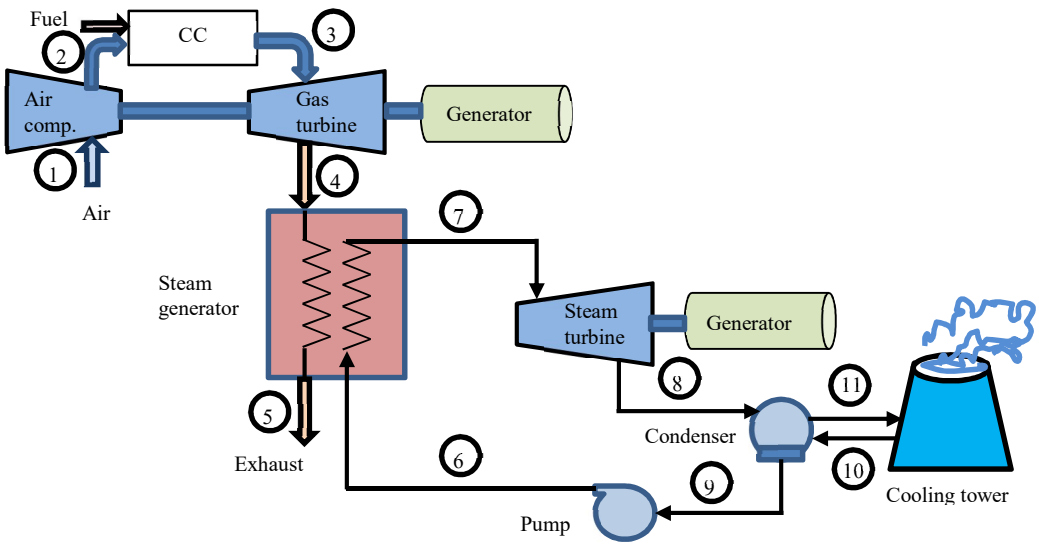

Figure 10.1. Schematic diagram of the basic CCPP configuration (adopted from [5])

Chapter 11

Thermodynamic analyses of vapour-absorption refrigeration systems

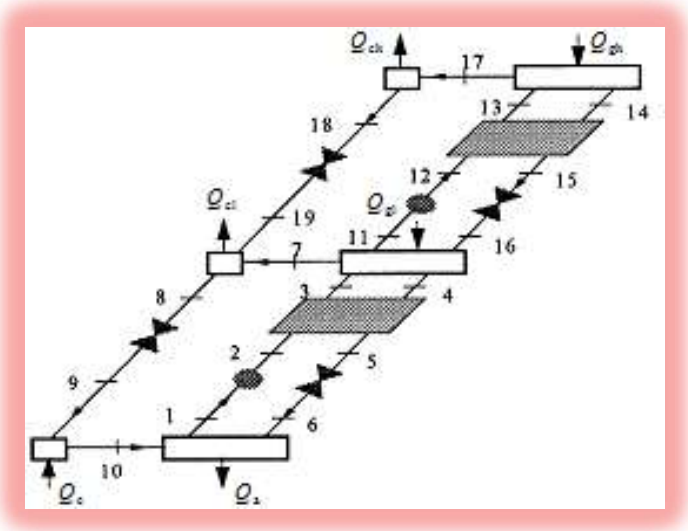

Vapour-absorption refrigeration (VAR) systems do not compress a vapour refrigerant as in the more commonly used vapour-compression refrigeration (VCR) systems. Instead, the refrigerant vapour is dissolved in a liquid absorbent at the lower pressure and released at the higher pressure by heating the solution. Thus, VAR systems require considerably less work input than VCR systems. Since a low-temperature heat source can be used for the heating process, VAR systems are important elements for efficient use of recovered energy and for the utilisation of renewable energies such as solar and geothermal energies. Thermax provides two sets of property functions for the two most commonly used absorbent-refrigerant combinations in VAR systems, which are lithium-bromide-water, with water as the refrigerant, and water-ammonia, with ammonia as the refrigerant. This chapter uses the functions to analyse different types of VAR systems. Initially, the chapter gives a brief description of VAR systems and discusses the temperature-pressure-concentration and enthalpy properties of water-lithium-bromide solutions. The functions for lithium-bromide-water are verified by comparing their results for analysing a basic VAR system, a single-effect system with a heat-exchanger, and a double-effect system with the data provided by Stoecker and Jones [1], ASHRAE [2], Abdulateef et. al. [3], and Kaynakli et al. [4]. The ammonia-water functions are verified by comparing their results for analysing the single-effect VAR system with those given by Sun [5].

11.1. Vapour-absorption refrigeration systems

A significant part of the energy released by burning fossil fuels in industrial, commercial, and residential buildings to produce thermal energy for different uses is rejected to the surrounding as waste energy [6]. Large amounts of waste heat are also released to the ambient from the internal combustion engines in the automotive industry and from marine engines [7]. With the increasing world population, the rate at which the non-renewable sources of fossil fuels are being consumed and the uncertainties regarding their future prospects have become major concerns. These concerns, and the increasing costs of fossil fuels, force the scientists and engineers to come up with ideas for making the energy systems more efficient by developing appropriate technologies to recover and utilise the waste heat [8]. Recovering the waste heat from the utility power plants that burn fossil fuels also helps to reduce the CO_2 emissions which is responsible for the global environmental problem of greenhouse effect [6]. One of the technologies that is suitable in terms of energy efficiency and economic feasibility is to utilise the waste heat for the implementation of vapour absorption refrigeration systems for air-conditioning and cooling purposes.

Figure 11.1 shows a line diagram of the basic VAR system. Like a VCR system, the cooling effect is achieved by the vaporisation of a refrigerant in the evaporator, but the operating principle of the VAR system has two major differences from that of the VCR system [9]. Firstly, unlike the VCR system, a secondary fluid is used in the VAR system as an absorbent for the refrigerant. Secondly, while a VCR system requires mechanical energy to drive it, the VAR system requires heat energy to drive it. A weak solution at state 1 is pumped from the absorber to the generator that *desorbs* the refrigerant from the absorbent at the high pressure. A heat source provides heat to the generator to vaporise

[2] J.M. Abdulateef, M.A. Alghoul, R. Sirwan, A. Zahrim, K. Sopian, Second law thermodynamic analysis of a solar single-stage absorption refrigeration system, *Models and Methods in Applied Sciences,* 2012 pp. 163 – 168.

[3] O. Kaynakli, K. Saka, F. Kaynakli, Energy and exergy analysis of a double effect absorption refrigeration system based on different heat sources, Energy Conversion and Management 106 (2015) 21–30

[4] D-W Sun. Comparison of the performances of NH_3-H_2O, NH_3-$LiNO_3$ and NH_3-NaSCN absorption refrigeration systems. *Energy Convers. Mgmt*, Vol. 39, No. 5/6, 1998, pp. 357-368

[5] S. H. Al-Tahaineh, M. Frihat, M. Al-Rashdan, Exergy Analysis of a Single-Effect Water-Lithium Bromide Absorption Chiller Powered by Waste Energy Source for Different Cooling Capacities, *Energy and Power* 2013, 3(6): 106-118

[6] N. Kurtulmuş, M. Bilgili, B. Şahin, Energy and exergy analysis of a vapor absorption refrigeration system in an intercity bus application, *Journal of Thermal Engineering*, Yildiz Technical University Press, Istanbul, Turkey, Vol. 5, No. 4, pp. 355-371, July, 2019

[7] Md. Meraj, M. Emran Khan, Rashid Imam, Thermodynamic Analysis of Single Effect Vapor Absorption Refrigeration Cycle, *International Journal of Science and Research* (IJSR), ISSN (Online): 2319-7064

[8] N. Sitotaw, Energy and Exergy Analysis of Single Effect Water-LiBr Vapour Absorption Refrigeration System, *International Journal of Advanced Science Computing and Engineering*, Vol. 4, No. 3, December 2022, pp. 175-187

[9] A. Bhatia. Online course. https://www.cedengineering.com/userfiles/M04-025%20%20Overview%20of%20Vapor%20Absorption%20Cooling%20System%20-%20US.pdf

[10] R. Nikbakhti, X. Wang, A. Hussein, and A. Iranmanesh, Absorption cooling systems – Review of various techniques for energy performance enhancement, *Alex. Eng. J.*, vol. 59, pp. 707–738. 2020.

[11] M. Harisha, A.N.R. Reddy, Design of Solar Based Vapour Absorption System, ICEMS-2014

[12] X. Wang and H. T. Chua, Absorption Cooling: A Review of Lithium Bromide-Water Chiller Technologies, Recent Patents on Mechanical Engineering 2009, 2, 193-213 193

[13] F. M. Kashkooli, M. Rezaeian, M. Sefidgar, M. Soltani, M. Mafi, Performance Evaluation of Series and Parallel Two-Stage Absorption Chillers Driven by Solar Energy: Energetic Viewpoint, Gas Processing Journal, Vol. 7, No. 2, 2019

[14] I. H. Yılmaz, K. Saka, Ö. Kaynaklı, Ö. Kaska, Performance Assessment and Solution Procedure for Series Flow Double-Effect Absorption Refrigeration Systems Under Critical Operating Constraints, Arabian Journal for Science and Engineering, March 2019, https://doi.org/10.1007/s13369-019-03805-x

[15] L. Jiang, Z. Gu, X. Feng, Y. Li, Thermo-economical analysis between new absorption–ejector hybrid refrigeration system and small double-effect absorption system, Applied Thermal Engineering 22 (2002) 1027–1036

12

Thermodynamic evaluation of a combined ORC-TFC cycle for power generation from low-grade energy sources

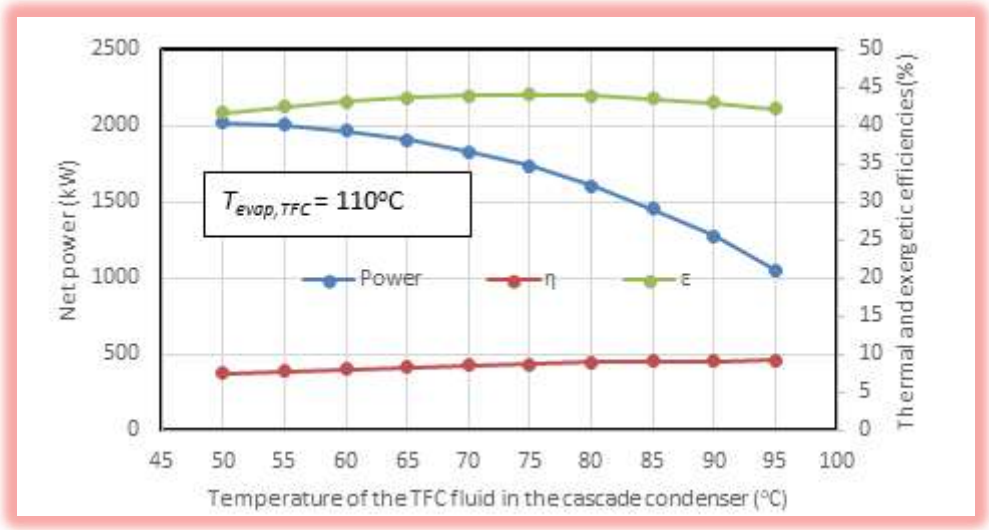

This chapter presents a new power generation cycle for utilising low-grade and renewable energy sources that combines the Organic Rankine Cycle (ORC) with the Trilateral Flash Cycle (TFC). By connecting the two cycles via a cascade condenser and applying the TFC in the high-temperature circuit, the combined cycle enjoys the merits of each cycle while minimising its drawbacks. The thermodynamic performance of the cycle is evaluated by using an Excel-based model that determines the fluid properties with Thermax functions for the refrigerants' group. The accuracy of these functions is first checked by comparing their estimations with relevant published data for the basic ORC and TFC cycles with a number of relevant fluids. The performance of the combined cycle with hot water at 120°C is compared to those of the simple TFC and ORC by using R152a as the working fluid in all three cycles. It is also compared to those of other two-stage and combined ORC-TFC cycles for a source temperature at 300°C using R245fa in the ORC circuit and water in the TFC circuit. Finally, the cycle is analysed with five fluids of low GWP, which are R1234yf in the ORC and R152a, R600, R600a, or R717 in the TFC. The performance of the best pair found, which is R152a/R1234yf, is compared with that of R152a as the single fluid at the cascade temperature that simultaneously maximises the cycle's power, thermal efficiency, and exergetic efficiency.

12.1. Literature review

Fossil-fuels are still the primary source of energy for electricity generation in both developed and developing countries. However, the mounting concerns about the damage to the environment and the climate changes have inspired intensive research for utilising renewable energy sources such as solar and geothermal energies. Another abundant source of energy that can also contribute to solving this problem is the wasted heat in the industrial, commercial, and transport sectors [1-3]. A common feature of these two energies is their low to moderate temperatures. Therefore, the development of appropriate technologies for utilising low/moderate energy sources is beneficial to both. In this respect, one of the promising technologies are the power generation systems that apply the ORC. Unlike the conventional Rankine cycle that requires steam at very high temperatures to drive the turbine, the ORC can be adapted to heat sources at low and moderate temperatures by using an organic working fluid instead of water. Low efficiency is the main drawback of the cycle particularly for the low-temperature (<100°C) energy sources that constitute 63% of the waste heat [4]. According to Iqbal et al. [5], the simple ORC is not economically feasible at temperatures lower than 80°C.

As for the conventional Rankine cycle, various improvements to the simple ORC have been considered such as reheating, regeneration, and recuperation [2]. However, such modifications do not address an inherent drawback of the cycle which is the mismatch between the temperature of the heating source and that of the working-fluid during the heat-addition process in the evaporator since the first remains constant while the second drops steadily. To solve this problem, the TFC has been proposed [5-9]. In this cycle, the heat recovery process is not allowed to vaporise the working which is taken directly as saturated liquid to expand in a two-phase expander. The problem with the TFC is that the technology of expanders is relatively immature and, therefore, they are less efficient

References

[1] A.A. Bidgoli and J.I. Yanagihar, Integration of the Compression Units of the Processing Plant with an Organic Rankin Cycle for Power Generation and Cooling Process, Proceedings of ECOS 2023 - the 36th International Conference on Efficiency, Cost, Optimization, Simulation and Environmental Impact of Energy Systems 25-30 June, 2023, Las Palmas De Gran Canaria, Spain

[2] J.J. Fierro, C. Hern´andez-G´omez, C.A. Marenco-Porto, C. Nieto-Londo˜no, A. Escudero-Atehortua, M. Giraldo, H. Jouhara, L.C. Wrobel, Exergo-economic comparison of waste heat recovery cycles for a cement industry case study, Energy Conversion and Management: X 13 (2022) 100180

[3] C. Wolf, E. Rothuizen, T. Ommen, Exergoeconomic Analysis of a Solar Powered ORC using Zeotropic Mixtures for Combined Heat & Power Generation, Proceedings of ECOS 2023 - the 36th International Conference on Efficiency, Cost, Optimization, Simulation and Environmental Impact of Energy Systems 25-30 June, 2023, Las Palmas De Gran Canaria, Spain

[4] Forman, C., Muritala, I.K., Pardemann, R., Meyer, B. Estimating the Global Waste Heat Potential. Renew. Sustain. Energy Rev. 2016, 57, 1568–1579.

[5] Md Arbab Iqbal et al. Trilateral Flash Cycle (TFC): a promising thermodynamic cycle for low grade heat to power generation, 2nd International Conference on Energy and Power, ICEP2018, 13–15 December 2018, Sydney, Australia, / Energy Procedia 160 (2019) 208–214

[6] A. Skiadopoulos, C. Antonopoulou, K. Atsonios, P. Grammelis, A. Gkountas, P. Bakalis, G. Kosmadakis, and D. Manolakos, Trilateral Flash Cycle for efficient low temperature solar heat harvesting- A case study, Proceedings of ECOS 2023 - the 36th International Conference on Efficiency, Cost, Optimization, Simulation and Environmental Impact of Energy Systems 25-30 June, 2023, Las Palmas De Gran Canaria, Spain

[7] M. Yari, A.S. Mehr, V. Zare, S.M.S. Mahmoudi, M.A. Rosen, Exergoeconomic comparison of TLC (trilateral Rankine cycle), ORC (organic Rankine cycle) and Kalina cycle using a low grade heat source, Energy 83 (2015) 712-722

[8] K-Y. Lai, Y-T. Lee, M-R. Chen and Y-H. Liu, Comparison of the Trilateral Flash Cycle and Rankine Cycle with Organic Fluid Using the Pinch Point Temperature, Entropy (2019), 21, 1197

[9] P. Lykas, C. Antonopoulou, A. Gkountas, K. Atsonios, G. Itskos, N. Nikolopoulos, P. Grammelis, D. Manolakos and P. Bakalis, Thermodynamic and economic performance of novel organic cycle designs powered by low temperature waste heat, Proceedings of ECOS 2023 - the 36th International Conference on Efficiency, Cost, Optimization, Simulation and Environmental Impact of Energy Systems 25-30 June, 2023, Las Palmas De Gran Canaria, Spain

[10] L. Yu, W. Chen, A. Kan, Y. Zhang, S. Xue, J. Zeng, Investigation of a Dual-Loop ORC for the Waste Heat Recovery of a Marine Main Engine. Energies 2022, 15, 8365. https://doi.org/10.3390/en15228365

[11] X. Li, T. Liu and L. Chen, Thermodynamic Performance Analysis of an Improved Two-Stage Organic Rankine Cycle, Energies 2018, 11, 2864; doi:10.3390/en11112864

[12] Z.-Q. Wang, Y. Hu, X. Xia, Comparison of Conventional and Advanced Exergy Analysis for Dual-Loop Organic Rankine Cycle used in Engine Waste Heat Recovery, Journal of Thermal Science 30(1) 1-14, 2020 https://doi.org/10.1007/s11630-020-1299-x

[13] G. Liu, Q. Wang, J. Xu, Z. Miao. Exergy Analysis of Two-Stage Organic Rankine Cycle Power Generation System. Entropy 2021, 23, 43. https://doi.org/ 10.3390/e23010043

[14] Z. Li, R. Huang, Y. Lu, A. P. Roskilly, X. Yu, Analysis of a combined trilateral cycle - organic Rankine cycle (TLC-ORC) system for waste heat recovery, 10th International Conference on Applied Energy (ICAE2018), 22-25 August 2018, Hong Kong, China, Energy Procedia 158 (2019) 1786–1791, Science Direct, Available online at www.sciencedirect.com

[15] X. Yu, Z. Li, Y. Lu, R. Huang and A. P. Roskilly, Investigation of an Innovative Cascade Cycle Combining a Trilateral Cycle and an Organic Rankine Cycle (TLC-ORC) for Industry or Transport Application, Energies 2018, 11, 3032; doi:10.3390/en11113032, www.mdpi.com/journal/energies

[16] J.C. Jiménez-García, A. Ruiz, A. Pacheco-Reyes, W.A. Rivera, Comprehensive Review of Organic Rankine Cycles. Processes 2023, 11, 1982. https://doi.org/10.3390/pr11071982

[17] S. Trædal, Analysis of the Trilateral Flash Cycle for Power Production from Low Temperature Heat Sources. Master's Thesis, Institutt for Energi-og Prosessteknikk, Kolbjørn Hejes v 1B, Trondheim, 2014.

[18] C.O.C. Oko and, E.O. Diemuodeke, MS Excel spreadsheet add-in for thermodynamic properties and process simulation of R152a, Energy Science and Technology, Vol. 5, No. 2, 2013, pp. 63-69.

[19] M. Schlueter, J. Rueckmann, M. Gerdts. A Numerical Study of MIDACO on 100 MINLP Benchmarks, Optimization: A Journal of Mathematical Programming and Operations Research, 61,2012,7, 873-900.

[20] N.H. Mokarram, A.H. Mosaffa. Investigation of the thermoeconomic improvement of integrating enhanced geothermal single flash with transcritical organic Rankine cycle. Energy Convers. Manag. 2020, 213, 112831.

[21] M.J. Moran and H.N. Shapiro, Fundamentals of Engineering Thermodynamics, 5th edition, John Wiley, & Sons. Inc. 2006

[22] ASHRAE Handbook–Refrigeration, 2017, American Society of Heating, Refrigerating and Air-Conditioning Engineers, Inc., (SI Edition).

[23] M.M. El-Awad, A Solver-TOPSIS technique for multi-objective optimisation of innovative multi-stage VCR systems by using Microsoft Excel, Journal of Engineering Research. Faculty of Engineering-University of Tripoli, Issue (38), November 2024, 25-42, https://www.jer.ly/search_articles.php?f=38

[11] X. Li, T. Liu and L. Chen, Thermodynamic Performance Analysis of an Improved Two-Stage Organic Rankine Cycle, Energies 2018, 11, 2864; doi:10.3390/en11112864

[12] Z.-Q. Wang, Y. Hu, X. Xia, Comparison of Conventional and Advanced Exergy Analysis for Dual-Loop Organic Rankine Cycle used in Engine Waste Heat Recovery, Journal of Thermal Science 30(1) 1-14, 2020 https://doi.org/10.1007/s11630-020-1299-x

[13] G. Liu, Q. Wang, J. Xu, Z. Miao. Exergy Analysis of Two-Stage Organic Rankine Cycle Power Generation System. Entropy 2021, 23, 43. https://doi.org/ 10.3390/e23010043

[14] Z. Li, R. Huang, Y. Lu, A. P. Roskilly, X. Yu, Analysis of a combined trilateral cycle - organic Rankine cycle (TLC-ORC) system for waste heat recovery, 10th International Conference on Applied Energy (ICAE2018), 22-25 August 2018, Hong Kong, China, Energy Procedia 158 (2019) 1786–1791, Science Direct, Available online at www.sciencedirect.com

[15] X. Yu, Z. Li, Y. Lu, R. Huang and A. P. Roskilly, Investigation of an Innovative Cascade Cycle Combining a Trilateral Cycle and an Organic Rankine Cycle (TLC-ORC) for Industry or Transport Application, Energies 2018, 11, 3032; doi:10.3390/en11113032, www.mdpi.com/journal/energies

[16] J.C. Jiménez-García, A. Ruiz, A. Pacheco-Reyes, W.A. Rivera, Comprehensive Review of Organic Rankine Cycles. Processes 2023, 11, 1982. https://doi.org/10.3390/pr11071982

[17] S. Trædal, Analysis of the Trilateral Flash Cycle for Power Production from Low Temperature Heat Sources. Master's Thesis, Institutt for Energi-og Prosessteknikk, Kolbjørn Hejes v 1B, Trondheim, 2014.

[18] C.O.C. Oko and, E.O. Diemuodeke, MS Excel spreadsheet add-in for thermodynamic properties and process simulation of R152a, Energy Science and Technology, Vol. 5, No. 2, 2013, pp. 63-69.

[19] M. Schlueter, J. Rueckmann, M. Gerdts. A Numerical Study of MIDACO on 100 MINLP Benchmarks, Optimization: A Journal of Mathematical Programming and Operations Research, 61,2012,7, 873-900.

[20] N.H. Mokarram, A.H. Mosaffa. Investigation of the thermoeconomic improvement of integrating enhanced geothermal single flash with transcritical organic Rankine cycle. Energy Convers. Manag. 2020, 213, 112831.

[21] M.J. Moran and H.N. Shapiro, Fundamentals of Engineering Thermodynamics, 5th edition, John Wiley, & Sons. Inc. 2006

[22] ASHRAE Handbook–Refrigeration, 2017, American Society of Heating, Refrigerating and Air-Conditioning Engineers, Inc., (SI Edition).

[23] M.M. El-Awad, A Solver-TOPSIS technique for multi-objective optimisation of innovative multi-stage VCR systems by using Microsoft Excel, Journal of Engineering Research. Faculty of Engineering-University of Tripoli, Issue (38), November 2024, 25-42, https://www.jer.ly/search_articles.php?f=38

Appendices

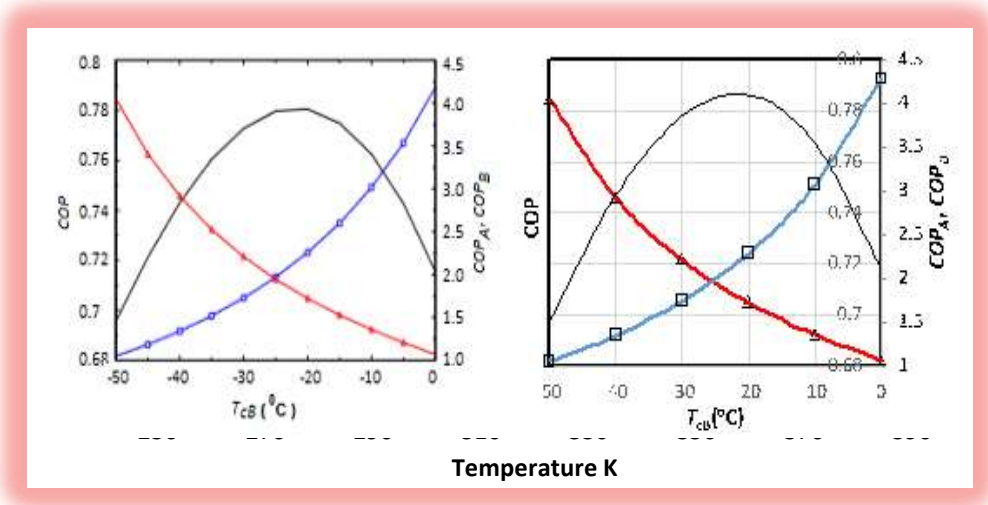
0.8
0.78
0.76
0.74
0.72
0.7
0.68
COP
4.5
4.0
3.5
3.0
2.5
2.0
1.5
1.0
COP_A, COP_B
-50
-40
-30
-20
-10
0
T_cB (°C)
COP
0.78
0.76
0.74
0.72
0.7
0.68
4
3.5
3
2.5
2
1.5
1
COP_A, COP_B
50
40
30
20
10
0
T_cb (°C)
Temperature K

Appendix A: Ideal gases, refrigerants, and chemical reactants supported by Thermax

Thermax functions for ideal gases, refrigerants, and combustion analyses deal with multiple substances and, therefore, require the name of the particular substance in the analysis to be provided. This appendix lists the various substances in these three groups with their Thermax names.

A: Ideal gases

Table A.1 lists 29 gases included in the gas-group (Gas) with their respective reference names used by Thermax.

Table A.1. Gases supported by the ideal-gas group (Gas)

#	Gas	Formula	Thermax name
1	Nitrogen	N_2	N2
2	Oxygen	O_2	O2
3	Air	—	Air
4	Hydrogen	H_2	H2
5	Carbon monoxide	CO	CO
6	Carbon dioxide	CO_2	CO2
7	Water vapour	H_2O	H2O
8	Nitric oxide	NO	NO
9	Nitrous oxide	N_2O	N2O
10	Nitrogen dioxide	NO_2	NO2
11	Ammonia	NH_3	NH3
12	Sulphur	S_2	S2
13	Sulphur dioxide	SO_2	SO2
14	Sulphur trioxide	SO_3	SO3
15	Acetylene	C_2H_2	C2H2
16	Benzene	C_6H_6	C6H6
17	Methanol	CH_4O	CH4O
18	Ethanol	C_2H_6O	C2H6O
19	Hydrogen chloride	HCl	HCl
20	Methane	CH_4	CH4
21	Ethane	C_2H_6	C2H6
22	Propane	C_3H_8	C3H8 or R290
23	*n*-Butane	C_4H_{10}	C4H10n or R600
24	*i*-Butane	C_4H_{10}	C4H10i or R600a
25	*n*-Pentane	C_5H_{12}	C5H12
26	*n*-Hexane	C_6H_{14}	C6H14
27	Ethylene	C_2H_4	C2H4
28	Propylene	C_3H_6	C3H6
29	Octane	C_8H_{18}	C8H18

B: Vapour-compression refrigerants

Table A.2 lists the 28 refrigerants for VCR systems supported by the refrigerants group (Ref) that include 18 halocarbon refrigerants, three inorganic refrigerants (ammonia, water, and carbon dioxide), and seven hydrocarbon refrigerants included by ASHRAE [2].

Table A.2. Refrigerants supported by the refrigerants group (Ref)

#	ASHRAE designation [2]	Thermax name	#	ASHRAE designation [2]	Thermax name
1	R-12 (dichlorodifluoromethane)	R12	15	R-404A [R-125/143a/134a (44/52/4)]	R404A
2	R-22 (chlorodifluoromethane)	R22	16	R-407C [R-32/125/134a (23/25/52)]	R407C
3	R-23 (trifluoromethane) .	R23	17	R-410A [R-32/125 (50/50)]	R410A
4	R-32 (methylenefluoride)	R32	18	R-507A [R-125/143a (50/50)]	R507A
5	R-123 (dichlorotrifluroethane)	R123	19	R-717 (ammonia)	R717
6	R-124 (2-chloro-1,1,1,2-tetrafluoroethane)	R124	20	R-718 (water/steam)	R718
7	R-125 (pentafluoroethane)	R125	21	R-744 (carbon dioxide)	R744
8	R-134a (tetrafluoroethane)	R134a	22	R-50 (methane)	R50
9	R-143a (1,1,1-trifluoroethane)	R143a	23	R-170 (ethane).	R170
10	R-152a (difluoroethane)	R152a	24	R-290 (propane)	R290
11	R-245fa (1,1,1,3,3-pentafluoropropane)	R245fa	25	R-600 (butane)	R600
12	R-1233zd (trans-1-chloro-3,3,3-trifluoroprop-1-ene)	R1233zd	26	R-600a (isobutane)	R600a
13	R1234yf (2,3,3,3-tetrafluoroprop-1-ene)	R1234yf	27	R-1150 (ethylene)	R1150
14	R1234ze (trans-1,3,3,3-tetrafluoropropene)	R1234ze	28	R-1270 (propylene)	R1270

C: Combustion and chemical reactions

Thermax provides three general functions, called **Chm_f1**, **Chm_f2**, and **Chm_f3**, for the analyses of combustion process and chemical reactions. The three functions require as input the intended property as well as the substance name. Table A.3 lists the 29 fuels and reactive substances which are the subjects of the first function **Chm_f1** and Table A.4 shows the four properties associated with this function which are the molar mass (M), the molar enthalpy of formation ($\bar{h}_f^0$), the molar Gibbs function of formation ($\bar{g}_f^0$), and the molar absolute entropy ($\bar{s}^0$). Table A.5 lists the 20 substances supported by the second function **Chm_f2**, while Table A.6 shows the nine properties associated with this function for a general substance of the chemical representation $C_\alpha H_\beta O_\gamma N_\delta$.

Table A.3. List of common reactants and reaction products in **Chm_f1** function

#	Substance	Phase	Thermax name
1	Carbon	Gas	C
2	Hydrogen	Gas	H2
3	Nitrogen	Gas	N2
4	Oxygen	Gas	O2
5	Carbon monoxide	Gas	CO
6	Carbon dioxide	Gas	CO2
7	Steam	Gas	H2O
8	Water	Liquid	H2OL
9	Hydrogen peroxide	Gas	H2O2
10	Ammonia	Gas	NH3
11	Methane	Gas	CH4
12	Acetylene	Gas	C2H2
13	Ethylene	Gas	C2H4
14	Ethane	Gas	C2H6
15	Propylene	Gas	C3H6
16	Propane	Gas	C3H8
17	*n*-Butane	Gas	C4H10
18	*n*-Octane	Gas	C8H18
19	*n*-Octane	Liquid	C8H18L
20	*n*-Dodecane	Gas	C12H26
21	Benzene	Gas	C6H6
22	Methyl alcohol	Gas	CH3OH
23	Methyl alcohol	Liquid	CH3OHL
24	Ethyl alcohol	Gas	C2H5OH
25	Ethyl alcohol	Liquid	C2H5OHL
26	Oxygen1	Gas	O
27	Hydrogen1	Gas	H
28	Nitrogen1	Gas	N
29	Hydroxyl	Gas	OH

Table A.4. Properties provided by the first function, **Chm_f1**

	Property [unit]	Thermax name
1	Molar mass (*M*), [kg/kmol]	M
2	Molar enthalpy of formation ($\bar{h}_f^0$), [kJ/kmol]	hf0
3	Molar Gibbs function of formation ($\bar{g}_f^0$), [kJ/kmol]	gf0
4	Molar absolute entropy ($\bar{s}^0$), [kJ/kmol.K]	as0

Table A.5. List of fuels and reacting substances in **Chm_f2** function

#	Substance	Formulae	Thermax name
1	Gasoline	C_8H_{15}	C8H15
2	Light diesel	$C_{12.3}H_{22.2}$	LDL
3	Heavy diesel	$C_{14.6}H_{24.8}$	HDL
4	Isooctane	C_8H_{18}	C8H18
5	Methanol	CH_3OH	CH3OH
6	Ethanol	C_2H_5OH	C2H5OH
7	Methane	CH_4	CH4
8	Propane	C_3H_8	C3H8
9	Nitromethane	CH_3NO_2	CH3NO2
10	Heptane	C_7H_{16}	C7H16
11	Cetane	$C_{16}H_{34}$	C16H34
12	Heptamethylnonane	$C_{12}H_{34}$	C12H34
13	α-methylnaphthalene	$C_{11}H_{10}$	C11H10
14	Carbon monoxide	CO	CO
15	Coal (carbon)	C	C
16	Butene-1	C_4H_8	C4H8
17	Triptane	C_7H_{16}	C7H16
18	Isodecane	$C_{10}H_{22}$	C10H22
19	Toluene	C_7H_8	C7H8
20	Hydrogen	H_2	H2

Table A.6. Properties provided by the second function, **Chm_f2**

	Property [unit]	Thermax name
1	Molar mass (M), [kg/kmol]	M
2	Gravimetric higher heating values (Q_H), [kJ/kg]	QH
3	Gravimetric lower heating value (Q_L), [kJ/kg]	QL
4	Heat of vaporisation (H_v), [kJ/kg]	HOV
5	Stoichiometric air-fuel ratio (AFR_s)	AF
6	Carbon content of the fuel (α)	ALFA
7	Hydrogen content of the fuel (β)	BETA
8	Oxygen content of the fuel (γ)	GAMA
9	Nitrogen content of the fuel (δ)	DELTA

Note that for **Chm_f1**, steam is referred to by "H2O", while liquid water is referred to by "H2OL". The respective properties for the fuels and reactive substances listed in Table A.3 and Table A.5 are based on those given by Cengel and Boles [1] and Pulkrapek [3], respectively. Case 8 in Table 2.1 shows how the function **Chm_f1** can be used to determine the molar mass (M) of benzene (C_6H_6).

The third function, **Chm_f3**, returns the values of the specific heat, enthalpy, internal energy, and temperature-dependent entropy change of the ideal gases listed in Table A.1

on a unit-mole basis. Table A.7 shows the four properties for ideal gases associated with **Chm_f3** expressed on a unit-mole basis. Case 9 in Table 2.1 shows how the function **Chm_f3** can be used to determine the molar mass of Hydrogen (H_2). Chapter 7 illustrates the use of the three functions in this group for the analyses of combustion processes.

Table A.7. Properties provided by the third function, **Chm_f3**

	Property [unit]	Thermax name
1	Molar specific heat ($\bar{c}_p$), [kJ/kmol.K]	cpm
2	Sensible molar internal energy ($\bar{u}$), [kJ/kmol]	um
3	Sensible molar enthalpy ($\bar{h}$), [kJ/kmol]	hm
4	Temperature-dependent molar entropy ($\bar{s}_0$), [kJ/kmol.K]	s0m

References

[1] Y. A. Cengel and M.A. Boles. *Thermodynamics an Engineering Approach*, McGraw-Hill, 7th Edition, 2007.

[2] American Society of Heating, Refrigeration and Air-Conditioning Engineers, (ASHRAE), Handbook of fundamentals, Atlanta, 2017.

[3] W.W. Pulkrabek, *Engineering Fundamentals of the Internal Combustion Engine*, Second Edition, Pearson Prentice Hall, 2004.

Appendix B: Determining the thermodynamic properties of ideal gases and humid air

This appendix describes the thermodynamic relationships used to develop the property functions provided by Thermax for ideal-gases and humid-air. The basic relationships for ideal gases and humid air are the familiar relationships given in standard textbooks [1]. The functions for humid air needed auxiliary functions to determine the enthalpy of saturated liquid water and water vapour as well as the saturation pressure and saturation temperature for water in the temperatures range 0 – 100°C.

A. Properties of ideal gases

Properties of ideal gases at a given temperature are obtained by suitable integration of the following equation for the molar specific heat at constant pressure ($\tilde{c}_p$) [1]:

$$\tilde{c}_p = a_0 + a_1 T + a_2 T^2 + a_3 T^3 \qquad \text{[kJ/kmol.K]} \qquad \text{(B.1)}$$

Where T is the absolute temperature and a_0, a_1, a_2, and a_3 are constants that have different values for the 29 gases listed in Table A.1.

Accordingly, the molar enthalpy ($\tilde{h}$), molar internal energy ($\tilde{u}$), and temperature-dependent molar entropy change ($\tilde{s}^0$) of an ideal gas are calculated from [1]:

$$\tilde{h} = \tilde{h}_0 + \int_{T_0}^{T} \tilde{c}_p(T)dT \qquad \text{(B.2)}$$

$$\tilde{u} = \tilde{u}_0 + \int_{T_0}^{T} \tilde{c}_v(T)dT = \tilde{u}_0 + \int_{1}^{2} (\tilde{c}_p(T) - R_u)dT \qquad \text{(B.3)}$$

$$\tilde{s}^0 = \tilde{s}_0^0 + \int_{T_0}^{T} \frac{\tilde{c}_p(T)}{T} dT \qquad \text{(B.4)}$$

Where, $\tilde{h}_0$, $\tilde{u}_0$, and $\tilde{s}_0^0$ are specified values at a reference temperature (T_0) and R_u is the universal gas constant. For $\tilde{h}$ and $\tilde{u}$, the reference temperature is taken as 300K and the corresponding values of $\tilde{h}_0$ and $\tilde{u}_0$ are those given by Cengel and Boles [1]. However, for $\tilde{s}^0$ the reference temperature is taken as 298K and the corresponding value of $\tilde{s}_0^0$ is the absolute entropy of the gas. Thermax functions do not return the molar properties of the ideal-gases as given above, but per kg, i.e., h, u and s^0, given by:

$$h = \tilde{h} / M \tag{B.5}$$

$$u = \tilde{u} / M \tag{B.6}$$

$$s^0 = \tilde{s}^0 / M \tag{B.7}$$

Where M is the molar mass of the gas. The relative pressure (P_r) and relative volume (v_r) of the ideal gases, respectively, are obtained from [1]:

$$P_r = \exp(s°/R) \tag{B.8}$$

$$v_r = T / P_r \tag{B.9}$$

Table A.1 in Appendix A shows the respective add-in reference names for the 29 gases. Chapter 3 illustrates the use of the Gas functions for the analyses of gas-power cycles.

B. Properties of humid air

For psychrometric analyses the enthalpy of humid air (h) is calculated from [1]:

$$h = c_{pa} T + \omega h_v \tag{B.10}$$

Where, c_{pa} is the specific heat at constant pressure for dry air (c_{pa} =1.005 kJ/kg.K), T is the temperature in °C, ω is the absolute humidity, and h_v is the enthalpy of water vapour at the air temperature and partial-pressure of the water-vapour (P_v). The absolute humidity (ω) in Equation (B.24) is determined from:

$$\omega = 0.622 P_v / (P - P_v) \tag{B.11}$$

Where, P is the atmospheric pressure, which is total pressure of the air-water-vapour mixture, and P_v is the partial pressure of water-vapour in the air. The partial pressure of water vapour itself is determined from:

$$P_v = \phi P_{sat} / 100 \tag{B.12}$$

Where ϕ is the relative humidity and P_{sat} is the saturation pressure of water at the given dry-bulb temperature. The enthalpy of water vapour (h_v) in Equation (B.10) is approximated by the following equation [1]:

$$h_v \approx 2500.09 + 1.82T \tag{B.13}$$

Where 2500.09 (kJ/kg) is the enthalpy of saturated water vapour at 0°C and 1.82 is the average c_p value of water vapour in the temperature range -10 to 50°C. Property functions of this group determine the relative humidity from the following relationship:

$$\phi = \omega P / (0.622 + \omega) P_g \tag{B.14}$$

This group needs functions that determine the saturation pressure (P_{sat}) and saturation temperature (T_{sat}) for water in the temperatures range 0 – 100°C usually met in common air-conditioning practice. For the convenience of making this group independent from the water-group, it has its own functions (**PsyPsat_T** and **PsyTsat_P**) that determine these two properties from [2]:

$$P_{sat} = 0.1333 \times 10^{A - \frac{B}{C+T}} \tag{B.15}$$

$$T_{sat} = B / \left[A - \log\left(\frac{P}{0.1333} \right) \right] - C \tag{B.16}$$

Where, T is in °C, P in kPa and the three constants A, B, and C, respectively, have values of 8.07131, 1730.63, 233.426 for $1 < T < 100$°C and 8.14019, 1810.94, 244.485 for $99 < T < 374$°C.

A third auxiliary function in this group determines the enthalpy of saturated liquid water (h_L) at a given temperature. This is obtained from the following equation which was obtained by curve-fitting the data for water in the range 0 – 100°C using Excel's trendline feature:

$$h_L = 0.146 + 4.184T \tag{B.17}$$

The function (**PsyhL_T**) that uses equation (B.17) also makes the Psy group independent from the Wat group. Chapter 6 illustrates the use of this group of functions for the analyses of typical air-conditioning processes and systems.

References

[1] Y. A. Cengel and M. A. Boles. *Thermodynamics an Engineering Approach*, McGraw-Hill, 7th Edition, 2007.

[2] Wikipedia contributors, "Antoine equation", Wikipedia, The Free Encyclopaedia, internet, https://en.wikipedia.org/wiki/Antoine_equation

Appendix C: Validation of Thermax functions for superheated refrigerants

Although the thermodynamic properties of superheated refrigerants can be determined on the basis of accurate representations such as the Benedict-Webb-Rubin (BWR) equation of state [1,2], this approach requires considerable time and effort to develop the property functions. Therefore, Thermax functions in the Ref group adopt a simpler approach bearing in mind that the add-in is primarily intended for educational purposes. While the functions for saturated refrigerants calculate the refrigerants properties by interpolating the trustful data provided by ASHRAE [3], the functions for superheated refrigerants apply modified ideal-gas relationships. This appendix describes the mathematical relationships applied by the functions for superheated refrigerants and compares their estimations with those given by ASHRAE [3] for refrigerant R134a.

A. Specific volume

The molar specific volume ($\tilde{v}$) of a superheated refrigerant is obtained from the following Soave-Redlich-Kwong (SRK) equation of state [4]:

$$P = \frac{R_u T}{\tilde{v} - b} - \frac{a\alpha}{\tilde{v}(\tilde{v} + b)} \tag{C.1}$$

The constants a, b and α, which depend on the refrigerant's pressure and temperature at the critical point, are given by:

$$a = 0.4278\, R_u^2\, T_c^{\,2} / P_c \tag{C.2}$$

$$b = 0.0867\, R_u\, T_c / P_c \tag{C.3}$$

$$\alpha = \left[1 + S\left(1 - \sqrt{T_r}\right)\right]^2 \tag{C.4}$$

Where, T_c and P_c are the temperature and pressure at the critical point, $T_r = T/T_c$ is the reduced temperature, and S is the following function for the acentric factor (ω):

$$S = 0.48508 + 1.55171\, \omega - 0.15613\, \omega^2 \tag{C.5}$$

Values of the acentric factor itself for the various refrigerants are mostly obtained from ASHRAE [3] or other relevant sources. It can also be calculated from [5]:

$$\omega = -\log_{10}\left(p_r^{sat}\right) - 1, \text{ at } T_r = 0.7 \tag{C.6}$$

Where $P_r^{sat} = P_{sat}/P_c$ is the reduced saturation pressure. Values of T_c, P_c, and ω for the 28 refrigerants supported by Thermax are shown in Table C.1.

Table C.1. Properties of the refrigerants supported by the refrigerants group (Ref)

#	ASHRAE designation	Thermax name	M [kg/kmol]	T_c [K]	P_c [MPa]	ω
1	R-12 (dichlorodifluoromethane)	R12	120.91	385.12	4.136100	0.1795
2	R-22 (chlorodifluoromethane)	R22	86.468	369.3	4.990000	0.2208
3	R-23 (trifluoromethane) .	R23	70.0	299.29	4.832000	0.263
4	R-32 (methylenefluoride)	R32	52.02	351.26	5.782000	0.2769
5	R-123 (dichlorotrifluroethane)	R123	152.93	456.83	3.661800	0.2819
6	R-124 (2-chloro-1,1,1,2-tetrafluoroethane)	R124	136.5	395.43	3.624300	0.2881
7	R-125 (pentafluoroethane)	R125	120.0	339.17	3.617700	0.3052
8	R-134a (tetrafluoroethane)	R134a	102.03	374.21	4.059300	0.3268
9	R-143a (1,1,1-trifluoroethane)	R143a	84.0	345.86	3.761000	0.2615
10	R-152a (difluoroethane)	R152a	66.05	386.41	4.516800	0.2752
11	R-245fa (1,1,1,3,3-pentafluoropropane)	R245fa	134.05	427.16	3.651000	0.3776
12	R-1233zd (trans-1-chloro-3,3,3-trifluoroprop-1-ene)	R1233zd	130.5	438.75	3.580000	0.3414
13	R1234yf (2,3,3,3-tetrafluoroprop-1-ene)	R1234yf	114.0	367.85	3.382200	0.276
14	R1234ze (trans-1,3,3,3-tetrafluoropropene)	R1234ze	114.04	382.52	3.636200	0.313
15	R-404A [R-125/143a/134a (44/52/4)]	R404A	97.604	345.2	3.729000	0.275
16	R-407C [R-32/125/134a (23/25/52)]	R407C	86.204	359.18	4.630000	0.3268
17	R-410A [R-32/125 (50/50)]	R410A	72.585	344.51	4.903000	0.296
18	R-507A [R-125/143a (50/50)]	R507A	98.859	343.77	3.705000	0.2793
19	R-717 (ammonia)	R717	17.02	405.4	11.333000	0.256
20	R-718 (water/steam)	R718	18.0	647.1	22.064000	0.3443
21	R-744 (carbon dioxide)	R744	44.0	304.1	7.380000	0.239
22	R-50 (methane)	R50	16.044	190.56	4.599200	0.0114
23	R-170 (ethane).	R170	30.07	305.32	3.872200	0.0995
24	R-290 (propane)	R290	44.097	369.89	4.251200	0.1521
25	R-600 (butane)	R600	58.124	425.13	3.796000	0.201
26	R-600a (isobutane)	R600a	58.124	407.81	3.629000	0.184
27	R-1150 (ethylene)	R1150	28.05	282.35	5.041800	0.0866
28	R-1270 (propylene)	R1270	42.08	365.57	4.664600	0.146

Equation (C.1), which is a non-linear equation that requires a numerical solution, is solved by using a Newton-Raphson solver provided by Thermax. The specific volume (v), in m^3/kg, is then obtained from the molar specific volume, $\tilde{v}$, as follows:

$$v = \tilde{v} / M \tag{C.7}$$

Where M is the molar mass of the refrigerant and its values for the 28 refrigerants supported by Thermax are shown in Table C.1. Figure C.1 compares the densities for refrigerant R134a calculated by using the function **Refv_PT** with those given by ASHRAE [3] for R134a at pressures of 0.1 MPa, 1.4 MPa, and 3.0 MPa. The figure confirms the accuracy of the function's estimations at all three pressure levels.

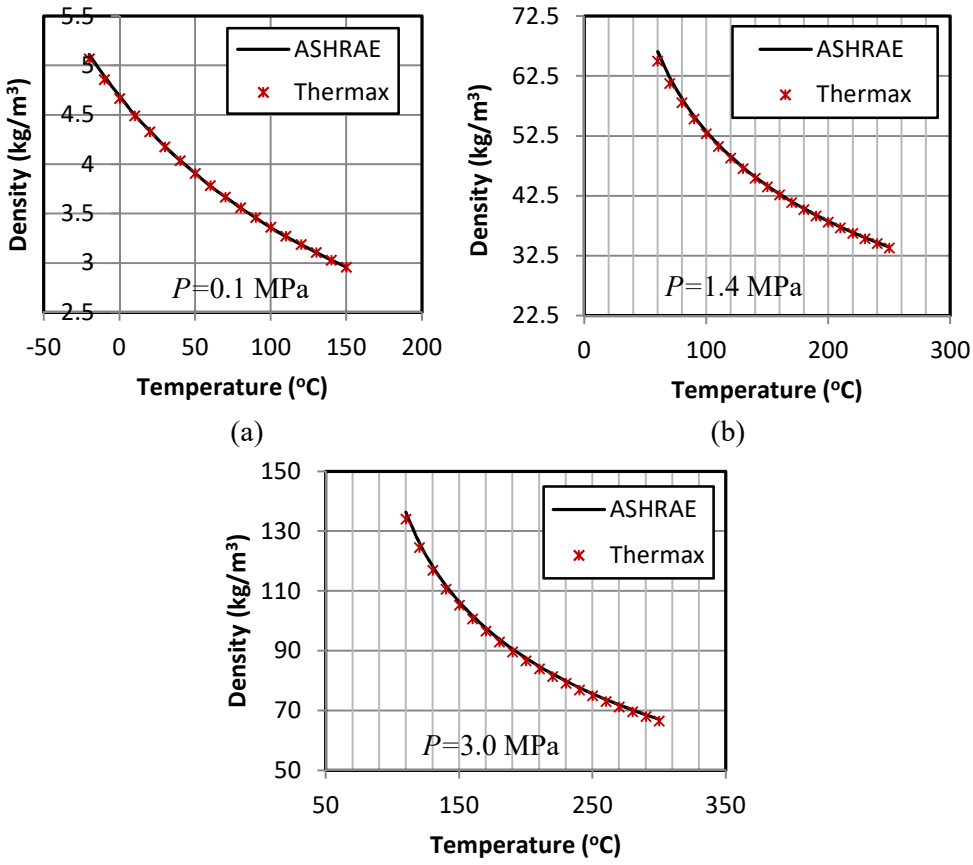

Figure C.1: Accuracy of the computed densities for R134a

B. Enthalpy

Enthalpy (h) of a superheated refrigerant at a given pressure and temperature is determined from the following relationship:

$$h = h_g + Cp_g^*(T - T_s) \tag{C.8}$$

Where h_g and T_s are the enthalpy and temperature of the saturated vapour refrigerant at the given pressure, which are obtained from ASHRAE data [3], while Cp_g^* is the value of its specific heat evaluated at an adjusted – usually reduced - pressure (P*) given by:

$$P^* = f \times P \tag{C.9}$$

Where P is the actual pressure and f is the adjustment factor which can be considered a measure of deviation from ideal-gas behaviour applied to the enthalpy equation like the compressibility factor Z applied to the specific volume.

Figure C.2 compares the values of enthalpy determined by Thermax function **Refh_PT** on the basis of Equations (C.8) and (C.9) at the three pressures with the corresponding values given by ASHRAE [3]. The Figure shows that the values obtained with f= 1.0 deviate considerably from ASHRAE data, especially at P = 3.0 MPa. Equation (C.8) leads to a good accuracy at P 3.0 MPa by using f= 0.5, but not at P = 0.1 or 1.4 MPa.

The accuracy of Equation (C.8) can be improved by making the factor f in Equation (C.9) a function of the pressure ratio to the critical pressure. In this respect, two options were investigated the first of which used the following formula that was obtained by fitting the computed enthalpy values for R134a to ASHRAE data at the three pressures:

$$f = 1.3 \times e^{\left(-\frac{1.55P}{P_c}\right)} \tag{C.10}$$

Where P_c is the critical pressure (for R134a P_c = 4.0593 MPa). Note that according to Equation (C.10), the value of f converges to 0.276 as the pressure approaches P_c and to a value of 1.3 at low pressures.

The second pressure-dependent function tried for f makes it equal to the compressibility factor (Z), i.e.:

$$f = Z = Pv_g / RT_s \tag{C.11}$$

Where T_s and v_g are the saturation temperature and specific volume of the saturated vapour at the given pressure, respectively, and R is the gas constant. The value of v_g was determined from ASHRAE data by using the relevant Thermax function. The enthalpy values computed with f given by Equation (C.10) "f=exp" and by Equation (C.11) "f=Z" are also shown on Figure C.2. The figure shows that both options give similar or better accuracy than f = 0.5 at the three pressure levels, but Equation (C.10) is more accurate than Equation (C.11) at P = 3.0 MPa. The largest deviations of the computed enthalpy values from ASHRAE data occur at P=0.1 MPa, which increase as the temperature increases, i.e. when the gas tends to behave more ideally.

C. Entropy

Entropy (s) of a superheated refrigerant at a given pressure and temperature is determined from the following relationship:

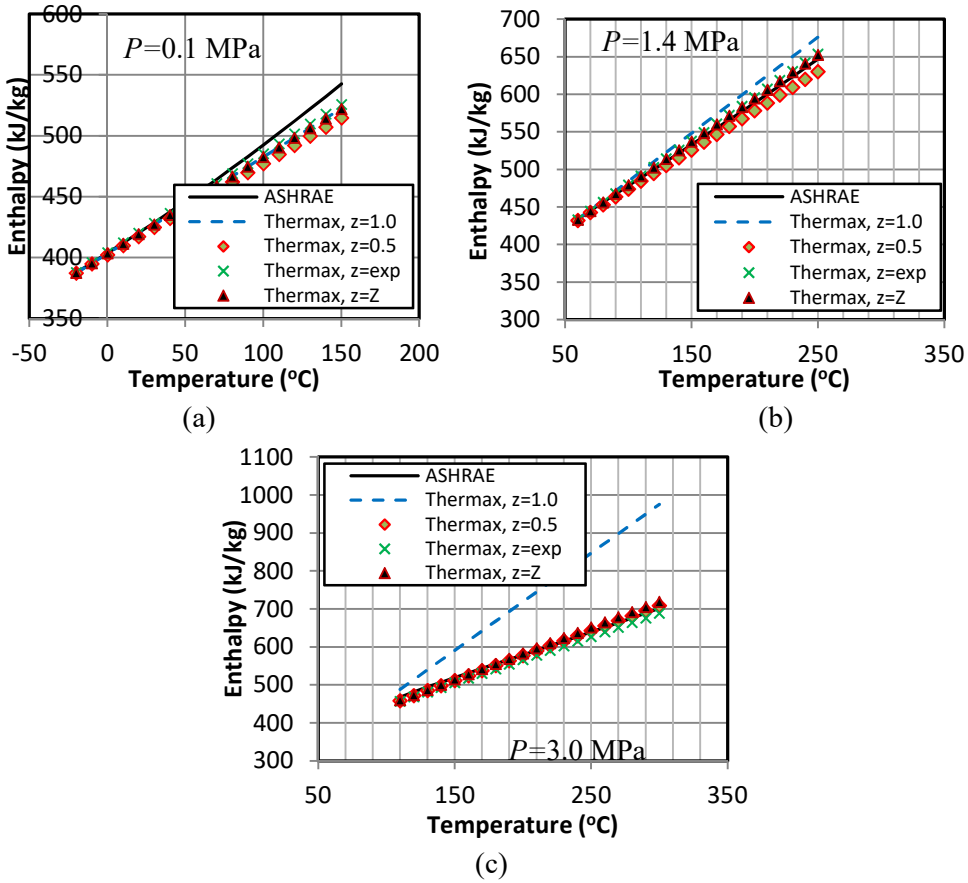

Figure C.2. The accuracy tests for different estimations of computed enthalpy values for R134a at: (a) 0.1 MPa, (b) 1.4 MPa, and (c) 3.0 MPa

$$s = s_g + \frac{Cp_g^*(T - T_s)}{(T_{av} + 273)} \tag{C.12}$$

Where s_g is the entropy of saturated vapour refrigerant at the given pressure, Cp_g^* is the value of the specific heat evaluated at the adjusted pressure (P*) given by Equation (C.9), and T_{av} is an average temperature in °C calculated as follows:

$$T_{av} = (T + T_s)/2 \tag{C.13}$$

Figure C.3 compares the values of entropy determined by the function **Refs_PT** on the basis of Equation (C.12) with the corresponding values given by ASHRAE for R134a at the three pressure levels of 0.1, 1.4, and 3.0 MPa. The figure shows the computed entropy values obtained with f=1.0, f=0.5, f given by Equation (C.10), and f given by Equation

(C.11). As the figure shows, the last three options are reasonably accurate, but best agreement with ASHRAE data is obtained with *f* given by Equation (C.11).

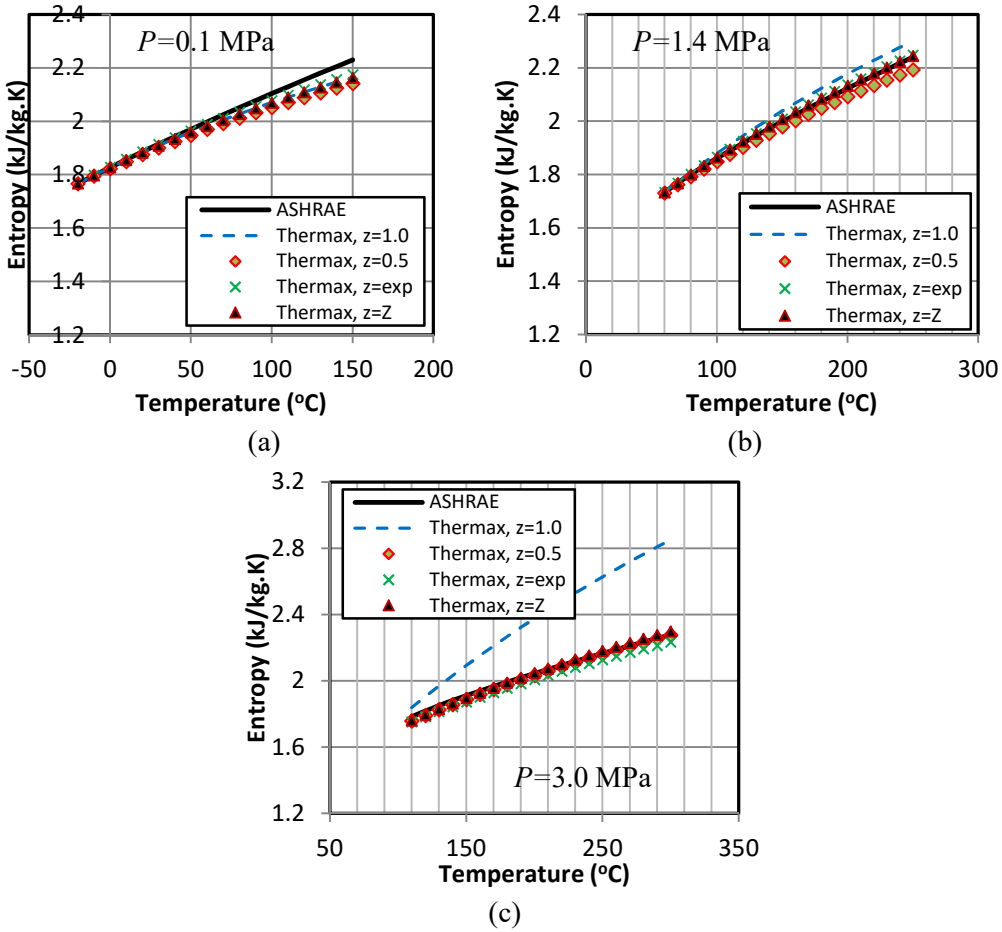

Figure C.3. The accuracy tests for different estimations of computed entropy values for R134a at: (a) 0.1 MPa, (b) 1.4 MPa, and (c) 3.0 MPa

D. The temperature at a given pressure and enthalpy or entropy

Two functions in this subgroup determine the temperature (*T*) of a superheated refrigerant given its pressure (*P*) and its enthalpy (*h*) or entropy (*s*). To determine *T* from *P* and *h*, Equation (C.8) is rearranged as follows:

$$T = T_s + \left(h - h_g\right) / Cp_g^* \tag{C.14}$$

Where T_s and h_g are values of the saturation temperature and enthalpy of saturated refrigerant vapour at the given pressure, but Cp_g^* is the value of the specific heat of saturated refrigerant vapour determined at the adjusted pressure *P**.

Similarly, when the pressure and entropy of the superheated refrigerant are known and its temperature is to be determined, the following equation is obtained from Equation (C.12):

$$T = \left(T_g + 273\right) e^{\frac{s - s_g}{Cp_g^*}} - 273 \qquad \text{(C.15)}$$

Where T_g and s_g are the temperature and entropy of saturated vapour refrigerant at the given pressure, while Cp_g^* is the value of the specific heat of saturated refrigerant vapour determined at the adjusted pressure P^*.

E. Closure

This appendix describes the mathematical relationships used to develop Thermax functions for superheated refrigerants and checks their accuracy by comparing their estimations of the density, enthalpy, and entropy for superheated refrigerant R134a with the values given by ASHRAE [3]. The estimations of the functions for other refrigerants have also been compared with those obtained by using REFPROP and EES [6]. Chapter 5 illustrates the use of the functions for the analyses of different VCR systems, while Chapter 12 uses them to analyses the performance of organic refrigerants as working fluids for the Organic Rankine Cycle (ORC) and the Trilateral Flash Cycle (TFC).

References

[1] B. A. Younglove and M. O. Mclinden, An International Standard Equation of State for the Thermodynamic Properties of Refrigerant 123 (2,2-Dichloro-1, 1,1-Trifluoroethane), Journal of Physical and Chemical Reference Data 23, 731 (1994); https://doi.org/10.1063/1.555950

[2] S. L. Outcalt and M. O. Mclinden, A Modified Benedict-Webb-Rubin Equation of State for the Thermodynamic Properties of R152a (1, 1-difluoroethane), Journal of Physical and Chemical Reference Data 25, 605 (1996); https://doi.org/10.1063/1.555979

[3] American Society of Heating, Refrigeration and Air-Conditioning Engineers, (ASHRAE), Handbook of fundamentals, Atlanta, 2017.

[4] Y. A. Cengel and M. A. Boles. *Thermodynamics an Engineering Approach*, McGraw-Hill, 7th Edition, 2007.

[5] Wikipedia contributors, "Acentric factor", Wikipedia, The Free Encyclopaedia, internet: https://en.wikipedia.org/wiki/Acentric_factor, (last accessed November 30, 2015.

[6] M.M. El-Awad, M.S. Al Nabhani, K.S. Al Hinai, A. Younis. 2019. Development and Validation of an Excel Add-In for Determining the Properties of Various Refrigerants, Proceedings of First National Conference on Recent Trends in Applied Science, Engineering and Technology (CASET 2K19), Ipri College of Technology, June 11, 2019.

Appendix D: Additional first-law analyses of combustion processes

This appendix shows how the Excel sheet developed in Chapter 7 for combustion analyses can be used to deal with additional standard combustion analyses. The analyses considered in this appendix include determining a fuel's enthalpy of combustion and heating value and first-law analyses of combustion in closed systems.

A. Enthalpy of combustion and heating value of a fuel

Since the chemical compositions of fuels like coal, oil, or biogas vary widely, their enthalpy of formation cannot be obtained easily from tables. Therefore, the analysis method presented in the chapter 7 by using the enthalpy of formation is not suitable for dealing with these fuels. A more appropriate method in this case is to use the fuel's enthalpy of combustion instead of its enthalpy of formation. The enthalpy of combustion of a fuel is defined as the amount of heat released during a steady-flow combustion process when 1 kmol (or 1 kg) of fuel is burned completely at a specified temperature and pressure [1]. The enthalpy of combustion can be measured experimentally for any fuel. Equation (7.33) can be rearranged in the following form:

$$Q - W = \underline{\sum_P N_P \tilde{h}_{fP}^0 - \sum_R N_R \tilde{h}_{fR}^0} + \sum_P N_P \Delta\tilde{h}_P - \sum_R N_R \Delta\tilde{h}_R \tag{D.1}$$

The underlined term on the right side of the above equation is nothing but the enthalpy of combustion at the standard temperature and pressure ($\tilde{h}_C^0$). Therefore, the above equation can be written as:

$$Q - W = \tilde{h}_C^0 + \sum_P N_P \Delta\tilde{h}_P - \sum_R N_R \Delta\tilde{h}_R \tag{D.2}$$

If the combustion process involves no work transfer, Equation (D.2) reduces to:

$$Q = \tilde{h}_C^0 + \sum_P N_P \Delta\tilde{h}_P - \sum_R N_R \Delta\tilde{h}_R \tag{D.3}$$

Equation (D.3) indicates that the rate of heat-transfer from the combustion process can be obtained by adding the fuels' enthalpy of combustion at the standard state ($\tilde{h}_C^0$) to the difference in enthalpy deviations of the products and reactant from their respective values at the standard state of 25°C, 1 atm. Thus, Equation (D.3) provides an alternative method to determine the heat-transfer from a combustion process.

The positive value of $\tilde{h}_C^0$ is known as the heating value (HV) of the fuel. Depending on the state of water in the products of combustions, two heating values for a given fuel are quoted; which are the higher heating value (HHV) and the lower heating value (LHV).

The higher heating value is obtained when all the water formed by combustion is a liquid, while the lower heating value is obtained when all the water formed by combustion is a vapour. The two heating values differ by the amount of energy that would be required to vaporise the liquid water in the products. Thermax function "**Chm_f2**" returns the higher and lower heating values per kg for the fuels listed in Table A.5. The following example illustrates how the heat of combustion can be determined by using Equation (D.3).

Example D.1. Combustion analysis using the enthalpy of combustion
Determine the amount of heat transferred in the spark-ignition engine considered in Example 7.2 which operates on stoichiometric propane fuel (C_3H_8) using the heating-value of propane.

Solution
Figure D.1 shows the Excel sheet developed for this example that uses the heating value of propane instead of its enthalpy of formation. The formula window reveals the formula in cell R4 that calculates the heat transfer (Q2_) according to Equation (D.3). The calculated value for the heat transfer is -1,577,339 kJ/kmol of fuel. The value found in Example 7.2 by using the data for enthalpy of formation is 1,577,317 kJ/kmol of fuel.

Q2_ | =-ChmLHV_1(Fuel)*M+Sumh_P2-Sumh_R2

	B	C	D	E	F	G	H	I	J	K	L	M	N	O	P	Q	R	S
1	**Fuel name and temp.**			**Fuel data**			**N of reactants**			**Δh for reactants**			**Air-fuel ratio**			**Steady heat transfer**		
2	**Fuel**	C3H8		α	3		Fuel_R	1		ΔhR_fuel	44774.3		AFR	15.57242		Sumh_R2	333224.8	kJ/kmol fuel
3	Tin_fuel	700	K	β	8		O2_R	5		ΔhR_O2	12613.3		**Air humidity**			Sumh_P2	799898.1	kJ/kmol fuel
4				M	44.09		N2_R	18.8		ΔhR_N2	11988.5		Pv_R	0		**Q2**	-1577339	kJ/kmol fuel
5	**Combustion air**			hf_fuel	-103850		H2O_R	0		ΔhR_H2O	14250.7		ω	0				
6	γ	0	%				Nreactants	24.8					**Products dew point**					
7	ϕ	0	%				**N of products**			**Δh for products**			Pv_P	15.65891	kPa			
8	Tin_air	700	K				CO2_P	3		ΔhP_CO2	44492		TdP	54.91237	°C			
9	Pin_air	101	kPa				CO_P	0		ΔhP_H2O	34506.8		**Fration of condensed water**					
10							H2O_P	4		ΔhP_N2	28106.1		Pratio	4073973				
11	**Discharge temperature**						O2_P	0		ΔhP_O2	29871.4		Nwv_ex	4	kmol			
12	**T_ex**	1200	K				N2_P	18.8		ΔhP_CO	28436.7		Nwl_ex	0	kmol			
13							Nproducts	25.8										
14																		

Figure D.1. Excel sheet developed for combustion analysis using the enthalpy of combustion

B. Enthalpy of combustion from enthalpy of formation
The enthalpy of combustion at standard temperature and pressure ($\tilde{h}_C^0$) can be determined by using the data for enthalpy of formation:

$$\tilde{h}_C^0 = \sum_P N_P \tilde{h}_{fP}^0 - \sum_R N_R \tilde{h}_{fR}^0 \qquad \text{(D.4)}$$

The following example illustrates the procedure of determining the heating value from the enthalpy of formation data.

Example D.2. Calculating enthalpy of combustion for methane
Calculate the enthalpy of combustion of gaseous methane, in kJ per kg of fuel, (a) at 25°C, 1 atm with liquid water in the products, (b) at 25°C, 1 atm with water vapour in the products. (c) Repeat part (b) at 1000 K, 1 atm.

This example is adopted from Moran and Shapiro [1], Example 13.7.

Solution
(a) Figure D.2 shows the modified Excel sheet for part (a) of this example in which the amount of excess air (γ) has been assigned a zero value and all the temperatures have been assigned a value of 298K. The formula window reveals the formula in cell O11 that determines the fraction of water vapour in the products (Nwv_ex). As the formula window shows, this fraction has been forced to be zero so that all the water in the products (2 moles) will be in the liquid phase. Dividing the heat of combustion (Q_p = 890,330 kJ/kmol of fuel) by the molar mass for methane, which is 16.04, gives the heating value (HV). The calculated value, which is 55,506.9 kJ/kg, agrees with the higher heating value of methane determined by Moran and Shapiro [1], which is 55,507 kJ/kg.

Nwv_ex | 0

	B	C	D	E	F	G	H	I	J	K	L	M	N	O	P	Q	R	S
1	**Fuel name and temp.**			**Fuel data**			**N of reactants**			**Δh for reactants**			**Air-fuel ratio**			**Steady heat transfer**		
2	**Fuel**	CH4		α	1		Fuel_R	1		ΔhR_fuel	0		AFR	17.1219		Sumh_R	-74850	kJ/kmol fuel
3	Tin_fuel	298	K	β	4		O2_R	2		ΔhR_O2	0		**Air humidity**			Sumh_P	-965180	kJ/kmol fuel
4				M	16.04		N2_R	7.52		ΔhR_N2	0		Pv_R	0		**Q**	-890330	kJ/kmol fuel
5	**Combustion air**			hf_fuel	-74850		H2O_R	0		ΔhR_H2O	0		ω	0				
6	γ	0	%				Nreactants	10.52					**Products dew point**			**HV**	-55506.9	kJ/kg
7	ϕ	0	%	**Enthalpy of formation**			**N of products**			**Δh for products**			Pv_P	19.20152	kPa			
8	Tin_air	298	K	hf_O2	0		CO2_P	1		ΔhP_CO2	0		TdP	59.20403	°C			
9	Pin_air	101	kPa	hf_N2	0		CO_P	0		ΔhP_H2O	0		**Fration of condensed water**					
10				hf_CO2	-393520		H2O_P	2		ΔhP_N2	0		Pratio	0.031405				
11	**Discharge temperature**			hf_CO	-110530		O2_P	0		ΔhP_O2	0		Nwv_ex	0	kmol			
12	T_ex	298	K	hf_H2O	-241820		N2_P	7.52		ΔhP_CO	0		Nwl_ex	2	kmol			
13				hf_H2OL	-285830		Nproducts	10.52										
14																		

Figure D.2. Excel sheet for determining the higher heating value for methane

(b) Figure D.3 shows the sheet developed for part (b) in which all the water in the products has been forced to be in the vapour phase by making the necessary change to the formula in cell O11. The value of the heating value (HV) has now changed to 50,019.3 kJ/kg, which is the lower heating value for methane as determined by Moran and Shapiro [1], which is 50,019 kJ/kg fuel.

(c) Figure D.4 shows the Excel sheet as modified for this part. Note that the temperatures of the fuel, combustion air, and products of combustion are all assigned a value of 1000K. When the combustion products are at a temperature of 1000K and atmospheric pressure, all the water in the products will be in the vapour phase. The heating value determined in this case is 49,920.0 kJ/kg. The value obtained by Moran and Shapiro [1] is 49,910.0 kJ/kg.

Nwv_ex | 2

	B	C	D	E	F	G	H	I	J	K	L	M	N	O	P	Q	R	S
1	**Fuel name and temp.**			**Fuel data**			**N of reactants**			**Δh for reactants**			**Air-fuel ratio**			**Steady heat transfer**		
2	**Fuel**	CH4		α	1		Fuel_R	1		ΔhR_fuel	0		AFR	17.1219		Sumh_R	-74850	kJ/kmol fuel
3	Tin_fuel	298	K	β	4		O2_R	2		ΔhR_O2	0		**Air humidity**			Sumh_P	-877160	kJ/kmol fuel
4				M	16.04		N2_R	7.52		ΔhR_N2	0		Pv_R	0		**Q**	-802310	kJ/kmol fuel
5	**Combustion air**			hf_fuel	-74850		H2O_R	0		ΔhR_H2O	0		ω	0				
6	γ	0	%				Nreactants	10.52					**Products dew point**			**HV**	-50019.3	kJ/kg
7	ϕ	0	%	**Enthalpy of formation**			**N of products**			**Δh for products**			Pv_P	19.20152	kPa			
8	Tin_air	298	K	hf_O2	0		CO2_P	1		ΔhP_CO2	0		TdP	59.20403	°C			
9	Pin_air	101	kPa	hf_N2	0		CO_P	0		ΔhP_H2O	0		**Fration of condensed water**					
10				hf_CO2	-393520		H2O_P	2		ΔhP_N2	0		Pratio	0.031405				
11	**Discharge temperature**			hf_CO	-110530		O2_P	0		ΔhP_O2	0		Nwv_ex	2	kmol			
12	**T_ex**	298	K	hf_H2O	-241820		N2_P	7.52		ΔhP_CO	0		Nwl_ex	0	kmol			
13				hf_H2OL	-241820		Nproducts	10.52										
14																		

Figure D.3. Excel sheet for determining the lower heating value for methane

R6 | =Q/M

	B	C	D	E	F	G	H	I	J	K	L	M	N	O	P	Q	R	S
1	**Fuel name and temp.**			**Fuel data**			**N of reactants**			**Δh for reactants**			**Air-fuel ratio**			**Steady heat transfer**		
2	**Fuel**	CH4		α	1		Fuel_R	1		ΔhR_fuel	38226.8		AFR	17.1219		Sumh_R	170551.5	kJ/kmol fuel
3	Tin_fuel	1000	K	β	4		O2_R	2		ΔhR_O2	22815.6		**Air humidity**			Sumh_P	-630165	kJ/kmol fuel
4				M	16.04		N2_R	7.52		ΔhR_N2	21481.9		Pv_R	0		**Q**	-800716	kJ/kmol fuel
5	**Combustion air**			hf_fuel	-74850		H2O_R	0		ΔhR_H2O	26040.5		ω	0				
6	γ	0	%				Nreactants	10.52					**Products dew point**			**HV**	-49920	kJ/kg
7	ϕ	0	%	**Enthalpy of formation**			**N of products**			**Δh for products**			Pv_P	19.20152	kPa			
8	Tin_air	1000	K	hf_O2	0		CO2_P	1		ΔhP_CO2	33370.4		TdP	59.20403	°C			
9	Pin_air	101	kPa	hf_N2	0		CO_P	0		ΔhP_H2O	26040.5		**Fration of condensed water**					
10				hf_CO2	-393520		H2O_P	2		ΔhP_N2	21481.9		Pratio	19931.53				
11	**Discharge temperature**			hf_CO	-110530		O2_P	0		ΔhP_O2	22815.6		Nwv_ex	2	kmol			
12	**T_ex**	1000	K	hf_H2O	-241820		N2_P	7.52		ΔhP_CO	21727.8		Nwl_ex	0	kmol			
13				hf_H2OL	-285830		Nproducts	10.52										
14																		

Figure D.4. Excel sheet for determining the heat value for methane at 1000K

C. Determining the heating values for gaseous fuels

For gaseous fuels (treated as ideal gasses), the heating values are usually stated on a volumetric basis rather on a mass basis. If the heating value on a mole basis (HV) is known, one can obtain that per cubic meter (HV′) from the following relation [2]:

$$HV' = \frac{HV}{24.5} \qquad [\text{kJ/m}^3] \qquad \text{(D.5)}$$

The following example that demonstrates the use of the combustion sheet for determining HV′ for fuel mixtures is based on Example 11-4 by Annamalai and Puri [2].

Example D.3. Determining the heating values for biogas

If biogas is assumed to consist of 60% methane and 40% carbon dioxide (volume %), what is its higher heating value at 298K?

Solution

The sheet developed for this example requires some extensions to the sheet developed for determining the mass-based heat value of a single fuel. Figure D.5 shows these

extensions that determine the heating value for CH_4 per m^3 when water vapour is in the vapour phase. Note that formula window in Figure D.5 reveals the formula in cell R6 that determines the volumetric heat value for CH_4 according to Equation (D.5).

HV_CH4 | =Q/24.5

	B	C	D	E	F	G	H	I	J	K	L	M	N	O	P	Q	R	S
1	**Fuel name and temp.**			**Fuel data**			**N of reactants**			**Δh for reactants**			**Air-fuel ratio**			**Steady heat transfer**		
2	**Fuel**	CH4		α	1		Fuel_R	1		ΔhR_fuel	0		AFR	17.1219		Sumh_R	-74850	kJ/kmol fuel
3	Tin_fuel	298	K	β	4		O2_R	2		ΔhR_O2	0		**Air humidity**			Sumh_P	-965180	kJ/kmol fuel
4				M	16.04		N2_R	7.52		ΔhR_N2	0		Pv_R	0		**Q**	-890330	kJ/kmol fuel
5	**Combustion air**			hf_fuel	-74850		H2O_R	0		ΔhR_H2O	0		ω	0				
6	γ	0	%				Nreactants	10.52					**Products dew point**			HV_CH4	-36340	kJ/m3
7	ϕ	0	%	**Enthalpy of formation**			**N of products**			**Δh for products**			Pv_P	19.20152	kPa	HV_CO2	0	kJ/m3
8	Tin_air	298	K	hf_O2	0		CO2_P	1		ΔhP_CO2	0		TdP	59.20403	°C	**HV_biogas**	-21804	kJ/m3
9	Pin_air	101	kPa	hf_N2	0		CO_P	0		ΔhP_H2O	0		**Fration of condensed water**					
10				hf_CO2	-393520		H2O_P	2		ΔhP_N2	0		Pratio	0.031405				
11	**Discharge temperature**			hf_CO	-110530		O2_P	0		ΔhP_O2	0		Nwv_ex	0	kmol			
12	T_ex	298	K	hf_H2O	-241820		N2_P	7.52		ΔhP_CO	0		Nwl_ex	2	kmol			
13				hf_H2OL	-285830		Nproducts	10.52										
14																		

Figure D.5. Determining the higher volumetric heat value for biogas

The volumetric heating vale for biogas is given by:

$$HV'_{biogas} = 0.6HV'_{CH4} + 0.4HV'_{C2O}$$

Since the heat value for CO_2 is zero, the heat value for biogas is 60% of that of CH_4. The heat value thus determined, which is 21,804 kJ per m^3, is the same as that obtained by Annamalai and Puri [2].

D. First-law analyses of closed system combustion

For combustion in a closed system, the first-law of thermodynamics reads:

$$Q - W = \sum_P N_P \tilde{u}_P - \sum_R N_R \tilde{u}_R \tag{D.6}$$

Where, $\tilde{u}$ is the molar internal energy of the reactant or product of combustion. For ideal gases:

$$\tilde{u} = \tilde{h} - R_u T \tag{D.7}$$

Where, R_u = 8.314 kJ/kmol.K is the universal gas constant. Substituting in Equation (D.6):

$$Q - W = \sum_P N_P \left(\tilde{h}_P - R_u T_P\right) - \sum_R N_R \left(\tilde{h}_R - R_u T_R\right) \tag{D.8}$$

Replacing $\tilde{h}$ by $\tilde{h}_f^0 + \Delta\tilde{h}$ and rearranging:

$$Q - W = \underline{\sum_P N_P \left(\tilde{h}_{fP}^0 + \Delta\tilde{h}_P\right) - \sum_R N_R \left(\tilde{h}_{fR}^0 + \Delta\tilde{h}_R\right)} - R_u T_P \sum_P N_P + R_u T_R \sum_R N_R \qquad \text{(D.9)}$$

The underlined term on the right side of the equation is equal to the heat transfer in a steady, constant-pressure combustion. Representing this heat transfer by (Q_p), Equation (D.9) can be written as:

$$Q - W = Q_p - R_u \left(T_P \sum_P N_P - T_R \sum_R N_R \right) \qquad \text{(D.10)}$$

The following examples illustrate the use of the combustion sheet to determine the heat-transfer (Q) and adiabatic flame temperature (T_{af}) when combustion takes place in a closed system.

Example D.4. Closed-system heat transfer from the combustion of pentane
A closed, rigid vessel initially contains a gaseous mixture of 1 kmol of pentane (C_5H_{12}) and 150% of theoretical air at 25ºC, 1 atm. If the mixture burns completely, determine the heat transfer from the vessel, in kJ, and the final pressure in atm, for a final temperature of 800 K.

This example is based on problem 13.40 given by Moran and Shapiro [1].

Solution
The sheet developed for steady-flow combustion analyses can also be used for closed-system combustion by adding a single cell in the results part to determine Q_v from Q according to Equation (D.10). The formula window in Figure D.6 reveals the formula in this cell, which is cell R6. The calculated value for Qv, which is 2,561,006 kJ/kmol, closely agree with the value given by Moran and Shapiro [1], which is 2,563,732 kJ/kmol.

R6 =Q-8.314*(Nproducts*T_ex-Nreactants*Tin_fuel)

	B	C	D	E	F	G	H	I	J	K	L	M	N	O	P	Q	R	S
1	**Fuel name and temp.**			**Fuel data**			**N of reactants**			**Δh for reactants**			**Air-fuel ratio**			**Steady heat transfer**		
2	**Fuel**	C5H12		α	5		Fuel_R	1		ΔhR_fuel	0		AFR	22.83869		Sumh_R	-146440	kJ/kmol fuel
3	Tin_fuel	298	K	β	12		O2_R	12		ΔhR_O2	0		**Air humidity**			Sumh_P	-2451572	kJ/kmol fuel
4				M	72.15		N2_R	45.12		ΔhR_N2	0		Pv_R	0		**Q**	-2305132	kJ/kmol fuel
5	**Combustion air**			hf_fuel	-146440		H2O_R	0		ΔhR_H2O	0		ω	0				
6	γ	50	%				Nreactants	58.12					**Products dew point**			**Qv**	-2561006	kJ/kmol fuel
7	ϕ	0	%	**Enthalpy of formation**			**N of products**			**Δh for products**			Pv_P	10.07984	kPa			
8	Tin_air	298	K	hf_O2	0		CO2_P	5		ΔhP_CO2	22743.5		TdP	46.06383	°C			
9	Pin_air	101	kPa	hf_N2	0		CO_P	0		ΔhP_H2O	18060.9		**Fration of condensed water**					
10				hf_CO2	-393520		H2O_P	6		ΔhP_N2	15094.2		Pratio	1175.446				
11	**Discharge temperature**			hf_CO	-110530		O2_P	4		ΔhP_O2	15953.8		Nwv_ex	6	kmol			
12	**T_ex**	800	K	hf_H2O	-241820		N2_P	45.12		ΔhP_CO	15247.2		Nwl_ex	0	kmol			
13				hf_H2OL	-285830		Nproducts	60.12										
14																		

Figure D.6. Excel sheet developed for closed-system combustion of pentane

Example D.5. Adiabatic flame temperature for liquid octane in a closed system
Liquid octane enters a rigid closed system reactor with 40% excess air. Determine the adiabatic flame temperature with both the fuel and air being at 298 K and 1 atm.

This example is based on Example 9 given by Annamalai and Puri [2] in Chapter 11.

Solution
The sheet for this example was developed by making the necessary modifications to that of the previous example. Figure D.7 shows the modified sheet in which the fuel is C8H18L and the amount of excess air is 40%.

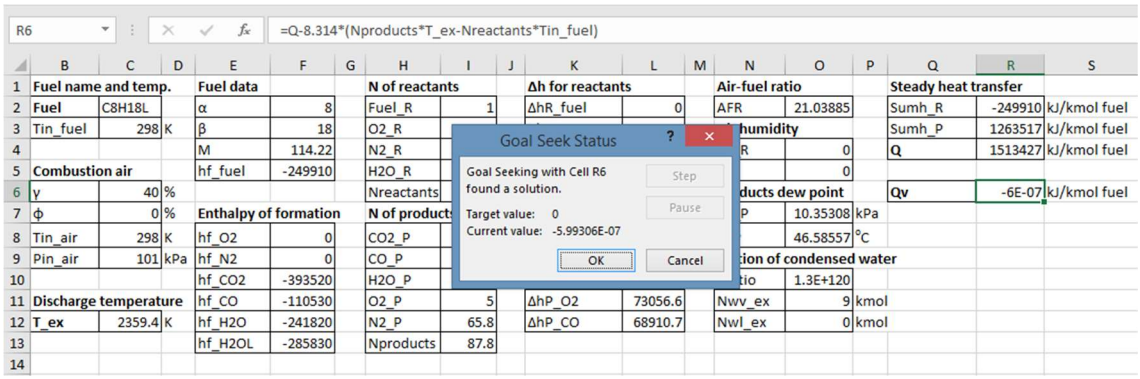

Figure D.7. Adiabatic flame temperature of liquid octane in a constant volume device

Since the fuel is liquid, the fuel's enthalpy change (ΔhR_fuel) in cell L2 is zero. Goal Seek was used to find the adiabatic flame temperature, which is the exhaust temperature (T_ex) at which Qv is zero. Figure D.7 shows the solution obtained, which is 2359.4K. The solution obtained by Annamalai and Puri [2] is 2340K.

References
[1] M.J. Moran and H.N. Shapiro, *Fundamentals of Engineering Thermodynamics*, 5th edition, John Wiley & Sons, Inc, 2006.
[2] K. Annamalai and I.K. Puri. *Advanced Thermodynamics Engineering*, CRC 2002

Appendix E: Second-law analyses of combustion processes

This appendix extends the Excel sheet developed in Chapter 7 for combustion analyses to deal with second-law analyses that determine the rate of entropy production in the combustion process and the maximum work that can be done during the process.

A. Second-law equations

The purpose of fuel combustion is to release the fuel's chemical energy in the form of heat as a necessary step towards converting it into useful work via a heat engine. In this respect, first-law analyses of combustion reactions are useful for quantifying the amount of thermal energy that can be obtained from the combustion process, but they give no indication of the inherent irreversibility of combustion process that leads to significant losses in the work potential of the fuel's chemical energy. By applying the second law of thermodynamics, we can determine the amount of available (reversible) work from the fuel's energy and rate of exergy destruction in the combustion process.

Exergy and reversible work in combustion processes

The property that measures the work potential of the energy content of a fluid stream is its exergy χ (also called availability). Disregards mixing and chemical reactions, the thermo-mechanical exergy is defined as:

$$\chi = \left(\tilde{h} - \tilde{h}_0\right) - T_0\left(\tilde{s} - \tilde{s}_0\right) + \frac{V^2}{2} + gz \tag{E.1}$$

Where, h_0 and s_0 are enthalpy and entropy of the stream at the dead state at (T_0, P_0), respectively, V is the velocity, and z the elevation. Exergy values of the reactants and products enable us to determine the reversible work W_{rev}, which is the maximum work that can be done during a process. In the absence of any changes in kinetic and potential energies, the reversible work relation for a steady-flow combustion process that involves heat transfer with only the surroundings at T_0 can be expressed as [1]:

$$W_{rev} = \sum_R N_R\left(\tilde{h}_f^0 + \tilde{h} - \tilde{h}^0 - T_0\tilde{s}\right)_R - \sum_P N_P\left(\tilde{h}_f^0 + \tilde{h} - \tilde{h}^0 - T_0\tilde{s}\right)_P \tag{E.2}$$

$$W_{rev} = \sum_R N_R\left(\tilde{h}_f^0 + \Delta\tilde{h} - T_0\tilde{s}\right)_R - \sum_P N_P\left(\tilde{h}_f^0 + \Delta\tilde{h} - T_0\tilde{s}\right)_P \tag{E.3}$$

Note that the enthalpy term $\tilde{h} - \tilde{h}^0$ in Equation (E.1) has been replaced by $\tilde{h}_f^0 + \tilde{h} - \tilde{h}^0$, where $\tilde{h}_f^0$ is the enthalpy of formation at the standard reference state.

Exergy destruction and entropy production in the combustion process

The exergy destroyed $\psi_{destroyed}$ associated with a chemical reaction can be determined from:

$$\psi_{destroyed} = T_0 \sigma \tag{E.4}$$

Where σ is the total entropy change or the entropy generation. In combustion processes, entropy is produced by the chemical reaction itself and also as a result of heat-transfer to the surroundings which are usually at a lower temperature. The entropy produced (σ) per unit mole of fuel in a closed or steady-flow reacting system is given by [1]:

$$\sigma = S_p - S_R - \sum_i \frac{Q_i}{T_i} \geq 0 \tag{E.5}$$

Where S_P and S_R are the total entropy of the combustion products and reactants, respectively, per mole of fuel and Q_i is the portion of total heat transfer crossing the section of the system's boundary where the temperature is T_i. Equation (E.5) adopts the usual sign convention that the positive direction of heat transfer is into the system. In terms of entropies of the reactants and products components, Equation (E.5) reads:

$$\sigma = \sum_P N_P \tilde{s}_P - \sum_R N_R \tilde{s}_R - \sum_i \frac{Q_i}{T_i} \geq 0 \tag{E.6}$$

Where $\tilde{s}_P$ and $\tilde{s}_R$ are the absolute molal entropy of the components in the products and reactants, respectively. For component i of a mixture of ideal gases, the absolute entropy at any temperature T and partial pressure P_i can be obtained from [1]:

$$\tilde{s}(T, P_i) = \underline{\tilde{s}_i^o(T, P_0)} - R_u \ln \frac{y_i P_m}{P_0} \tag{E.7}$$

Where y_i is the molal fraction of the gas, P_m is the total pressure of the mixture, and P_0 = 1 atm.

B. Extending the workbook for second-law combustion analyses

Thermax function "**Chms0m_TK**" returns the absolute molal entropy at P_0 = 1 atm and any temperature T, which is the underlined term in Equation (E.7), for all the gases supported by Thermax. Another function, "**Chmas0_1**", returns the absolute molal entropy at the standard temperature and pressure (T_0 = 25ºC, P_0 = 1 atm) of the all the substances supported by Thermax as listed in Table A.4. The following examples extend the general Excel sheet for performing second-law analyses to determine the reversible work of a combustion process and the rate of entropy production.

Example E.1. Second-law analysis of adiabatic combustion of ethylene

Consider the steady-flow adiabatic combustion of gaseous ethylene (C_2H_4) with stoichiometric air, both at 25ºC, and assume complete combustion. If T_0=25ºC, determine (a) the entropy change and (b) the reversible work, both in kJ/kmol of fuel.

This example is adopted from Wark [2], Example 10-5.

Solution

Figure E.1 shows the general Excel sheet that performs first-law analysis of the combustion process with the data part modified to account for the present case in which the fuel is ethylene (C2H4), γ =0%, Tin_air = 298K, and Pin_air =101 kPa. Since the combustion process is adiabatic, Goal Seek was used to determine the adiabatic flame temperature following the procedure of Example 7.5. The value determined by Goal Seek, which is 2606.02K, is higher than that given by Wark [2], which is 2570K, but the error is 1.4%.

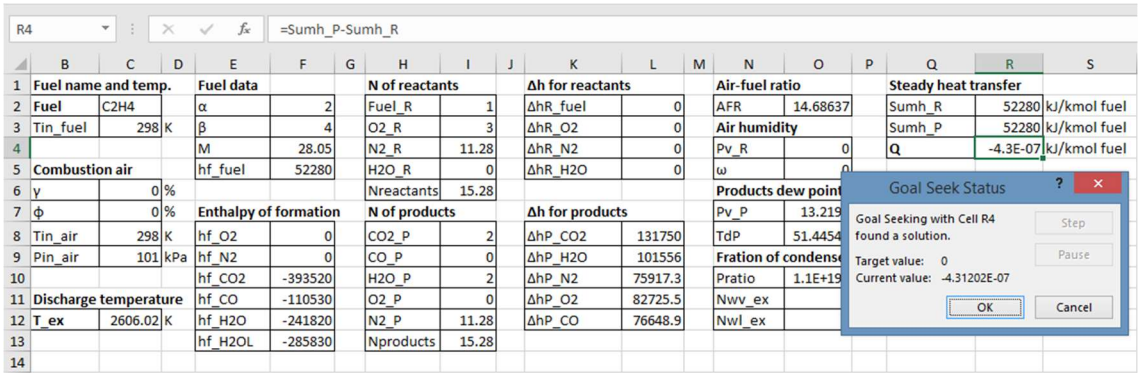

1	**Fuel name and temp.**			**Fuel data**			**N of reactants**			**Δh for reactants**			**Air-fuel ratio**			**Steady heat transfer**		
2	**Fuel**	C2H4		α	2		Fuel_R	1		ΔhR_fuel	0		AFR	14.68637		Sumh_R	52280	kJ/kmol fuel
3	Tin_fuel	298	K	β	4		O2_R	3		ΔhR_O2	0		**Air humidity**			Sumh_P	52280	kJ/kmol fuel
4				M	28.05		N2_R	11.28		ΔhR_N2	0		Pv_R	0		**Q**	-4.3E-07	kJ/kmol fuel
5	**Combustion air**			hf_fuel	52280		H2O_R	0		ΔhR_H2O	0		ω	0				
6	γ	0	%				Nreactants	15.28					**Products dew point**					
7	ϕ	0	%	**Enthalpy of formation**			**N of products**			**Δh for products**			Pv_P	13.219				
8	Tin_air	298	K	hf_O2	0		CO2_P	2		ΔhP_CO2	131750		TdP	51.4454				
9	Pin_air	101	kPa	hf_N2	0		CO_P	0		ΔhP_H2O	101556		**Fration of condens**					
10				hf_CO2	-393520		H2O_P	2		ΔhP_N2	75917.3		Pratio	1.1E+19				
11	**Discharge temperature**			hf_CO	-110530		O2_P	0		ΔhP_O2	82725.5		Nwv_ex					
12	**T_ex**	2606.02	K	hf_H2O	-241820		N2_P	11.28		ΔhP_CO	76648.9		Nwl_ex					
13				hf_H2OL	-285830		Nproducts	15.28										
14																		

Figure E.1. 1st law analysis of the adiabatic combustion of methane gas

Figure E.2 shows the sheet that performs second-law analysis of the combustion process. The analysis is placed in a separate sheet with its data part that shows the specified values of the surroundings pressure (Pref) and temperature (Tref), which are 101 kPa and 298K, respectively. Based on these data, the sheet determines the rate of entropy production (σ_production). The value determined by the sheet, which is 1190.3 kJ/kmol of C_2H_4 agrees well with that given by Wark [2], which is 1189.55 kJ/kmol of C_2H_4.

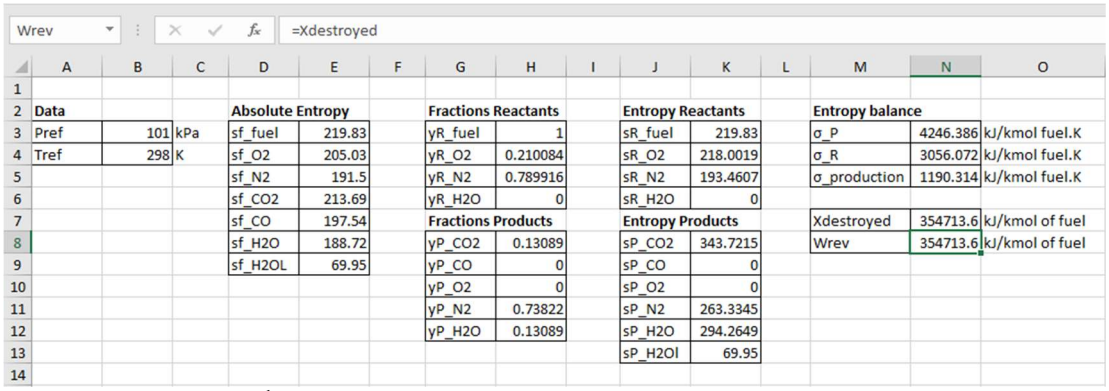

1																		
2	**Data**			**Absolute Entropy**			**Fractions Reactants**			**Entropy Reactants**			**Entropy balance**				
3	Pref	101	kPa	sf_fuel	219.83		yR_fuel	1		sR_fuel	219.83		σ_P	4246.386	kJ/kmol fuel.K		
4	Tref	298	K	sf_O2	205.03		yR_O2	0.210084		sR_O2	218.0019		σ_R	3056.072	kJ/kmol fuel.K		
5				sf_N2	191.5		yR_N2	0.789916		sR_N2	193.4607		σ_production	1190.314	kJ/kmol fuel.K		
6				sf_CO2	213.69		yR_H2O	0		sR_H2O	0							
7				sf_CO	197.54		**Fractions Products**			**Entropy Products**			Xdestroyed	354713.6	kJ/kmol of fuel			
8				sf_H2O	188.72		yP_CO2	0.13089		sP_CO2	343.7215		Wrev	354713.6	kJ/kmol of fuel			
9				sf_H2OL	69.95		yP_CO	0		sP_CO	0							
10							yP_O2	0		sP_O2	0							
11							yP_N2	0.73822		sP_N2	263.3345							
12							yP_H2O	0.13089		sP_H2O	294.2649							
13										sP_H2Ol	69.95							
14																		

Figure E.2. 2nd law analyses of the adiabatic combustion of methane gas

The extension required by the present example is the determination of the rate of exergy destruction (Xdestroyed) and reversible work (Wrev) using Equation (E.3). Since there is no useful work in this process, the reversible work, which is the same as the exergy destruction. The reversible work is determined as 354,713.6 kJ/kmol of C_2H_4, which is close to the value given by Wark [2] of 354,660 kJ/kmol of C_2H_4.

Example E.2. Second-law analysis of isothermal combustion of methane
Methane (CH_4) gas enters a steady-flow combustion chamber at 25°C and 1 atm and is burned with 50 percent excess air, which also enters at 25°C and 1 atm. After combustion, the products are allowed to cool to 25°C. Assuming complete combustion, determine (a) the heat transfer per kmol of CH_4, (b) the entropy generation, and (c) the reversible work and exergy destruction. Assume that T_0 = 298 K and the products leave the combustion chamber at 1 atm pressure.

This example is adopted from Cengel and Boles [1], Example 15.11.

Solution
Figure E.3 shows the modified Excel sheet for this example in which T_ex is entered as 298K. Note is that for gaseous methane the enthalpy change (ΔhR_fuel) is automatically adjusted to zero by the sheet. The value determined for the heat transfer is 871,617 kJ/kmol of fuel. This agrees well with the value obtained by Cengel and Boles [1], which is 871,400 kJ/kmol of fuel.

Q =Sumh_P-Sumh_R

	B	C	D	E	F	G	H	I	J	K	L	M	N	O	P	Q	R	S
1	**Fuel name and temp.**			**Fuel data**			**N of reactants**			**Δh for reactants**			**Air-fuel ratio**			**Steady heat transfer**		
2	**Fuel**	CH4		α	1		Fuel_R	1		ΔhR_fuel	0		AFR	25.68284		Sumh_R	-74850	kJ/kmol fuel
3	Tin_fuel	298	K	β	4		O2_R	3		ΔhR_O2	0		**Air humidity**			Sumh_P	-946230	kJ/kmol fuel
4				M	16.04		N2_R	11.28		ΔhR_N2	0		Pv_R	0		**Q**	-871380	kJ/kmol fuel
5	**Combustion air**			hf_fuel	-74850		H2O_R	0		ΔhR_H2O	0		ω	0				
6	γ	50	%				Nreactants	15.28					**Products dew point**			**Qv**	-871380	kJ/kmol fuel
7	ϕ	0	%	**Enthalpy of formation**			**N of products**			**Δh for products**			Pv_P	13.2199	kPa			
8	Tin_air	298	K	hf_O2	0		CO2_P	1		ΔhP_CO2	0		TdP	51.44542	°C			
9	Pin_air	101	kPa	hf_N2	0		CO_P	0		ΔhP_H2O	0		**Fration of condensed water**					
10				hf_CO2	-393520		H2O_P	2		ΔhP_N2	0		Pratio	0.031405				
11	**Discharge temperature**			hf_CO	-110530		O2_P	1		ΔhP_O2	0		Nwv_ex	0.430581	kmol			
12	T_ex	298	K	hf_H2O	-241820		N2_P	11.28		ΔhP_CO	0		Nwl_ex	1.569419	kmol			
13				hf_H2OL	-285830		Nproducts	15.28										
14																		

Figure E.3. 1st law analysis of the isothermal combustion of methane gas

Figure E.4 shows the sheet that performs the second-law analysis of the combustion process. The sheet calculates the entropy generation as 2,745.02 kJ/kmol.K. The value obtained by Cengel and Boles [1] is 2,746.0 kJ/kmol.K. The exergy destruction, which equals the reversible is calculated as 818,014.6 kJ/kmol of methane. This also agrees with value given by Cengel and Boles [1], which is 818,000.0 kJ/kmol of methane.

For the special case considered in this example in which the reactants, the products, and the surroundings are all at 25°C and the partial pressure P_i = 1 atm for each component of the reactants and the products, Equation (E.3) reduces to [3]:

$$W_{rev} = \sum_{R} N_R \tilde{g}^0_{fR} - \sum_{P} N_P \tilde{g}^0_{fP} \qquad \text{(E.8)}$$

Where, $\tilde{g}^0_f$ is the Gibbs function of formation. Using Thermax functions that return values of the Gibbs function of formation for the reactants and products, Figure E.5 shows that the sheet determines the reversible work as 814,251.3 kJ/kmol of CH_4, which is only marginally different from the value obtained above by using Equation (E.3).

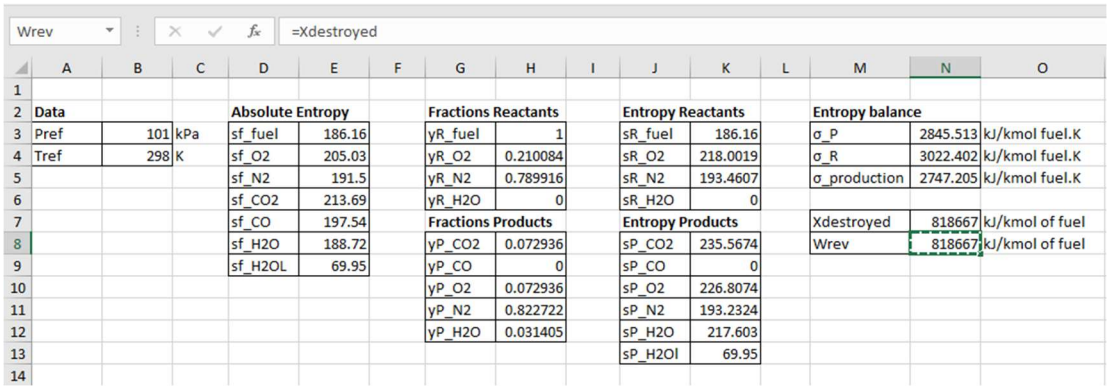

	A	B	C	D	E	F	G	H	I	J	K	L	M	N	O
1															
2	Data			Absolute Entropy			Fractions Reactants			Entropy Reactants			Entropy balance		
3	Pref	101	kPa	sf_fuel	186.16		yR_fuel	1		sR_fuel	186.16		σ_P	2845.513	kJ/kmol fuel.K
4	Tref	298	K	sf_O2	205.03		yR_O2	0.210084		sR_O2	218.0019		σ_R	3022.402	kJ/kmol fuel.K
5				sf_N2	191.5		yR_N2	0.789916		sR_N2	193.4607		σ_production	2747.205	kJ/kmol fuel.K
6				sf_CO2	213.69		yR_H2O	0		sR_H2O	0				
7				sf_CO	197.54		Fractions Products			Entropy Products			Xdestroyed	818667	kJ/kmol of fuel
8				sf_H2O	188.72		yP_CO2	0.072936		sP_CO2	235.5674		Wrev	818667	kJ/kmol of fuel
9				sf_H2OL	69.95		yP_CO	0		sP_CO	0				
10							yP_O2	0.072936		sP_O2	226.8074				
11							yP_N2	0.822722		sP_N2	193.2324				
12							yP_H2O	0.031405		sP_H2O	217.603				
13										sP_H2Ol	69.95				
14															

Figure E.4. 2nd law analyses of the isothermal combustion of methane gas

.

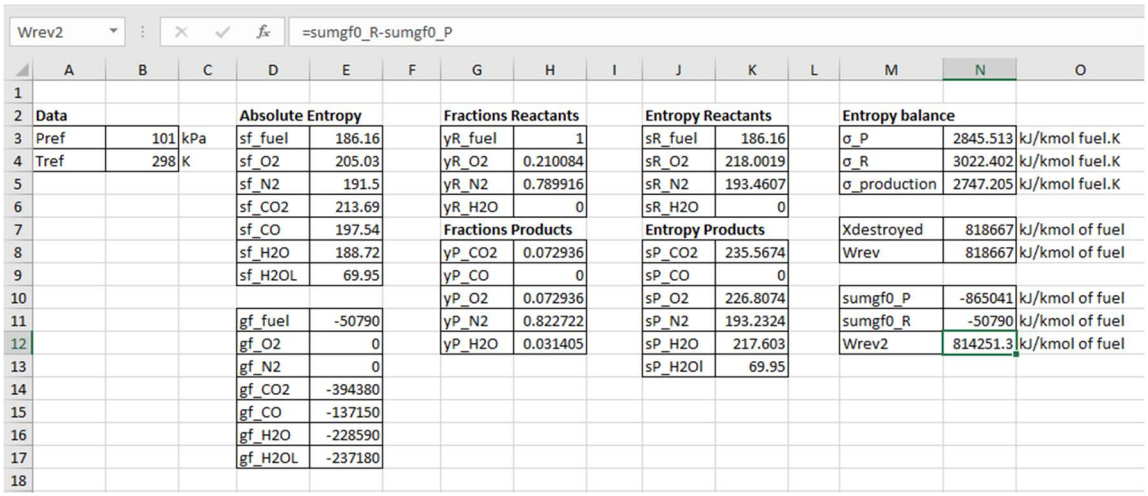

	A	B	C	D	E	F	G	H	I	J	K	L	M	N	O
1															
2	Data			Absolute Entropy			Fractions Reactants			Entropy Reactants			Entropy balance		
3	Pref	101	kPa	sf_fuel	186.16		yR_fuel	1		sR_fuel	186.16		σ_P	2845.513	kJ/kmol fuel.K
4	Tref	298	K	sf_O2	205.03		yR_O2	0.210084		sR_O2	218.0019		σ_R	3022.402	kJ/kmol fuel.K
5				sf_N2	191.5		yR_N2	0.789916		sR_N2	193.4607		σ_production	2747.205	kJ/kmol fuel.K
6				sf_CO2	213.69		yR_H2O	0		sR_H2O	0				
7				sf_CO	197.54		Fractions Products			Entropy Products			Xdestroyed	818667	kJ/kmol of fuel
8				sf_H2O	188.72		yP_CO2	0.072936		sP_CO2	235.5674		Wrev	818667	kJ/kmol of fuel
9				sf_H2OL	69.95		yP_CO	0		sP_CO	0				
10							yP_O2	0.072936		sP_O2	226.8074		sumgf0_P	-865041	kJ/kmol of fuel
11				gf_fuel	-50790		yP_N2	0.822722		sP_N2	193.2324		sumgf0_R	-50790	kJ/kmol of fuel
12				gf_O2	0		yP_H2O	0.031405		sP_H2O	217.603		Wrev2	814251.3	kJ/kmol of fuel
13				gf_N2	0					sP_H2Ol	69.95				
14				gf_CO2	-394380										
15				gf_CO	-137150										
16				gf_H2O	-228590										
17				gf_H2OL	-237180										
18															

Figure E.5. Determining the reversible work from the difference in Gibbs function of formation

The two previous examples applied the second law to analyse two important special cases of adiabatic and isothermal combustion at atmospheric pressure. The following example demonstrates the application of second-law analysis to the more general case in which the process is neither adiabatic nor isothermal and the pressure is not atmospheric.

Example E.3. Second-law analysis of a more general combustion process

1 kmole of butane enters a steady state steady flow reactor at 298 K and 250 kPa with 50% excess air. Combustion is assumed to be complete, and the products leave the reactor at 1000 K and 250 kPa. Determine the heat transfer, reactant and product entropies, the absolute availability of the reactants and products, the entropy change between the exit and inlet, the entropy generation, the optimum work and the irreversibility.

This example is adopted from Annamalai and Puri [4], Example 2 in Chapter 13.

Solution

Figures E.6 and E.7 show the sheets that perform first and second-law analyses of the combustion process, respectively. Note that pressure (Pin_air) has been set to 250 kPa, while the products exit temperature (T_ex) has been set to 1000K.

Q =Sumh_P-Sumh_R

	B	C	D	E	F	G	H	I	J	K	L	M	N	O	P	Q	R	S
1	**Fuel name and temp.**			**Fuel data**			**N of reactants**			**Δh for reactants**			**Air-fuel ratio**			**Steady heat transfer**		
2	**Fuel**	C4H10		α	4		Fuel_R	1		ΔhR_fuel	0		AFR	23.0359		Sumh_R	-126150	kJ/kmol fuel
3	Tin_fuel	298	K	β	10		O2_R	9.75		ΔhR_O2	0		**Air humidity**			Sumh_P	-1657820	kJ/kmol fuel
4				M	58.12		N2_R	36.66		ΔhR_N2	0		Pv_R	0		**Q**	-1531670	kJ/kmol fuel
5	**Combustion air**			hf_fuel	-126150		H2O_R	0		ΔhR_H2O	0		ω	0				
6	γ	50	%				Nreactants	47.41					**Products dew point**					
7	ϕ	0	%	**Enthalpy of formation**			**N of products**			**Δh for products**			Pv_P	25.55715	kPa			
8	Tin_air	298	K	hf_O2	0		CO2_P	4		ΔhP_CO2	33370.4		TdP	65.44627	°C			
9	Pin_air	250	kPa	hf_N2	0		CO_P	0		ΔhP_H2O	26040.5		**Fration of condensed water**					
10				hf_CO2	-393520		H2O_P	5		ΔhP_N2	21481.9		Pratio	8052.338				
11	**Discharge temperature**			hf_CO	-110530		O2_P	3.25		ΔhP_O2	22815.6		Nwv_ex	5	kmol			
12	**T_ex**	1000	K	hf_H2O	-241820		N2_P	36.66		ΔhP_CO	21727.8		Nwl_ex	0	kmol			
13				hf_H2OL	-285830		Nproducts	48.91										
14																		

Figure E.6. First-law analysis of the combustion of butane

Wrev =Xdestroyed

	A	B	C	D	E	F	G	H	I	J	K	L	M	N	O
1															
2	**Data**			**Absolute Entropy**			**Fractions Reactants**			**Entropy Reactants**			**Entropy balance**		
3	Pref	101	kPa	sf_fuel	310.03		yR_fuel	0.021093		sR_fuel	334.577		σ_P	11371.31	kJ/kmol fuel.K
4	Tref	298	K	sf_O2	205.03		yR_O2	0.205653		sR_O2	210.6438		σ_R	9210.876	kJ/kmol fuel.K
5				sf_N2	191.5		yR_N2	0.773255		sR_N2	186.1026		σ_production	7300.266	kJ/kmol fuel.K
6				sf_CO2	213.69		yR_H2O	0		sR_H2O	0				
7				sf_CO	197.54		**Fractions Products**			**Entropy Products**			Xdestroyed	2175479	kJ/kmol of fuel
8				sf_H2O	188.72		yP_CO2	0.081783		sP_CO2	282.4941		Wrev	2175479	kJ/kmol of fuel
9				sf_H2OL	69.95		yP_CO	0		sP_CO	0				
10							yP_O2	0.066449		sP_O2	258.7307				
11							yP_N2	0.74954		sP_N2	223.1062				
12							yP_H2O	0.102229		sP_H2O	244.2767				
13										sP_H2Ol	69.95				
14															

Figure E.7. Second-law analysis of the combustion of butane

Since butane is one of the fuels supported by Thermax, no special changes are required to the calculations part. Figure E.6 shows that the heat transfer from the combustion process is –1,531,670 kJ per kmole of butane. This compares well with the value given by Annamalai and Puri. [4], which is –1,533,044 kJ per kmole of butane. The second-

law analysis sheet shows that 7,300.3 kJ/K of entropy is generated and 2,175,479 kJ of reversible work is available per kmole of butane. The corresponding values given by Annamalai and Puri. [4] are 7,294 kJ/K and 2,175,291 kJ, respectively. Since no actual work has been produced, the irreversibility is equal to the reversible work, i.e., 2,175,479 kJ per kmol of butane.

References

[1] Y. A. Cengel and M.A. Boles. *Thermodynamics an Engineering Approach*, McGraw-Hill, 7th Edition, 2007

[2] K. Wark, JR, *Advanced Thermodynamics for Engineers*, McGraw Hill, 1995

[3] M.J. Moran and H.N. Shapiro, *Fundamentals of Engineering Thermodynamics*, 5th edition, John Wiley & Sons, Inc, 2006.

[4] K. Annamalai and I.K. Puri. *Advanced Thermodynamics Engineering*, CRC 2002

Appendix F: Analysis of a parallel-flow double effect VAR system

This appendix supplements Chapter 11 that deals with thermodynamic analyses of vapour-absorption refrigeration (VAR) systems by analysing a parallel-flow double-effect VAR system. The system considered in the analysis uses a water-lithium bromide solution with the input data given by ASHRAE [1].

A. The parallel-flow double-effect VAR system

Figure F.1 shows a schematic diagram of the parallel-flow double-effect VAR system. Like the series-flow cycle, there are three pressure levels in the cycle and the water vapour taken from the weak solution in each generator enters a distinct condenser. The high-pressure generator separates the refrigerant from the absorbent and the vapour produced there moves to the condenser where it is condensed into a liquid. The diluted absorbent then flows to the low-pressure generator where the heat from the condenser is used to further separate the refrigerant from the solution. The resulting vapour is taken to a second low-pressure condenser. The mixed liquid refrigerants from the two condensers then flow to the evaporator where it evaporates, creating the cooling effect.

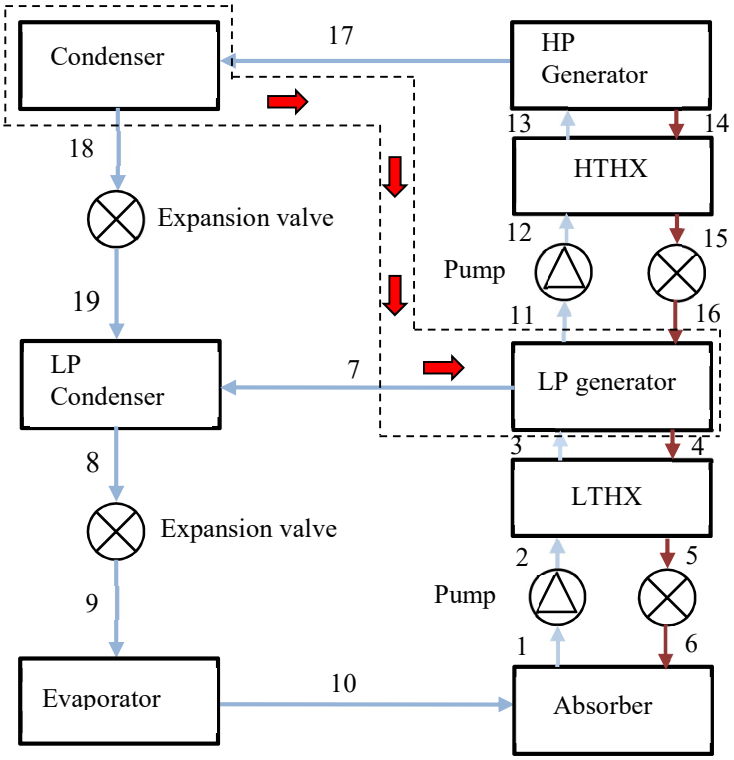

Figure F.1. Schematic drawing of the parallel flow double-effect VAR system

The system considered in the following analysis uses a water-lithium bromide solution with the particulars shown on Table F.1 as given by ASHRAE [1].

Table F.1. Inputs for the model of the parallel-flow double-effect system

Input	Value
Capacity (Q_e)	1760 kW
Evaporator temperature (T_{10})	5°C
Desorber solution exit temperature (T_{14})	170.7°C
Condenser/absorber low temperature ($T_1 = T_8$)	42.4°C
Temperature difference between the high-temperature condenser T_{18} and low-temperature generator T_4	5°C
Solution heat exchanger effectiveness (ε)	0.6

B. The analytical model

Mass and energy balances of the system are calculated with the following assumptions:

- The solution is saturated after it passes through the absorber and the generator, i.e., at state points 1, 4, 11, and 14.
- State points at 8 and 18 are saturated liquid water.
- Upper loop solution flow rate is selected such that upper condenser heat exactly matches lower generator heat requirement
- Vapour leaving both generators, i.e. T_7 and T_{17}, is superheated water vapour at equilibrium temperatures of entering solution streams.

As for the series-flow system, the temperature at state point 4 or 18 that determine the high pressure level at the HT condenser and HT generator is not given, but the difference between T_{18} and T_4 is specified as 5°C. Therefore, determining one of the temperatures will fix the other. In this mode, an initial value for T_4 which is then adjusted by using Excel's Solver to satisfy all the mass and energy balances in the cycle.

Solution concentrations

The solution concentrations at points 1 and 4 are determined from the known values of the temperatures and pressures using Thermax function **LibX_PrT** and the enthalpies h_1 and h_4 is then determined by using the function **LiBh_TX**. Unlike the series-flow system that has three concentration levels, various previous analyses [1, 2] show that there are only two concentration levels in this system. Therefore, the concentrations of the solution at state points 11 and 14 are takes as equal to those at 1 and 4, respectively, Accordingly:

$$X_{11} = X_{12} = X_{13} = X_1 \tag{F.1}$$

$$X_{13} = X_{14} = X_{15} = X_4 \tag{F.2}$$

State temperatures

The temperatures of the weak solution after the two heat-exchangers at state points 3 and 13 are determined as follows:

$$T_3 = T_2 + \varepsilon\left(T_4 - T_2\right) \tag{F.3}$$

$$T_{13} = T_{12} + \varepsilon\left(T_{14} - T_{12}\right) \tag{F.4}$$

The temperatures T_6 and T_{16} are determined from the calculated values of enthalpy and concentration using the function **LibT_hX**. Neglecting the work in the two pumps, the temperatures and enthalpy values at state points 2 and 12 after the pumps are taken as equal to their corresponding values at points 1 and 11 before the pumps.

State enthalpies

The enthalpies at state points 3 and 13 are determined by using the function **LiBh_TX** from which the enthalpies at state points 5 and 15 are determined from energy balances:

$$h_5 = h_4 - \left(\dot{m}_1 / \dot{m}_5\right)\left(h_3 - h_2\right) \tag{F.5}$$

$$h_{15} = h_{14} - \left(\dot{m}_{11} / \dot{m}_{15}\right)\left(h_{13} - h_{12}\right) \tag{F.6}$$

The temperatures T_5 and T_{15} are then determined by using the function **LiBT_hX**.

Since the flow restrictors are adiabatic, the enthalpies of the strong solution h_6 and h_{16} are given by:

$$h_6 = h_5 \tag{F.7}$$

$$h_{16} = h_{15} \tag{F.8}$$

Similarly, enthalpies of the pure refrigerant h_9 and h_{19} are given by:

$$h_9 = h_8 \tag{F.9}$$

$$h_{19} = h_{18} \tag{F.10}$$

Mass flow rates

The mass flow rates of the water vapour in and out of the evaporator are determined from the specified cooling capacity, Q_e, as follows:

$$\dot{m}_9 = \dot{m}_{10} = Q_e / \left(h_{10} - h_9\right) \tag{F.11}$$

The other mass flow rates are determined as follows:

$$\dot{m}_1 = \dot{m}_{10} + \dot{m}_6 \tag{F.12}$$

$$\dot{m}_3 = \dot{m}_2 = \dot{m}_1 \tag{F.13}$$

$$\dot{m}_4 = \dot{m}_3 X_3 / X_4 \tag{F.14}$$

$$\dot{m}_6 = \dot{m}_5 = \dot{m}_4 \tag{F.15}$$

$$\dot{m}_7 = \dot{m}_3 - \dot{m}_4 - \dot{m}_{11} + \dot{m}_{16} \tag{F.16}$$

$$\dot{m}_8 = \dot{m}_9 \tag{F.17}$$

$$\dot{m}_{16} = \dot{m}_{11} X_{11} / X_{16} \tag{F.18}$$

$$\dot{m}_{14} = \dot{m}_{15} = \dot{m}_{16} \tag{F.19}$$

$$\dot{m}_{11} = \dot{m}_{16} + \dot{m}_{17} \tag{F.20}$$

Heat and work transfer rates

$$Q_{\text{evap}} = \dot{m}_9 \left(h_{10} - h_9 \right) \tag{F.21}$$

$$Q_{\text{abs}} = \dot{m}_{10} h_{10} + \dot{m}_6 h_6 - m_1 h_1 \tag{F.22}$$

$$Q_{\text{cond}} = \dot{m}_7 h_7 + \dot{m}_{19} h_{19} - \dot{m}_8 h_8 \tag{F.23}$$

$$Q_{lpg} = \dot{m}_7 h_7 + \dot{m}_{11} h_{11} - \dot{m}_{16} h_{16} - \dot{m}_3 h_3 + \dot{m}_4 h_4 \tag{F.24}$$

$$Q_{hpc} = \dot{m}_{17} \left(h_{17} - h_{18} \right) \tag{F.25}$$

$$W_{pump1} = \dot{m}_1 v_1 \left(P_{LTG} - P_{evap} \right) \tag{F.27}$$

$$W_{pump2} = \dot{m}_{11} v_{11} \left(P_{HTG} - P_{LTG} \right) \tag{F.27}$$

Energy balance over the HTC and LPG

$$Q_{hpc} = Q_{lpg} \tag{F.28}$$

C. The Excel model

Figure F.2 shows the Excel sheet developed for this analysis and Figure F.3 reveals the formulae used in it with Thermax functions. The input data given in Table F.1 are stored on the top left side of the sheet. An initial value for T_4 of 100°C is assumed. The sheet then determines the pressures in the various system's components and the temperatures, concentrations, mass flow rates, and enthalpies at the 19 state points in the cycle.

Diff =ABS(Q_ch-Q_gl)

	A	B	C	D	E	F	G	H	I	J	K	L	M	N	O	P	Q	R
1	Input data																	
2	Q_E	1760	kW	T_1	42.4		x_1	59.060		m_1	8.246		h_1	115.523		Energy balance		
3	T_E	5	oC	T_2	42.4		x_2	59.060		m_2	8.246		h_2	115.523		Q_ch	904.8387	
4	T_HTG	170.7	oC	T_3	76.96		x_3	59.060		m_3	8.246		h_3	183.137		Q_gl	1183.143	
5	T_A	42.4	oC				x_4	65.009		m_4	7.491		h_4	253.282				
6				T_5	58.431		x_5	65.009		m_5	7.491		h_5	178.857		Q_a	2281.263	
7	ε	0.6		T_6	54.525		x_6	65.009		m_6	7.491		h_6	178.857		Q_c	1020.181	
8				T_7	85.788		x_7	0		m_7	0.370		h_7	2662.036		Q_gh	1263.141	
9	T_4	100	oC	T_8	42.4		x_8	0		m_8	0.755		h_8	177.562				
10				T_9	5		x_9	0		m_9	0.755		h_9	177.562		Q_shx1	557.531	
11	P_E	0.870	kPa	T_10	5		x_10	0		m_10	0.755		h_10	2510.060		Q_shx2	419.645	
12	P_A	0.870	kPa															
13	P_cl	8.441	kPa	T_11	85.788		x_11	59.060		m_11	4.203		h_11	200.422		w_p1	0.037	
14	P_gl	8.441	kPa	T_12	85.788		x_12	59.060		m_12	4.203		h_12	200.422		w_p2	0.284	
15				T_13	136.735		x_13	59.060		m_13	4.203		h_13	300.268				
16	P_ch	120.900	kPa	T_14	170.7		x_14	65.009		m_14	3.818		h_14	380.005		COP	1.393	
17	P_gh	120.900	kPa	T_15	109.389		x_15	65.009		m_15	3.818		h_15	270.101				
18				T_16	100.000		x_16	65.0091		m_16	3.818		h_16	270.101		Diff	278.3041	
19	v_1	0.00059		T_17	158.433		x_17	0		m_17	0.385		h_17	2792.940				
20	v_11	0.000601		T_18	105		x_18	0		m_18	0.385		h_18	440.270				
21				T_19	42.367		x_19	0		m_19	0.385		h_19	440.270				
22																		

Figure F.2. The sheet developed for analysing the parallel-flow double-effect system

Q20

	A	B	C	D	E	F	G	H	I	J	K	L	M	N
1	Input d													
2	Q_E	1760	kW	T_1	=T_A		x_1	=LiBX_TPr(T_1,P_E)		m_1	=m_10+m_6		h_1	=LiBh_TX(T_1,x_1)
3	T_E	5	oC	T_2	=T_1		x_2	=x_1		m_2	=m_1		h_2	=h_1
4	T_HTG	170.7	oC	T_3	=T_2+ε*(T_4-T_2)		x_3	=x_1		m_3	=m_1		h_3	=LiBh_TX(T_3,x_3)
5	T_A	42.4	oC				x_4	=LiBX_TPr(T_4,P_cl)		m_4	=m_3*x_3/x_4		h_4	=LiBh_TX(T_4,x_4)
6				T_5	=LiBT_hx(h_5,x_5)		x_5	=x_4		m_5	=m_4		h_5	=h_4-(x_5/x_1)*(h_3-h_2)
7	ε	0.6		T_6	=LiBT_PrX(P_A,x_6)		x_6	=x_4		m_6	=m_4		h_6	=h_5
8				T_7	=LiBT_PrX(P_gl,x_3)		x_7	0		m_7	=m_3-m_4-m_11+m_16		h_7	=Wath_PT(P_gl,T_7)
9	T_4	100	oC	T_8	=T_A		x_8	0		m_8	=m_9		h_8	=Wath_Tx(T_8,0)
10				T_9	=T_E		x_9	0		m_9	=Q_E/(h_10-h_9)		h_9	=h_8
11	P_E	=WatPsat_T(T_E)	kPa	T_10	=T_E		x_10	0		m_10	=m_9		h_10	=Wath_Tx(T_10,1)
12	P_A	=P_E	kPa											
13	P_cl	=WatPsat_T(T_8)	kPa	T_11	=LiBT_PrX(P_gl,x_11)		x_11	=x_1		m_11	=m_16+m_17		h_11	=LiBh_TX(T_11,x_11)
14	P_gl	=P_cl	kPa	T_12	=T_11		x_12	=x_11		m_12	=m_11		h_12	=h_11
15				T_13	=T_12+ε*(T_14-T_12)		x_13	=x_11		m_13	=m_11		h_13	=LiBh_TX(T_13,x_13)
16	P_ch	=WatPsat_T(T_18)	kPa	T_14	=T_HTG		x_14	=x_4		m_14	=m_13*x_13/x_14		h_14	=LiBh_TX(T_14,x_14)
17	P_gh	=P_ch	kPa	T_15	=LiBT_hx(h_15,x_15)		x_15	=x_14		m_15	=m_14		h_15	=h_14-(x_15/x_11)*(h_13-h_12)
18				T_16	=LiBT_PrX(P_gl,x_16)		x_16	=x_14		m_16	=m_14		h_16	=h_15
19	v_1	=LiBv_TX(T_1,x_1)		T_17	=LiBT_PrX(P_gh,x_13)		x_17	0		m_17	=m_8-m_7		h_17	=Wath_PT(P_gh,T_17)
20	v_11	=LiBv_TX(T_11,x_11)		T_18	=T_4+5		x_18	0		m_18	=m_17		h_18	=Wath_Tx(T_18,0)
21				T_19	=WatTsat_P(P_cl)		x_19	0		m_19	=m_17		h_19	=h_18
22														

Figure F.3. The formulae used in the sheet for the parallel-flow double effect system

At the initial value of T_4, Figure F.2 shows that the rates of heat transfer in the HT condenser and LT generator are not equal and, therefore, Equation (F.28) is not satisfied. Solver's set-up for determining the required value of T_4 is similar to that shown on Figure 11.15 and Figure F.4 shows its solution by using the GRG Nonlinear method. Solver reduced the value of DIFF to 0.937 at T_4 = 97.64°C and Table F.2 shows the

corresponding values obtained by the model for the mass flow rate ($\dot{m}$), refrigerant concentration (X), solution temperature (T), and solution enthalpy (h).

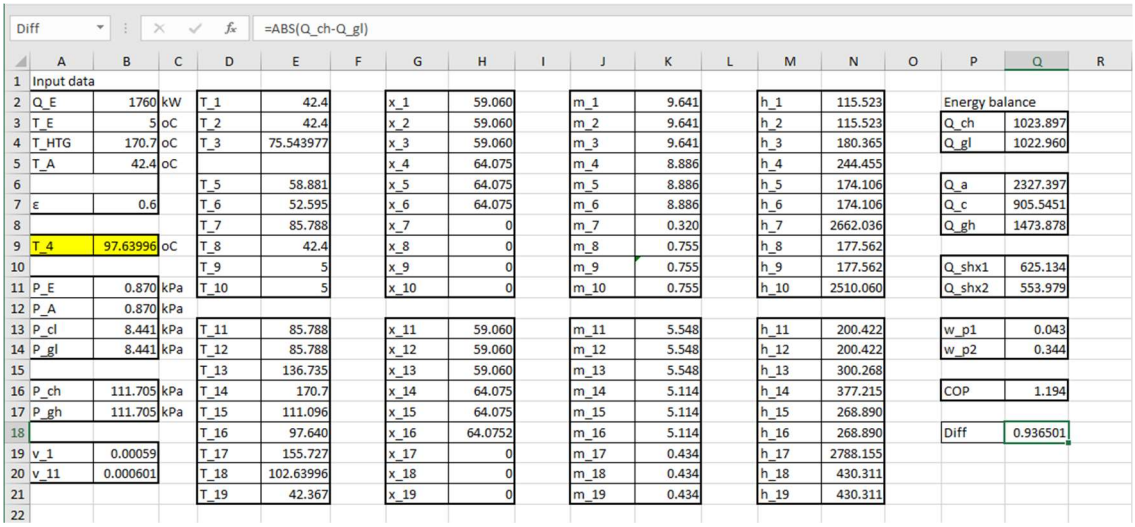

Figure F.4. Solver's solution of the parallel-flow double-effect VAR system

Table F.2. Results of the parallel-flow double-effect VAR cycle analysis

#	$\dot{m}$	X	T	h
1	9.641	59.060	42.4	115.523
2	9.641	59.060	42.4	115.523
3	9.641	59.060	75.54397	180.365
4	8.886	64.075	97.6399	244.455
5	8.886	64.075	58.881	174.106
6	8.886	64.075	52.595	174.106
7	0.320	0	85.788	2662.036
8	0.755	0	42.4	177.562
9	0.755	0	5	177.562
10	0.755	0	5	2510.060
11	5.548	59.060	85.788	200.422
12	5.548	59.060	85.788	200.422
13	5.548	59.060	136.735	300.268
14	5.114	64.075	170.7	377.215
15	5.114	64.075	111.096	268.890
16	5.114	64.075	97.640	268.890
17	0.434	0	155.727	2788.155
18	0.434	0	102.6399	430.311
19	0.434	0	42.367	430.311

Figure F.5, that shows the percentage deviation of the results obtained by the present model from those given by ASHRAE [1], shows that most of the model values deviated by less than 1% from their corresponding values in Ref. [1]. Table F.3 compares the different pressures and heat-transfer rates in the system's components as well as the pumps' work and cycle's COP with those given by ASHRAE [1]. The table shows close agreements between the calculated values and the reference data particularly the COP.

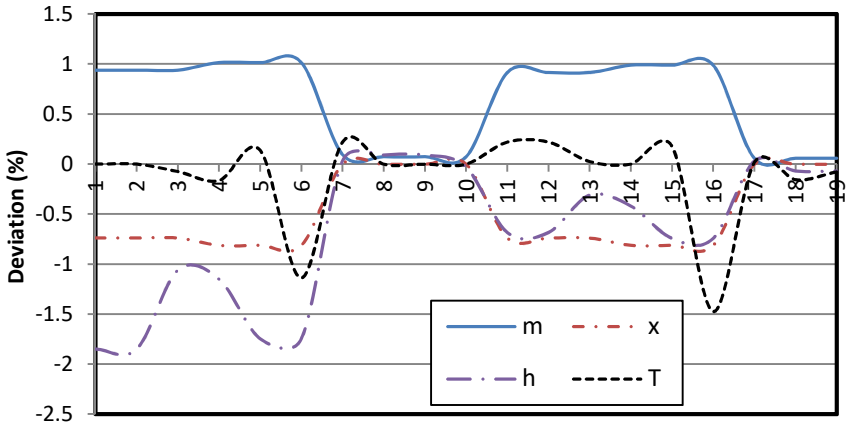

Figure F.5. Percentage deviations from ASHRAE [1] data

Table F.3. Comparison of the present estimations with those of Ref. [1]

	Ref. [1]	Present	% error
Evaporator pressure	0.88	0.870	1.14
Low-temperature generator pressure	8.36	8.441	-0.97
High-temperature generator pressure	111.8	111.705	0.08
Heat-transfer in absorber	2328	2327.397	0.03
Heat-transfer in low-temperature generator	1023	1022.960	0.00
Heat-transfer in low-temperature condenser	905	905.545	-0.06
Heat-transfer in high-temperature generator	1472	1473.879	-0.13
Heat-transfer in heat-exchanger 1	617	625.134	-1.32
Heat-transfer in heat-exchanger 2	546	553.980	-1.46
Work supplied to pump 1	0.043	0.043	-0.66
Work supplied to pump 2	0.346	0.344	0.51
COP	1.195	1.194	0.10

References

[1] ASHRAE Handbook–Refrigeration, 2017, American Society of Heating, Refrigerating and Air-Conditioning Engineers, Inc., (SI Edition).

[2] F. M. Kashkooli, M. Rezaeian, M. Sefidgar, M. Soltani, M. Mafi, Performance Evaluation of Series and Parallel Two-Stage Absorption Chillers Driven by Solar Energy: Energetic Viewpoint, Gas Processing Journal, Vol. 7, No. 2, 2019

Appendix G: Review exercises and mini projects

This appendix provides review exercises and mini projects related to the various types of energy-conversion systems considered in the book. The majority of the cases presented in the appendix have been adapted from standard textbooks and published studies from which more information about the cases and the basic principles involved can be obtained for validating the analytical models.

1. A 100-MWe steam power plant is to be designed on the basis of a reheat–regenerative Rankine cycle with one open feedwater heater, one closed feedwater heater, and one reheater as shown on Figure G.1. Steam enters the turbine at 15 MPa and 600°C and is condensed in the condenser at a pressure of 10 kPa. Some steam is extracted from the turbine at P_{10} for the closed feedwater heater, and the remaining steam is reheated at the same pressure to 600°C. The extracted steam is completely condensed in the heater and is pumped to 15 MPa before it mixes with the feedwater at the same pressure. Steam for the open feedwater heater is extracted from the low-pressure turbine at P_{12}.

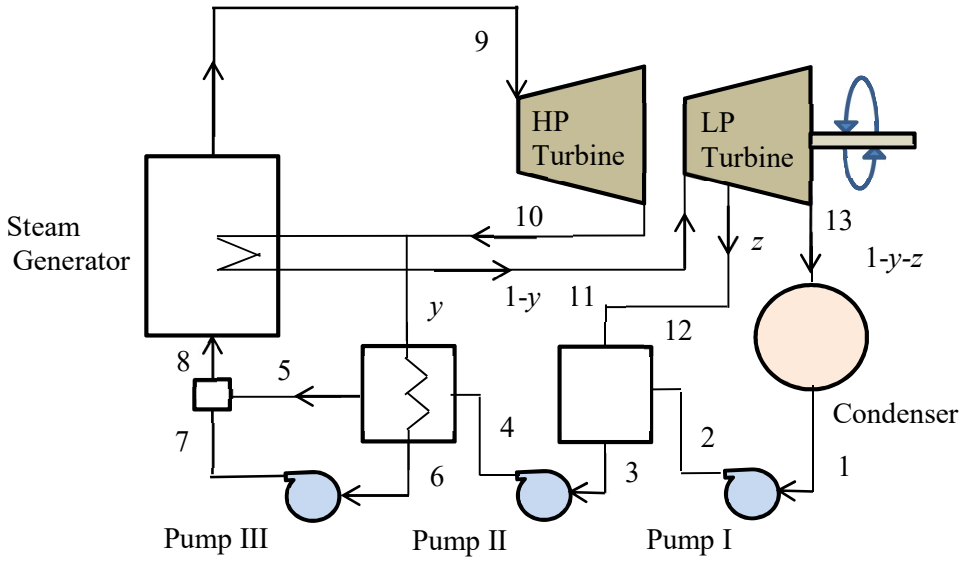

Figure G.1. A reheat–regenerative Rankine cycle with open and closed feedwater heaters (Adapted from Cengel and Boles [1])

(a) Develop an Excel sheet for thermodynamic analysis of the ideal cycle and verify your sheet by comparing the values obtained for the fractions of steam extracted from the turbine and the thermal efficiency of the cycle with the relevant values given by Cengel and Boles [1] in Example 10.6 for P_{10} = 4 MPa and P_{12} = 0.5 MPa.

(b) Extend your Excel sheet to model the actual cycle by taking suitable values for the isentropic efficiencies of the turbines and pumps.

(c) Use Solver to determine the optimum values of the two extraction pressures P_{10} and P_{12} that maximise the total annual revenue.

2. The regenerative Rankine cycle shown on Figure 4.13 requires a feed-water pump to be added per each closed FWH. The added pumps increase both the initial and running costs of the power plant. An alternative arrangement that saves these additional costs is shown on Figure G.2.

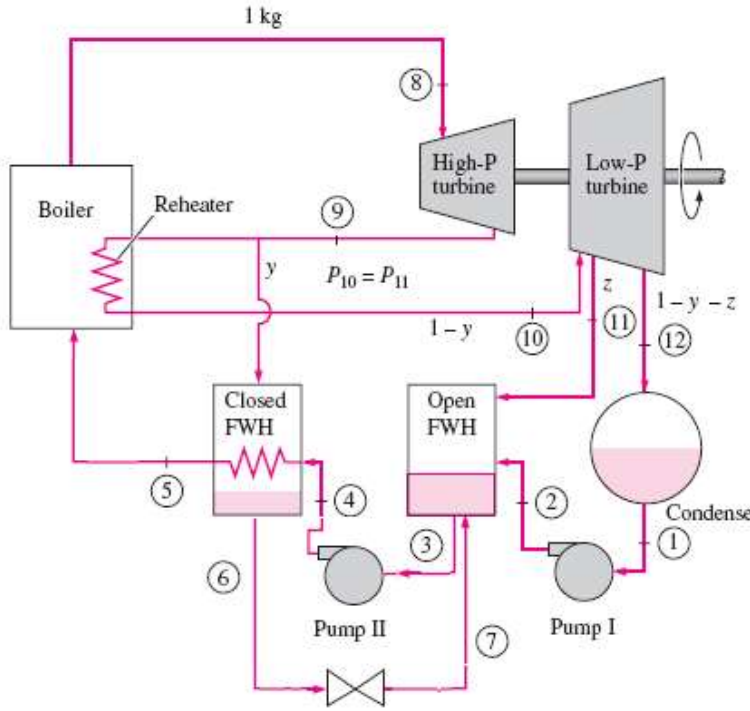

Figure G.2. (Adopted from Cengel and Boles [1])

According to this arrangement, instead of pumping the feed-water to the next upper level of pressure, the steam is throttled down to the feed-water heater with a lower pressure. The trap allows only the saturated liquid to pass to the open feed-water heater. Therefore, the vapour part has to be condensed first by losing its latent heat of vaporisation. (a) Develop an Excel sheet to analyse this cycle under the conditions similar to those of Example 4.4 and compare the two cycles. (b) What is the disadvantage of this system compared to that of Figure 4.13?

3. A regenerative steam-turbine cycle is shown on Figure G.3. A unit mass (m_t=1) of steam enters the turbine and expands to the first extraction point (4), where a mass of steam (m_4) is extracted and flows to the No. 4 feed-water heater. The remainder of the steam (1-m_4) expands to the second extraction point (3), where a mass of steam (m_3) is extracted and flows to the No. 3 heater. Subsequently, the steam continues to

expand with extraction at point (2) and (1). Heater No. 2 is a deaerating heater. Heater No. 3 and heater No. 4 are high-pressure closed heaters, and heaters No. 1 is a low-pressure closed heater. Heat rejected from the coolers of the generator, lubricating oil, etc. are presented by a single cooler - between the condensate pump and heater No. 1- that increases the enthalpy of the condensate by 58.3 kJ/kg. Determine the optimum extraction pressures for heaters No 1, 3, and 4.

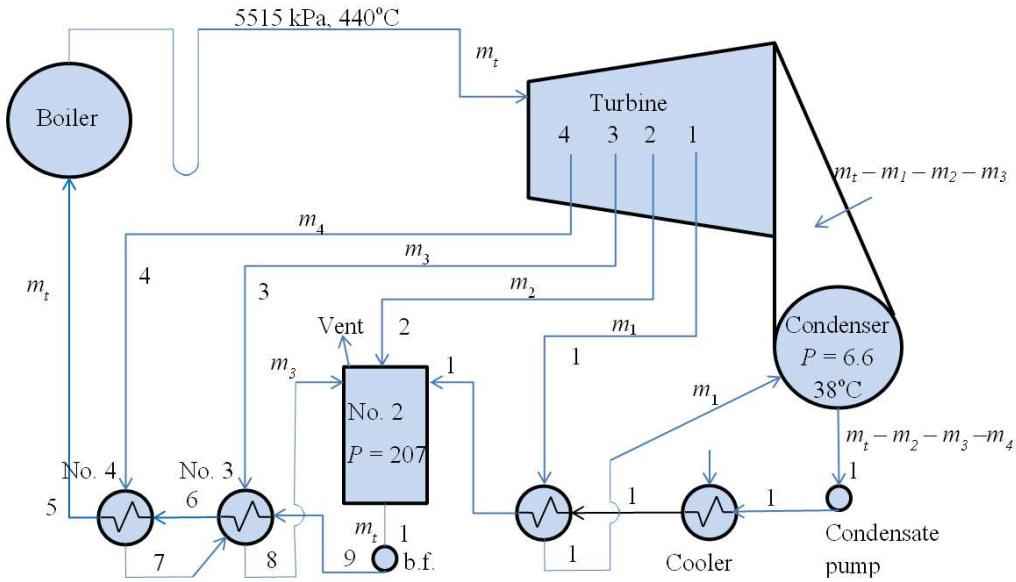

Figure G.3. A regenerative Rankine cycle (adapted from Sorensen [2])

4. Consider a combined gas–steam power plant that has a net power output of 450 MW. The pressure ratio of the gas-turbine cycle is 14. Air enters the compressor at 300 K and the turbine at 1400 K. The combustion gases leaving the gas turbine are used to heat the steam at 8 MPa to 400°C in a heat exchanger. The combustion gases leave the heat exchanger at 460 K. An open feedwater heater incorporated with the steam cycle operates at a pressure of 0.6 MPa. The condenser pressure is 20 kPa. Assuming all the compression and expansion processes to be isentropic, develop an Excel sheet to determine (a) the mass flow rate ration of air to steam, (b) the required rate of heat input in the combustion chamber, and (c) thermal efficiency of the combined cycle. Based on Problem 10.78 in Cengel and Boles [1].
5. A vapour-compression refrigeration system includes a counter-flow double-pipe heat exchanger as shown on Figure G.4. Ammonia leaves the evaporator as saturated vapour at 1.0 bar and is heated in the heat-exchanger at constant pressure to 5°C before entering the compressor. Following isentropic compression to 18 bar, the refrigerant passes through the condenser, exiting at 40°C, 18 bar. The liquid then passes through the heat exchanger, entering the expansion valve at 18 bar.

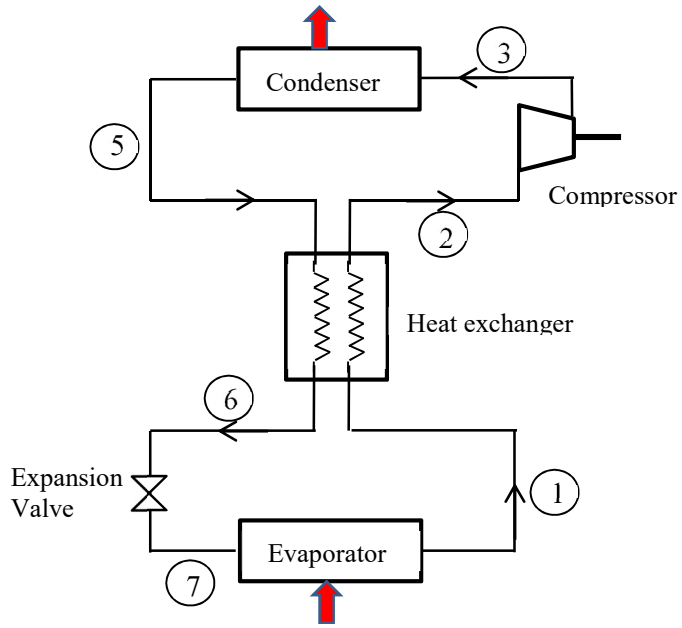

Figure G.4. Schematic of a VCR system with a counter-flow heat exchanger (adapted from Moran and Shapiro [3], Problem 10.19)

If the mass flow rate of refrigerant is 12 kg/min, use an Excel model to determine:

a. the exit temperature of the subcooled refrigerant at state 6
b. the refrigeration capacity, in tons of refrigeration
c. the compressor power input, in kW
d. the coefficient of performance

Discuss possible advantages and disadvantages of this arrangement and study the effect of the heat-exchanger effectiveness on the cycle's performance by increasing and decreasing the value of T_1.

6. The ideal vapour-compression refrigeration cycle considered in Example 5.1 with R-134a is modified to include a counter-flow double-pipe heat exchanger, as shown in Figure G.4. The refrigerant leaves the evaporator as saturated vapour at -10.0°C and is heated at constant pressure to state 2 before entering the compressor. Following isentropic compression to P_2 = 9 bar, the refrigerant passes through the condenser, exiting at saturated liquid. The liquid then passes through the heat exchanger where it is cooled to state 6 before entering the expansion valve at the same pressure. The mass flow rate of refrigerant is 0.08 kg/s. Determine:

(a) the refrigeration capacity, in tons of refrigeration.
(b) the compressor power input, in kW.
(c) the coefficient of performance.

7. It is required to compare the performance of refrigerant R22 and refrigerant R134a for heat-pump applications between an evaporator temperature of 10°C and a condenser temperature of 70°C. Four options are possible:

    a. A simple cycle with Refrigerant R22 alone
    b. A simple cycle with Refrigerant R134a alone
    c. A cascade system with R22 in the low-temperature cycle and R134a in the high-temperature cycle
    d. A cascade system with R134a in the low-temperature cycle and R22 in the high-temperature cycle

    Develop suitable Excel sheets to compare the compressor power (kW), heating capacity (kW), and coefficient of performance of the above options. For options (c) and (d), try various intermediate temperatures, e,g. 20, 30, 40°C
8. Extend the Excel sheet developed in Example 5.4 for analysing the three-stage compression VCR cycle for conducting a thermo-economic analysis of the system..
9. Extend the Excel sheet developed in Example 5.5 for analysing the cascade VCR cycle for conducting a thermo-economic analysis of the system.
10. Both the cooling and heating of the air in the design case of the air-conditioning system in Section 6.6 can be achieved by using a heat pump. Extend the Excel sheet developed for the design case of the air-conditioning system to account for the cost of this option based on its economic savings.
11. Cooling the air in the design case of the air-conditioning system described in Section 6.6 can be via vapour-compressions or vapour absorption systems. Similarly, heating the air can be done by using direct electric heating or by gas heating. These four options have different costs. By using suitable estimations of these costs, extend the Excel sheets developed for the design case of the air-conditioning system to account for the cost of cooling the air either by vapour-compressions or vapour absorption and heating it either by direct electric or gas heating. Evaluate the economic savings of the two operation modes shown on Figure 6.14 and prepare a table for the results with the four possible combinations.
12. Methane, CH_4, is burned with dry air. The fuel enters a combustion chamber at 400 K and 1 atm, where it is mixed with air entering at 500 K and 1 atm. The products of combustion exit at 1800 K and 1 atm. The molar analysis of the products on a dry basis is CO_2, 9.7%; CO, 0.5%; O_2, 2.95%; and N_2, 86.85%.

    (a) Show that the reaction equation is:

    $$CH_4 + 2.265\ O_2 + 11.515\ N_2 \rightarrow 0.951\ CO_2 + 0.049\ CO + 0.289\ O_2 + 11.515\ N_2 + 2\ H_2O$$

    (b) Determine the dew point temperature of the products, in °C, if the mixture were cooled at 1 atm.

(c) For operation at steady state, determine the rate of heat transfer from the combustion chamber in kJ per kmol of fuel. The average value for the specific heat of methane between 298 and 400 K is 38 kJ/kmol K.

13. Liquid octane at 25ºC, 1 atm enters a well-insulated reactor and reacts with air entering at the same temperature (298K) and pressure (1 atm). For steady-state operation and negligible effects of kinetic and potential energy, determine the adiabatic flame temperature of the combustion products for complete combustion with (a) the theoretical amount of air, (b) 400% theoretical air.
14. Study the effect of excess air and air humidity on the adiabatic flame temperature (T_{af}) of different fuels by determining the values of T_{af} for isooctane (C_8H_{18}), propane (C_3H_8), and methane (CH_4) at γ = 0%, 10%, 20%, 30%, 40%, and 50%. Use a macro and plot the results on an Excel chart.
15. Consider the simple vapour-compression refrigeration system shown in Figure G.5. The refrigerant can be assumed to leave the evaporator as saturated vapour and the condenser as saturated liquid. It is required to optimise the total lifetime cost of the system for a specified value of the cooling capacity $\dot{Q}_e$.

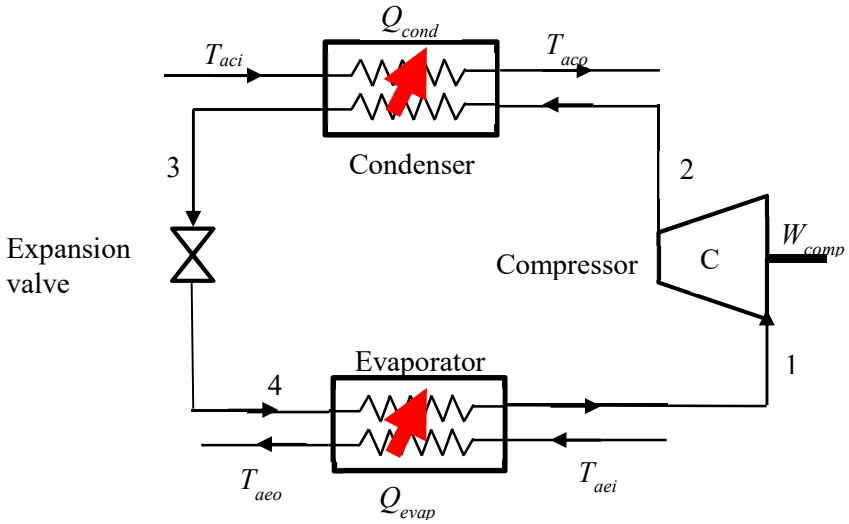

Figure G.5. Schematic diagram of a simple VCR system

For the system under consideration the objective function for optimisation is that of the total cost (C_T) given by:

$$C_T = IC + PW_{OC} \tag{G.1}$$

Where IC is the initial cost that includes the costs of the compressor, evaporator, and condenser, and PW_{OC} is the present worth value of the annual operating cost. The initial costs of the evaporator (IC_E) and condenser (IC_C), are given by:

$$IC_{evap} = A_e \times C_{uae} \tag{G.2}$$

$$IC_{cond} = A_c \times C_{uac} \tag{G.3}$$

Where A_e and C_{uae} are the area and cost per unit area for the evaporator and A_c and C_{uac} are their counterparts for the condenser. The areas of the evaporator and condenser depend on their rates of heat transfer, $\dot{Q}_e$ and $\dot{Q}_c$, and their overall heat-transfer coefficients, U_e and U_c. The initial cost of the compressor (IC_{Comp}) is given by:

$$IC_{comp} = \frac{C_{comp}}{(1-\eta_c)^2} \tag{G.4}$$

Where C_{comp} is a unified reference cost of the compressor (the lowest possible cost of a compressor) and η_c is the compressor's isentropic efficiency. The operating cost (OC), which is mainly the cost of electricity, can be obtained from;

$$OC = \dot{W}_{comp} \times \tau \times C_{elec} \tag{G.5}$$

Where $\dot{W}_{comp}$ is the compressor's power in kW, τ is the annual operating time in hours, and C_{elec} the cost of electricity per kW-hr.

The present worth value of the annualised cost of electricity (PW_{OC}) can be obtained from:

$$PW_{OC} = \frac{OC \times \left[(1+MARR)^N - 1\right]}{MARR \times (1+MARR)^N} \tag{G.6}$$

Where $MARR$ is the minimum attractive rate of return for investment and N is the life of the system in years.

Using Thermax, develop an Excel sheet that can be used to optimise the system for an application of your choice using refrigerant R134a, R22, R410A, or R717. Use your Excel sheet to optimise the VCR system for a cooling capacity $\dot{Q}_e$ = 10 kW, lifetime n = 25 years, and MARR = 0.20 based on Table G.1. This case is based on a paper contributed by Zietlow [4].

16. Meraj et. al. [5] analysed the single effect VAR cycle shown on Figure G.6 with H_2O-LiBr solution as working fluid for evaporator temperatures of 5, 7.5, 10 and 12.5°C and main condenser temperatures of 30 and 35°C.

Table G.1. Input data for Problem G.15

Variable Name	Value	Units
C_{comp}	25	$
C_{elec}	0.10	$/kW-hr
C_{uac}	200	$/m^2
C_{uae}	350	$/m^2
Time	3000	kW-hr/yr
T_{aci}	30	°C
T_{aei}	20	°C
U_c	0.20	kW/m^2-K
U_e	0.30	kW/m^2-K

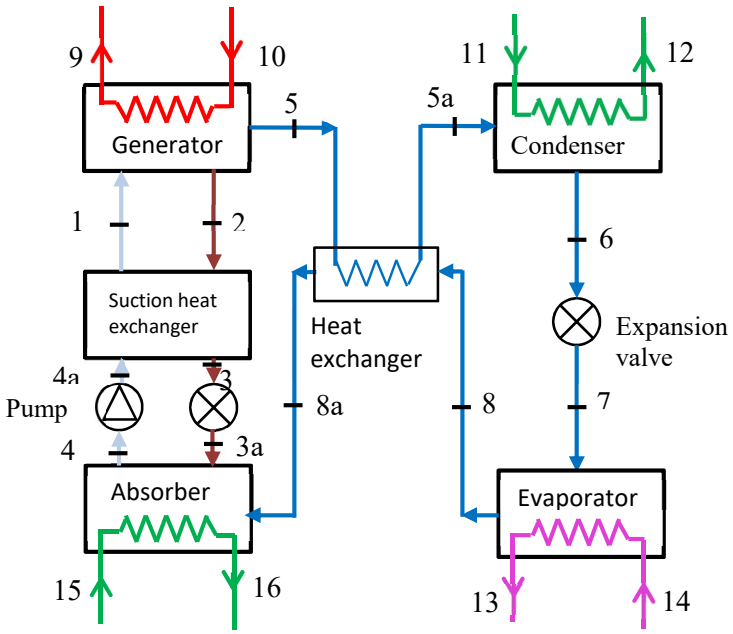

Figure G.6. Schematic of a single effect VAR system

Taking the absorber temperature to be equal to the condenser temperature, develop an Excel model using Thermax functions to analyse the system with the following assumptions:

- Refrigerant leaving the condenser is saturated water at condenser pressure, and refrigerant leaving the evaporator is saturated vapour at evaporator pressure.
- Condenser pressure is equal to generator pressure, and evaporator pressure is equal to absorber pressure.
- There is no pressure drop in the heat exchangers or piping systems.

- There are no heat losses or gains in the various components and piping systems.
- The solution pump efficiency is 0.9.

17. The ORC system shown on Figure G.7 adds a regenerator to the simple system between the superheated vapour at the expander's exit and the compressed liquid after the pump. Analyse the effect of this modification on the system's performance by using regenerator effectiveness from 65% to 85%.

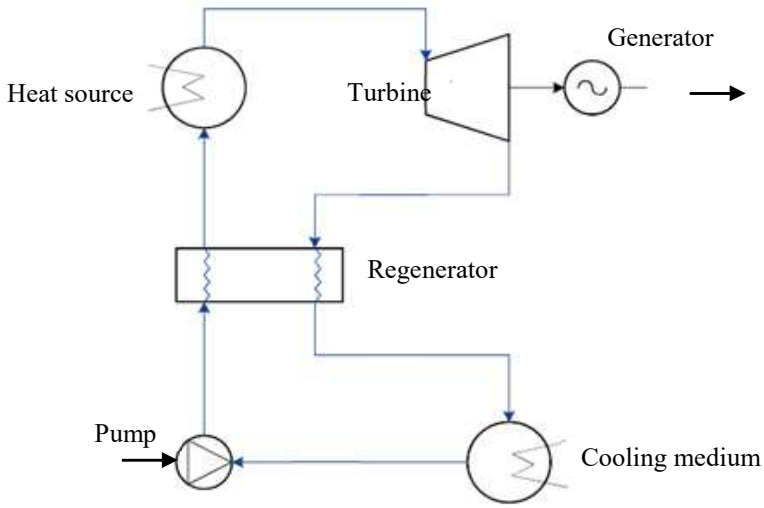

Figure G.7. Schematic of the ORC system with regeneration

18. Yu et. al. [6] proposed the innovative cascade system shown on Figure G.8 that combines a trilateral cycle and an organic Rankine cycle for industry or transport applications. Using their input data, develop an Excel sheet for the cycle using Thermax functions with R245fa in the LT circuit and water in the HT circuit and compare the system's net power, thermal efficiency, and exergetic efficiency at different temperatures in the HT circuit with those obtained by Yu et. al. [6].
19. The system shown on Figure G.8 differs from the combined TFC-ORC system presented in Section 12.3 in two respects:

    - The working fluid in the LT circuit is first heated by that of the HT circuit and then by the exhaust gas. In the system described in Section 12.3 the sequence is reversed.
    - The LT circuit is simple and does not include a preheater for the fluid.

    By using Thermax property functions, develop an Excel sheet for the system in Figure G.8 to analyse its performance with the low-temperature heat source of 120°C described in Section 12.3 under the same operating conditions:

(a) By using R152a in both the HTC and LTC
(b) By using R152a in the HTC and R1234yf in the LTC.

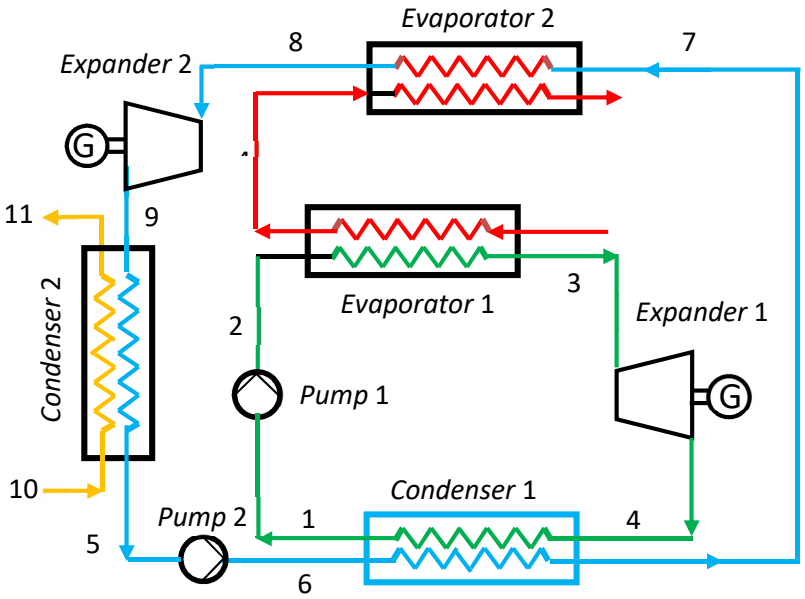

Figure G.8. Schematic of the combined ORC-TFC cycle proposed by Yu et. al. [6]

References

[1] Y. A. Cengel and M.A. Boles. *Thermodynamics an Engineering Approach*, McGraw-Hill, 7th Edition, 2007.
[2] H. A., Sorensen, Energy conversion systems, Publisher New York: J. Wiley, Publication date1983
[3] M. J. Moran and H.N. Shapiro, *Fundamentals of Engineering Thermodynamics*, 5th edition, John Wiley & Sons, Inc, 2006.
[4] D. C. Zietlow, Optimization of vapor compression cycles, 2014 ASEE Annual Conference & Exposition, 24.958. 1-24.958. 23
[5] M. M. Meraj, E. Khan, R. Imam, Thermodynamic Analysis of Single Effect Vapor Absorption Refrigeration Cycle, *International Journal of Science and Research* (IJSR), ISSN (Online): 2319-7064
[6] X. Yu, Z. Li,Y. Lu, R. Huang and A. P. Roskilly, Investigation of an Innovative Cascade Cycle Combining a Trilateral Cycle and an Organic Rankine Cycle (TLC-ORC) for Industry or Transport Application, Energies 2018, 11, 3032; doi:10.3390/en11113032, www.mdpi.com/journal/energies

Nomenclature

Symbol	Quantity	SI Unit
A	Area	m^2
AFR	Air-fuel ratio	-
BWR	Back-work ratio	-
c	Specific heat	kJ/kg.K
c_p	Specific heat at constant pressure	kJ/kg.K
$\bar{c}_p$	Specific heat at constant pressure (molar)	kJ/kmol.K
c_v	Specific heat at constant volume	kJ/kg.K
C	Degree celcius	^oC
COP	Coefficient of peformance for a refrigeration system	-
$\bar{g}_f^0$	Gibbs function of formation (molar)	kJ/kmol
h	Specific enthalpy	kJ/kg
$\tilde{h}$	Enthalpy (molar)	kJ/kmol
$\bar{h}_f^0$	Enthalpy of formation (molar)	kJ/kmol
$\tilde{h}_C^0$	Enthalpy of combustion at the standard state	kJ/kmol
HV	Heating value	kJ/kg
HHV	Higher heating value	kJ/kg
H_v	Heat of vaporization of fuel	kJ/kg
k	The ratio of specific heats c_p/c_v	-
k	Thermal conductivity	mW/(m.^oC)
K	Degree Kelvin	K
LHV	Lower heating value	kJ/kg
m	Mass	kg
M	Molar mass	Kg/mol
$MARR$	Minimum attractive rate of return	%
N	Number of moles	-
p	Pressure	kPa
Pr	Prandtl number	-
P_r	Relative pressure	-
P_{sat}	Saturation pressure	kPa
q	Quanitity of heat	kJ/kg
Q_H	Higher heating value of fuel	kJ/kg.K
Q_L	Lower heating value of fuel	kJ/kg.K
R	Gas constant	kJ/kg.K
s	Entropy (specific)	kJ/kg.K
s_f	Entropy of saturated liquid solution	kJ/kg.K
s_g	Entropy of sturated vapour soliution	kJ/kg.K
s^o	Entropy change with temperature (ideal gas)	kJ/kg.K

$\bar{s}^o$	Entropy change with temperature (molar)	kJ/kmol.K
$\bar{s}^o$	Entropy (absolute molar)	kJ/kmol.K
T	Temperature	^oC
T_{db}	Dry-bulb temperature	^oC
T_{dp}	Dew-point temperature	^oC
T_{sat}	Saturation temperature	^oC
u	Internal energy (specific)	kJ/kg
$\tilde{u}$	Internal energy (molar)	kJ/kmol
v	Specific volume (relative)	m^3/kg
v_r	Relative specific volume	-
V	Velocity	m/s
V_s	Velocity of sound	m/s
$\dot{V}$	Volume flow rate	m^3/s
w	Quantity of work (specific)	kJ/kg
W	Quantity of work	kJ
x	Quality (dryness fraction)	-
x_{dest}	Exergy destruction	kJ/kg
X	Concentration (of an absorption solution)	%
z	Elevation	m
α	Diffusivity	m^2/s
β	Volumetric expansion coefficient	$^oC^{-1}$
γ	Excess air provided for combustion	-
ε	Effectiveness of a heat-exchanger	-
η	Thermal efficiency	-
η	Isentropic efficiency	-
μ	Dynamic viscosity	μPa.s
ν	Kinematic viscosity	m^2/s
ρ	Density	Kg/m^3
σ	Surface tension	mN/m
τ	Annual operating time	hour
ϕ	Exergy	kJ/kg
ϕ	Relative humidity	%
ω	Specific or absolute humidity	kg H_2O/kg dry air

Index